AMERICAN UNIVERSITY OF BEIRUT

INVESTIGATION ON DAPC AND DBPC LIPOSOME
PROPERTIES AND THEIR BIOMEDICAL APPLICATIONS

by
MARIA KHALIL ESTEPHAN

A thesis
submitted in partial fulfillment of the requirements
for the degree of Master of Science
to the Department of Chemistry
of the Faculty of Arts and Sciences
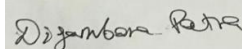at the American University of Beirut

Beirut, Lebanon
February 2021

AMERICAN UNIVERSITY OF BEIRUT

INVESTIGATION ON DAPC AND DBPC LIPOSOME
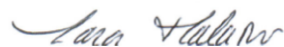PROPERTIES AND THEIR BIOMEDICAL APPLICATIONS

by
MARIA KHALIL ESTEPHAN

Approved by:

_____
[Dr. Digambara Patra, Professor]   Advisor
[Chemistry]

_____
[Dr. Lara Halaoui, Professor]   Member of Committee
[Chemistry]

_____
[Dr. Elias Baydoun, Professor]   Member of Committee
[Biology]

Date of thesis defense: February 22, 2021

AMERICAN UNIVERSITY OF BEIRUT

THESIS RELEASE FORM

Student Name: Estephan   Maria   Khalil
                         Last   First   Middle

I authorize the American University of Beirut, to: (a) reproduce hard or electronic copies of my thesis; (b) include such copies in the archives and digital repositories of the University; and (c) make freely available such copies to third parties for research or educational purposes:

☐ As of the date of submission

☐ One year from the date of submission of my thesis.

☒ Two years from the date of submission of my thesis.

☐ Three years from the date of submission of my thesis.

Maria Estephan

Signature

February 27, 2021

Date

ACKNOWLEDGMENTS

First and foremost, I would like to praise and thank God for granting me a life time opportunity to pursue my graduate studies at AUB, and have shadowed my journey all the way long through all the obstacles I faced.

My deepest gratitude goes to Professor Digambara Patra, my thesis supervisor, for his tremendous support, patience and help. I felt motivated and encouraged every time we met to discuss my results. Without his guidance, this thesis would not have materialized.

Sincere appreciation is also expressed to my committee members, Professor Lara Halaoui and Professor Elias Baydoun, for their valuable time, comments and suggestions that brought in threads of thought that made my research so much richer.

I would like to pay my special and heartful regards to Miss Riham El Kurdi, the greatest research assistant who turned out to be a very close friend, more like a big sister, and the ultimate 24/7 support during the lab work and the writing process. Words won't be fair to express my deepest gratitude for accompanying me in my challenging journey.

I am certainly lucky to have joined Dr.Patra's lab and met friends, especially Celine Arab, whose permanent encouragement has made me overcome difficulties and made the most valuable and unforgettable memories.

I would also like to thank, Georges, the very special person to my heart who stood by my side and supported me all throughout this long journey by making the toughest times easier.

Finally, I am extremely blessed and thankful to have my family: mom, dad, Mario and Elissa whose love and believe in me made me achieve my goals during these exceptional hard times that our country and world are facing.

In memory of my beloved Grandmother, my second mom, who supported me during my first year of graduate studies and was always looking forward to be with me on this day. It's for the first time that I accomplish a huge step in my life without her. Although she has physically parted from me, I know that she kept on watching on me from above and that she's proud of me.

ABSTRACT
OF THE THESIS OF

Maria Khalil Estephan   for   Master of Science
                                        Major: Chemistry

Title: Investigation on DAPC and DBPC liposome properties and their biomedical applications.

Nanotechnology is a promising developing field offering potential tools for the loading of curcumin in order to improve its various applications. Several types of nanoparticles have emerged one of which are liposomes vesicles. Formed by spontaneous self-assembly of lipids upon hydration, liposomes contribute a suitable alternative for curcumin delivery. Nevertheless, liposomes also suffered from low stability due to metabolic degradation which is why it was proposed to modify their surface by coating it with a polymeric layer such as chitosan oligosaccharide lactate.

In this thesis, we report in the first place the efficacy of curcumin as a fluorescence probe to determine the Tm, membrane permeability and partition coefficient of curcumin. These experiments were done for both DAPC and DBPC liposomes.

Actually, fluorescence intensity of curcumin – temperature profile was applied to determine the phase transition temperatures of these liposomes which were find to slightly affected with low curcumin's concentration.

Moreover, the encapsulation of curcumin was elaborated into two kinds of liposomes forming four types of nanocapsules: DAPC-curcumin; DAPC-curcumin-chitosan; DBPC-curcumin; DBPC-curcumin-chitosan. The partition coefficient of curcumin into these systems was evaluated and found to be higher with the polymer layer and dependent on the physical state of the liposomes. Quenching studies with hydrophobic and hydrophilic quenchers were conducted to locate curcumin in the systems. We concluded that curcumin binds strongly to the liposomes' membranes.

Furthermore, ionic liquids (ILs) are a type of green solvents that are recently being used for various applications. In that sense, the effect of 1-buytl-3-methyl imidazolium tetrafluoroborate (bmit) IL on the partition coefficient of curcumin was explored in this work by monitoring its interaction with DAPC and DBPC. The partition of curcumin was enhanced at low IL concentrations but depressed at higher concentrations while showing a dependence on the liposomes' physical state.

Indeed, the successful encapsulation of curcumin into DAPC liposome was verified through UV-Visible, fluorescence emission spectra, XRD and SEM. Additionally, the

effectiveness of chitosan as a protective layer was confirmed through zeta potential analysis and TGA study.

Moving on the application part, some biological applications for these nano-capsules were further investigated.

Mainly, DAPC based nanocapsules were used to study the anti-cancer activity of curcumin on MCF-7 breast cancer cells and Capan-1 pancreatic cancer cells along with evaluating the effect of the chitosan layer. It was observed that these nanoparticles inhibited up to 90% the proliferation of cancer cells after 72 hours.

On the other hand, DBPC based nanocapsules coated with chitosan layer (DBPC-CUR-Chi) played the role of potential, fast, easy, stable and selective nanosensors for the detection of RNA molecule. This was observed with the increase of the emission intensity of curcumin as the concentration of RNA was increased (0-20 and 30-500 μg/mL). The LOD attained were 36 ng/mL and 110 ng/mL. The recovery range was found to be 99.5 and 100.33%.

TABLE OF CONTENTS

ILLUSTRATIONS

Figure

TABLES

Table

ABBREVIATIONS

DAPC	1,2-diarachidoyl-sn-glycero-3-phosphocholine
DBPC	1,2-dibehenoyl-sn-glycero-3-phosphocholine
DMPC	1,2-dimyristoyl-sn-glycero-3-phosphocholine)
DSPC	1,2-Distearoyl-sn-glycero-3-phosphocholine
DAPC-Cur NCs	1,2-diarachidoyl-sn-glycero-3-phosphocholine-curcumin- nanocapsules
DAPC-Cur-Chi NCs	1,2-diarachidoyl-sn-glycero-3-phosphocholine-curcumin- chitosan nanocapsules
DBPC-Cur NCs	1,2-dibehenoyl-sn-glycero-3-phosphocholine-curcumin nanocapsules
DBPC-Cur-Chi NCs	1,2-dibehenoyl-sn-glycero-3-phosphocholine-curcumin - chitosan nanocapsules
MTT	3-(4,5-dimethylthiazol-2-yl)-2,5-diphenyltetrazolium bromide
DMEM	Dulbecco's Modified Eagle Medium
Bmit	1-buytl-3-methyl imidazolium tetrafluoroborate
CPB	Cetylpyridinium bromide
Chi	Chitosan oligosaccharide lactate
CUR	Curcumin
DNA	Deoxyribonucleic acid
DLS	Dynamic Light Scattering
EE	Encapsulation efficiency
IL	Ionic liquid
LC	Loading capacity
NCs	nanocapsules
Kp	Partition coefficient
Tm	Phase transition temperature
PC	Phosphatidylcholine
KI	Potassium iodide
RNA	Ribonucleic acid
RT	Room temperature
Ksv	Stern-Volmer constant

CHAPTER I

INTRODUCTION

A. Nanomaterials

1. Definition

Nanotechnology is a neoteric research field that is concerned with the development and production of particles, usually 1 to 100 nm in size, which are referred to as nanomaterials [1]. In 2010, upon the request of the European Commission, a new definition for nanomaterials was proposed. Liden stated the definition of nanoparticles in 3 different parts: the size distribution, the surface area and the size of the internal structural elements. Therefore, nanomaterial is a material that should meet at least one of the following criteria [2]:

- A nanomaterial consists with minimum one external dimension in the range of 1-100 nm for more than 1% of their number size distribution.

- A nanomaterial having a size smaller than 1 nm should have a specific surface area larger than 60 m^2/cm^{-3}.

- A nanomaterial has an internal or surface structure in the size range between 1-100 nm.

2. Classifications of nanoparticles

Nanoparticles are often classified based on three different criteria. They can be classified either by their origin (natural or anthropogenic), by their size (1-10 nm, 10-100

nm or larger than 100 nm) and by their chemical composition (inorganic substances, organic substances or element of the living kingdom) [3].

Examples of nanoparticles include metallic nanoparticles, metal oxide nanoparticles, micelles, dendrimers, nanocapsules, etc.

By definition, nanocapsules consist of nano-vesicular system designed in a shell-core model. They gained a lot of interest due to their use as drug delivery systems.

One instance of nanocapsules shells are liposomes.

B. Liposomes

1. Discovery of liposomes

The discovery of liposomes dates back to 1964 when Bangham and Horne described their observations by electron microscopy of the lipid phosphatidylcholine (lecithin) in water. The dispersions formed different sizes of "spherulites" which were not familiar with any known lamellar shell embracing a lipid bilayer [4].

The next year in 1965, Bangham et al. testified that ''the diffusion of univalent cations and anions out of spontaneously formed liquid crystals of lecithin is remarkably similar to the diffusion of such ions across biological membranes" [5].

Subsequently, possessing similar ions diffusion-rates as studied biological membranes, the self-assembling "spherulites" were given the name "liposomes" which is made up of two words, lipos (fat) and soma (body) [6].

2. Structure and composition of liposomes

Liposomes are spherical shaped lipid vesicles made up of phospholipids, which consist of a hydrophilic head group and a hydrophobic acyl chain. Due to the amphiphilic

nature of their lipid structure, they are built by closed membrane-like bilayers that organize concentrically around an aqueous cavity. Thus, liposomes possess a unique structural organization formed by a hydrophilic cavity in the core and a hydrophobic membrane. This special assembly allows them to encapsulate both hydrophobic and hydrophilic drugs in order to prevent them from degradation and metabolic processes, which made them a versatile tool in many biological application [7].

Phospholipids, which are the backbone of liposomes and act as the main building blocks in biological membranes, are lipids with a phosphate head group and composed of four components: the fatty acids, a glycerol or sphingosine backbone, a phosphate and an alcohol attached to it. Phospholipids differ by their head-groups, the lengths and the degree of saturation of the hydrocarbon chains.

Hence, the common alcohol head group components in the structural formula of the phospholipids includes choline, ethanolamine, glycerol, inositol and serine.

As for their sources, phospholipids can be classified as natural such as egg, soybean, rapeseed, and sunflower seed or synthetic with a unique predefined fatty acid chain or polar head group [8], [9].

Some of the synthetic saturated phospholipids with a choline head group include 1,2-Dimyristoyl-sn-glycero-3-phosphocholine (DMPC) and 1,2-dipalmitoyl-sn-glycero-3-phosphocholine (DPPC) which are used in liposomes formation and act as lipid bilayers models to study biological membranes [10].

3. *Vesicle formation*

In water and aqueous media, lipids with a low concentration are dissolved. However, as the concentration of the lipid is increased beyond a specific concentration known as the critical micelle concentration (CMC), the entropy of the interactions between water and hydrocarbon unfavorably increases which causes the spontaneous self-assembly of the lipid's molecules. In other words, the self-association of the hydrophobic acyl chains reduces the surface that is in contact with the aqueous media resulting in minimization of the energy for the formed molecular organization and relaxation of water structure driven by entropy.

This lipid organization harvests a variety of lipid architectures like micelles, bilayers, tubes, disks, liposomes, ribbons, cubic and hexagonal phases [11]–[13].

The different possible resulting structures mirror the organization of the lipids with the optimal packing. At this point, the lipids have a minimum energy where the confined head groups exert balanced hydrophobic forces and repulsive forces. These interactions are not the only governing factors that affect the resulting lipid's structure. Molecular parameters of the lipids as well as physical conditions also play a decisive role in influencing resulting structures of the lipid. These include geometrical and chemical properties, pH, salinity, temperature and pressure [14].

Hence, the interesting self-organizing of amphiphiles in aqueous media is a spontaneous process driven by and thermodynamic as well as by their molecular structure. A first attempt to relate the curvature of the formed membrane to the molecular structure of lipids was described in 1976 by Israelachvili et al. who introduced the concept of molecular packing parameter (P) which is known as the P value. (P) is defined in equation 1 by the

ratio between the volume occupied by the hydrophobic tails (*v*) with respect to their length (*l*) and the surface of the polar head group (*a*):

$P = v / l \cdot a.$

Subsequently, the lipid displays a cone-like shape when P<1/3 and will pack into micelles. For 1/3<P< ½, the lipid exhibits a truncated cone shape and will form cylindrical micelles. When 1/2 < P ≤ 1, the lipid adopts a shape between a truncated cone and a cylinder and will form vesicles or lamellar bilayers. Lastly, for P>1, the lipid has an inverted truncated cone shape and will pack into micelles [15], [16].

In that sense, lamellar bilayers form liposome structure by a spontaneous vesiculation process which has been defined to be a multi-step process beginning with the formation of the lamellar bilayers that will bend upon growing above a critical dimension. This is driven by the minimization of the energy at their edges by forming enclosed vesicles [17].

.

4. *Classification of liposomes*

Due to the several possibilities in modulating their physiochemical and structural properties, liposome can be classified into a wide number of categories, which offers them the probability to surpass other colloidal carrier systems. This flexibility in the properties of liposomes offers the ease for researchers to be fine-tuned towards specific applications. That being said, liposomes are classified based on structural parameter, physical properties and composition or sensitivity.

a) <u>Structural parameters</u>

Considering structural parameters, liposomes are categorized depending on the number of membrane bilayers (lamellae) and the size of the vesicle. The size of the liposomes could vary between 0.025 to2.5 µm.

Unilamellar liposomes have gained the main attention in research owing to their easy preparation and the ease in understanding the properties of their membrane. They are single-bilayer vesicles that are divided into three subtypes. Vesicles that are smaller than 100 nm are name small unilamellar vesicle (SUV). Vesicles ranging from 100 nm to 1 µm are called large unilamellar vesicles (LUV). Larger than 1 µm, the vesicles are called giant unilamellar vesicles (GUV).

Unilamellar vesicles have been the mostly investigated in many areas where the ones smaller than 200 nm are the most studied and of special interest in their usage for drug delivery pharmaceutical applications. The GUVs are typically used as basic models for biological membranes. In addition to the unilamellar liposomes, larger structures can also be formed from the assembly of many bilayers. These are described as oligolamellar vesicles (OLV), multilamellar vesicles (MLV) and multivesicular vesicles (MVV).

The drawback for these multi-lamellar vesicles is that their physical properties changes make them behave in different ways which render them less explorable as compared to the unilamellar liposomes [18]–[20].

b) <u>Liposomes composition and function</u>

Taking into description the surface functionalization of liposomes, they can be differentiated from each other and accordingly have different features which lead to a variety of applications.

On this basis, liposomes are classified into four subgroups: cationic, conventional, stealth and targeted.

Indeed, cationic liposomes have a positive net charge on the vesicle which renders this subgroup to be used as genetic delivery systems, as they form stable complexes with the negatively-charged DNA/RNA molecules [21].

On the other hand, the simplest liposomes are the conventional liposomes which are composed by a mixture of neutral or negatively charged surfaces, without any modifications, making a bilayer enclosing aqueous inner core in which a variety of drugs molecules can be incorporated accordingly [22].

Another subgroup is represented by the stealth liposomes, sometimes called stearic liposomes or long-circulating liposomes. This type of liposomes if coated with a layer of the hydrophilic molecule polyethylene glycol (PEG) chains, it will be attached via covalent bonds to the surface of the phospholipids. This formulation decreases the fast clearance of the liposomes from the body along with protecting it from destabilization [23].

Moving on to the last subgroup, target liposomes, as their nomenclature holds, have their surface functionalized by a ligand which is directed towards a specific receptor. This is usually achieved by attaching to the phospholipid's membranes an antibody, the reason why they are sometimes referred to as immuno-liposomes [24].

5. *Stability of liposomes*

Taking into considerations the pharmaceutical attentions, drugs that need to be delivered should be appropriately stable for at least 1 year of storage. Hence, liposomal carrier systems have to fulfil this criterion. At this level, the main issues addressed are the chemical and physical stability of phospholipid, especially phosphatidylcholine liposomes as they are the most used type.

a. Chemical stability

The shelf life of liposome might be limited by two degradation processes: oxidation and hydrolysis.

In the beginning, oxidation of phospholipids primarily happens in unsaturated fatty acyl chain. However, at high temperature, saturated chains can also be oxidized. The oxidation takes place through a free radical chain mechanism. Unsaturation induces delocalization of the unpaired electron along the acyl chain which explains why unsaturated fatty acids are the most prone to radical formation. To prevent oxidation, storage of liposome at low temperatures and in a dark place and protection from oxygen exposure are the most practical ways to apply. Furthermore, the use of antioxidants like a-tocopherol and butyl hydroxy toluene was suggested.

In what concerns hydrolysis, it's affected by the pH, ionic strength, solvent system and buffered species [25]–[27].

b. Physical stability

When hydrated in water, liposomes vesicles are spontaneously formed with varying sizes. As they are kept in storage, the formed vesicles aggregate with time, which lead to an increase of the size, which is thermodynamically favored. This phenomenon risks the encapsulated drug to leak, resulting in destabilization of the liposomal drug formulation. For that, it's necessary to assess the physical stability of any formulation before storage by measuring the size, size distribution and morphology of the vesicles [28].

6. Methods for liposome preparation

Since the groundbreaking discovery by Bangham that phospholipids dispersions in aqueous media form enclosed membranes, several potential methods have been widely outlined in the literature for the preparation of liposome. The choice of the right method influences both the size and lamellarity of the resulting vesicle.

Most of the procedures to prepare liposomes involve four basic stages starting with the formation of a dry lipid film out from an organic solvent followed by hydration of the thin film in aqueous solution. Then after purifying the resulting liposome solution, the product is analyzed [29].

Two essential methods are usually used to prepare liposomes: passive loading and active loading techniques.

The former technique consists of three different methods: mechanical dispersion, solvent dispersion and detergent removal method [30].

21

Mechanical dispersion method	Solvent dispersion method	Detergent removal method
• Sonication • Extrusion • Freeze-thawed liposomes • Lipid film hydration • Micro-emulsification • Membrane extrusion	• Ether injection • Ethanol injection • Reverse phase evaporation method	• Dialysis • Detergent removal of mixed micelles (absorption) • Gel permeation chromatography • Dilution

7. *Liposomes application*

Since their early discovery, liposomes were initially proposed as models of biological membranes. Few years later, Gregory Gregoriadis extended their future utility by launching the idea that they can entrap molecules, outlining by such their potential as carriers' systems in multiple fields [31]. This was owed to their structure special organization, their biocompatibility, their non-immunogenic nature as well as being biodegradable. All of these potential features of liposomes have positioned them to be an astonishing versatile tool in a vast range of scientific disciplines.

a. Topical liposomes drug

Due to the similarity between natural membrane and the liposome bilayer structure, liposomes have been used for skin treatment applications. This is achieved by the

capability of the lipid vesicle to modify the fluidity of the cell membrane and by such to merge in the dermatological field and showing moisturizing and restoring actions [32].

b. Cosmetic applications

Liposomes were also utilized to deliver ingredients in cosmetics. In 1986, Christian Dior lunched on market the first liposomal cosmetic product, the anti-ageing cream Capture. In addition, liposomes have been used to treat hair loss in products like "Regaine". The skin care profile of liposomes was valued by its ability to slow the transdermal water loss as well as by its suitability to treat dry skin [29], [33].

c. Anti-cancer activity

Liposomes attracted distinguished clinical acceptance and was recognized as chief platform for drug delivery in 1995 after the first liposomal anti-cancer drug "Doxil" have been approved by FDA [34].

Several studies have shown that the encapsulation of various anticancer agents in liposomal formulations has lower toxicity than the free drug itself without hindering its efficacy. Moreover, the great advantage offered by liposomes is their ability to functionalize their lipid membrane by attaching several target ligands which makes them targeted towards specific sites only, reducing by such the toxic side effects of the loaded drug. Liposomes usage is based on their ability to adapt the entrapped drug which becomes reliant only on the physiochemical properties of the liposomes resulting in enhancement in the penetration inside the targeted tissues.

That being said, liposomes improve the stability, efficacy and therapeutic index of the drug. Besides the mentioned advantages, liposomes are also able to reduce the contact between sensitive tissues and toxic drugs [35], [36].

d. Anti-inflammatory activity

Sterically stabilized liposomes may be an operative delivery system to deliver suitable drugs for inflammations treatment. In fact, infectious agents mostly exist in cells that are nearly inaccessible to chemotherapy like deep-tissue macrophages. Hence, a large fraction of stealth liposomes will accumulate in the skin, where many are eventually taken up by macrophages. It is thought that these cells host many bacterial and viral infections which long circulating liposomes can target [37].

One of the major drugs that is used in different field, and can be easily encapsulated into liposomes is curcumin.

C.   Curcumin

1. Origin

Curcumin, a natural chemical, was named in 1815 when Vogel and Pelletier testified the first isolation of a "yellow coloring-matter" from the rhizomes of *Curcuma Longa*. *C. longa*, native to tropical South Asia and India, is a perennial herb belonging to the Zingiberaceae family. The roots (rhizomes) of this plant are dried and crushed to obtain a powder golden spice generally known as turmeric[38], [39].

India is the primary producer of turmeric where it is extensively used in culinary activities. In Europe, turmeric was named "Indian Saffron" because of its color and taste. In addition to its utilization in food preservation, food coloring and food flavoring, turmeric has been also valued for its therapeutic activities such as it was used to cure jaundice, to heal wounds, to help with stomach problems, and most importantly it possesses anti-inflammatory properties to heal chest pains, colic and menstrual difficulties [39].

Turmeric contains many phytochemicals like the curcuminoids which happen to be its major polyphenolic compounds. The curcuminoids consist of curcumin, demethoxycurcumin and bis-demethoxycurcumin (See Figure 1). Curcumin is the main bioactive component of the three curcuminoids. Estimated to constitute 70%, curcumin is responsible for both the color and therapeutic effects of turmeric [40]. Curcumin acquired popularity and got nicknamed as 'next generation multipurpose drug' due to its many-sided roles, such as antioxidant, anti-inflammatory, anticancer, antidiabetic, antiangiogenic and antimicrobial activities [41]–[45].
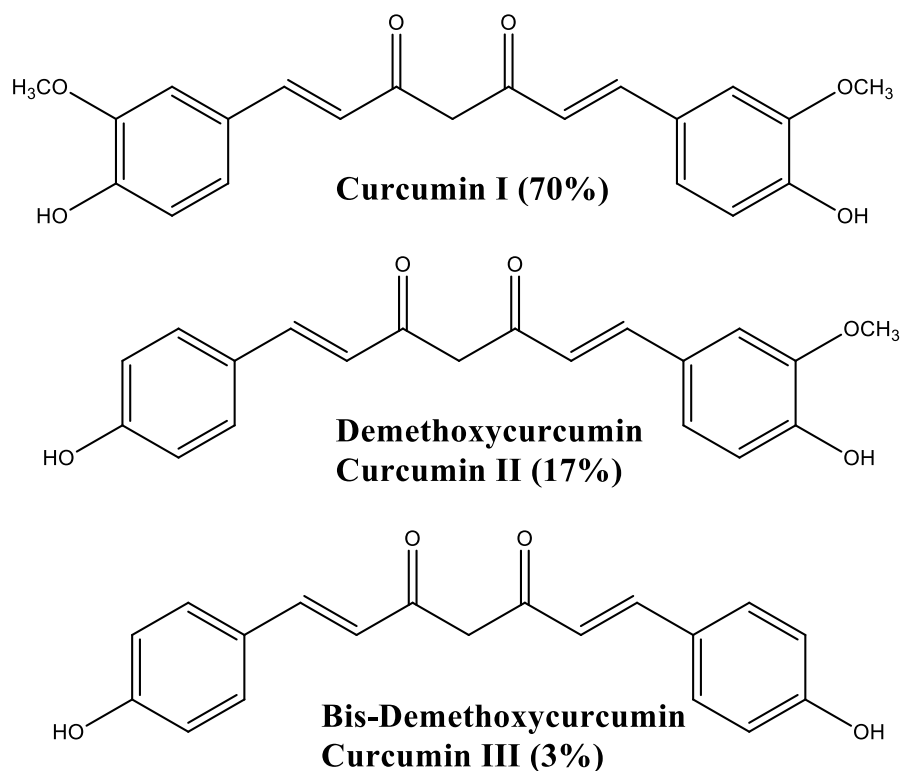
Figure 1 Major components of curcuminoides.

2. *Discovery of curcumin*

After the discovery of the yellow substance in 1815, it was later found to be a mixture of turmeric oil and resin. Then, it was until 1842 that Vogel got a preparation of pure curcumin.

The isolation of curcumin from turmeric was described by Perkin and Everest as follows: "*Pelletier and Vogel's method of isolating the curcumin consisted in first removing the fatty, resinous, and other impurities by extracting pulverised turmeric with water and carbon disulphide, then dissolving out the colouring matter with boiling alcohol, and purifying it by successive solution in ether and alcohol, precipitation with lead acetate,*

26

and subsequent treatment with hydrogen sulphide and extraction of the product with ether. It was thus obtained as an amorphous yellow powder." [46].

Vogel's product was liquid at 40°C and not pure, thus any proposed formula would have been incorrect which is why even though he offered elemental analysis data for his curcumin, he did not submit a molecular formula [47].

Afterward, several chemists described different possible structures for curcumin and after about half a century in 1910 that Lampe and Milobedska structurally identified the chemical structure of curcumin [48]. Three years later, the same group synthesized the compound [49]. After that in 1953, chromatography was used by Srinivasan to quantify and separate the components of curcumin [50].

3. *Chemistry of curcumin*

a. <u>Structural properties</u>

Diferuloylmethane is synonym of curcumin and 458-37-7 is its CAS number [51]. The IUPAC name of curcumin is (1*E*,6*E*)-1,7-bis(4-hydroxy-3-methoxyphenyl)-1,6-heptadiene-3,5-dione, with molecular formula $C_{21}H_{20}O_6$, and molecular weight of 368.38 Daltons [52].

In chemical terms, it's a symmetrical molecule composed of a chain of seven carbons that links two aromatic rings [53]. This special structure of curcumin makes it belong to the diarylheptanoid family. Moreover, curcumin has owned several functional active groups: a keto-enol moiety, two o-methoxy phenolic groups and two enone moieties.

Another chemical nomenclature for curcumin is bis-α,β-unsaturated β-diketone. Hence, the presence of carbonyl groups on the carbon number 3 and 5 in heptadienone

chain causes curcumin to exhibit a keto-enol tautomerism and a cis-trans isomerism which is dependent on the pH of its environment [54].

 The keto-form dominates at acidic pH. This is due to the highly active carbon atom in heptadienone chain that links the two methoxyphenol rings, which potentially donates its H-atom. The oxygens adjacent to this carbon have unpaired delocalized electrons which renders the C-H bond very weak. In contrast, as pH increases above 7, the enol-form becomes dominant as the phenolic part of curcumin donates electrons. The resonance-assisted in the enol form stabilizes the structure. However, both forms coexist in equilibrium under physiological conditions [55], [56] (See Figure 2).
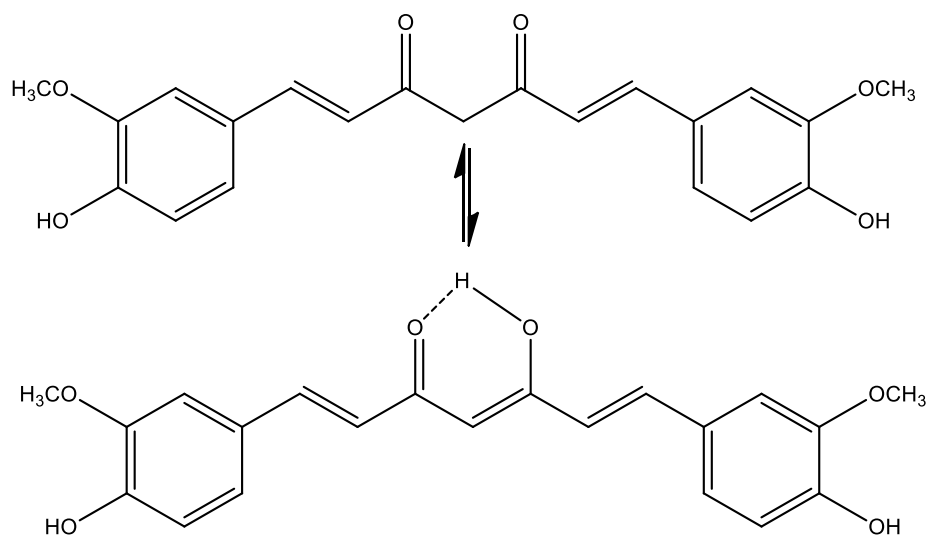
Figure 2 Tautomerization of curcumin.

Curcumin tautomerism is important as it plays a crucial role in its biological activities. For instance, in Alzheimer disease, the principal pathological feature is the formation amyloid beta (Aβ) aggregates. The anti-Alzheimer effect is exerted by curcumin

as it binds to these aggregates. Yanagisawa et al found that the binding activity of the keto form was much weaker than that of curcumin with the enol form [57].

b. Physical Properties of Curcumin

Three different pKa values have been reported for curcumin; pka_1 and pka_2 values are attributed to come from the two phenolic -OH groups, and pka_3 is from the enolic proton [58], [59].

Curcumin's melting point was determined to be equal to is 183°C [51]. It is a crystalline lipophilic polyphenol practically insoluble in water while being highly soluble in polar organic solvents such as ethanol and methanol but sparingly soluble in alicyclic and aliphatic organic solvents like cyclohexane and hexane. However, its solubility in water can be enhanced in alkali or extremely acidic medium, but it remains low to negligible at acidic and neutral pH [60], [61].

c. Stability of Curcumin

i. Aqueous stability

Aqueous media refers to the alkaline or acidic and biological media. Hence, the stability of curcumin depends on the pH of the media, which is demonstrated by change of the color of curcumin solution when pH is varied.

Accordingly, at very low pH <1, the protonated form dominates which results in a red color curcumin solution. In the 1-7 pH range, most of curcumin molecules are in their neutral form which gives a yellow color solution. For pH values > 7, curcumin solutions have an orange red color [62].

29

The kinetic degradation of curcumin was considered in several buffer systems at different pH. The results indicated that curcumin is unstable at neutral pH where it undergoes hydrolyzation to form smaller products as it degraded within 30 mins in phosphate buffer of pH 7.4. The study concluded that as pH increases, the degradation rate of curcumin similarly increases [63].

ii.   Spectral and Photophysical stability

Several studies were conducted to study the stability of curcumin in organic solvent as it possesses a very low solubility in aqueous media. The optical absorption for curcumin is solvent dependent and located between 408-430 nm, whereas its emission maximum when it's in his exited state ranges from 460 and 560 nm. It was concluded from different studies the rate of fluorescence decay and the acidity of the solution are directly proportional as well for the polarity of the solvents. That was illustrated when the fluorescence-decay spectra of curcumin were found to be much significant in methanol than in hexane.

Similarly, a bathochromic shift in the fluorescence maximum was noted when going to hexane from methanol, indicating a very polar excited state for curcumin [64]–[66].

iii.   Photochemical stability

An intensive study conducted by Tonnesen et al. [62] has investigated the photodegradation products of curcumin dissolved in isopropanol and then four other organic solvents: methanol, chloroform, ethyl acetate, and acetonitrile. After exposing the

solvent-curcumin solution to light (λ= 400–510 nm) for 4 h, the obtained degradation products were extracted by TLC and identified using mass spectrometry (MS) and nuclear magnetic resonance.

A compound that had the chemical composition $C_{12}H_{18}O_6$ was the main product resulting from the degradation of curcumin in isopropanol, chloroform and methanol and having a molecular ion at m/e = 366. This result reflects that the structure has lost two hydrogen atoms and that light irradiation induced a cyclization process.

In addition, other minor degradation products of curcumin were recognized like vanillic acid, vanillin, ferulic aldehyde and 4-vinylguaiacol.

In a second study, it was found that curcumin in dried form was more stable when exposed to sunlight than in solution [67].

These photochemical properties of curcumin are the reason behind storing curcumin in a brown glass as it transmits light of wavelengths higher than 500 nm at which curcumin has no absorption [68].

iv.   Thermal stability

After being exposed for 10 mins and up to 70°C, curcumin has been stable. However, above this temperature, it begins degrading. At 100°C, its rate of degradation increases as reflected by the drop in its absorbance value [69].

4. Safety profile of curcumin

Curcumin has been permitted to be a safe substance by Food and Drug Administration (FDA). Its safety was assessed by several studies. The maximum daily intake dose varies by ranging from 3 mg to 4-10 g per 1 kg body weight [70].

The safety of curcumin was tested in a clinical study where healthy subjects were administrated two different doses of curcumin: 8000mg and 12000 mg in a day. As a result, low levels of curcumin were detected only in the subjects who took the higher dose of curcumin. In addition, none of the subjects developed any side effects upon taking curcumin. Hence, a daily intake of 12 000 mg was regarded safe for healthy people [71].

As for individuals having health issues as cardiovascular diseases and cancer, a dose of up to 8000 mg/day was observed to be safe. In another study, mild and controllable gastrointestinal symptoms, headache and nausea were reported for subjects affected by primary sclerosing cholangitis taking up a dose of 1400 mg/day while consumption 8000 mg/day caused abdominal pain for patients with advanced pancreatic cancer and taking a prescription of gemcitabine [72].

5. Bioavailability of curcumin

The safety of curcumin consumption has been testified by several studies but unfortunately, its therapeutic use is limited by its very low bioavailability. Having low bioavailability means that its free levels in plasma and tissues is very low. This was explained by the fact that curcumin has a high-rate conjugation through sulfation and glucuronidation which causes its low absorption [73].

This drawback of curcumin limits its concentration in the gastrointestinal zone and its bioactivities such its potential as antitumor [74].

To overcome the poor bioavailability of curcumin and thus enhance its delivery, several studies have addressed different strategies such as incorporating curcumin into liposomes and phospholipids [75], surfactants [76], polymeric nanoparticles [77], polyethylene glycol [78] and cyclodextrin complexation [79].

6. *Pharmacological activities of curcumin*

Worldwide, curcumin is being used in many different forms for multiple potential health benefits. It is available in different forms such capsules, soaps, tablets, cosmetic, energy drinks and ointments [80].

Ever since curcumin has been identified, multiple pharmacological activities have been reported out of which few will be illustrated below including anti-cancer, anti-bacterial, anti-diabetic, anti-inflammatory and antioxidant activities.

a. <u>Anti-cancer effect</u>

Different studies have been done to show the selectivity of curcumin to tumor cells compared to normal healthy cells which boarded its usage for cancer treatment. Feng et al. reviewed the therapeutic effect of curcumin in several types of cancer including lung, cervical, prostate, breast, osteosarcoma and liver cancers[81].

Curcumin exerts its anti-cancer activities through its action on some of the biological pathways related to mutagenesis, oncogene expression, cell cycle regulation, apoptosis, tumorigenesis and metastasis. In fact, curcumin has been shown to regulate cell

33

proliferation and to act as an inhibitor of the NF-κB transcription nuclear factor which is an active player in human cancers. Moreover, curcumin influences multiple receptors of growth factor as well as cell adhesion molecules that engage in tumor growth [82].

Pancreatic cancer is responsible for approximately 6% of all deaths caused by cancer for men and women [83]. It was shown that in pancreatic cancer cells, curcumin inhibit the growth of the tumor by suppressing the expression of NF-κB factor and growth control molecules that are produced by NF-κB [84].

A phase II clinical trial was performed on subjects with advanced pancreatic cancer who received 8g of curcumin during 8 weeks on a daily basis. Despite its poor bioavailability, the expression of the NF-κB was down regulated by curcumin. One out of two patients had 73% tumor decrease after curcumin administration. It was found that curcumin is tolerable and non-toxic for 18 months. The study concluded that oral curcumin has a well-tolerated biological activity in some patients with pancreatic cancer despite its poor absorption. Oral curcumin is well tolerated and, despite its limited absorption, has biological activity in some patients with pancreatic cancer [85].

b. Anti-inflammatory effect

Inflammation has been linked to the development of many chronic diseases and conditions including Alzheimer, Parkinson's, epilepsy, cancer, allergy, asthma, diabetes, obesity and depression. In most diseases, the major mediator of inflammation is the tumor necrosis factor (α-TNF) and this is controlled by the activation of NF-κB. Accordingly, substances that downregulate NF-κB have a potential success in treating such diseases. It

has been proved that curcumin block NF-κB activation and by such suppresses inflammation [86].

A study considered this therapeutic activity of curcumin against cyclooxygenase-I (COX-I) and cyclooxygenase-II (COX-II) enzymes. These enzymes are known to produce an agent that promotes imflammation. Curcumin, at a concentration of 125 μg/ml, inhibited COX-I enzyme by 32% and COX-II enzyme by 89.7% [87].

c. <u>Anti-oxidant effect</u>

During natural cellular processes like cellular respiration, reactive oxygen species (ROS) are normally formed like superoxide radical ($O^{\bullet-}_2$), hydroxyl radicals ($OH^{\bullet}$), singlet oxygen ($O^{\bullet}$) and H_2O_2) [88].

The overproduction of ROS results in the oxidation of the components of cells which thereby provokes damage in the affected tissues. The damage caused by ROS can be attenuated by the human body's antioxidant defense systems such as superoxide dismutase (SOD), reduced glutathione (GSH), catalase (CAT) and others [89]. Sankar and his collaborators illustrated the ability to indirectly induce the upregulation of the antioxidant enzymes like CAT and SOD[90].

d. <u>Anti-diabetic effect</u>

Curcumin's potential therapeutic effect has been testified in different studies to manage diabetes mellitus via its hypoglycemic, hypolipidemic, antioxidative and anti-inflammatory effect[91]. Kim and his colleagues performed a study in which the glucose-lowering effect of curcumin was credited to its capability in reducing the hepatic glucose

output [92]. In addition, curcumin was also responsible for the reduction of the diabetic

complications such as diabetic retinopathy [93].

e. Anti-bacterial effect

In a study published by Ribeiro et al., the collected data exposed the antibacterial

activity against both *methicillin-sensitive S. aureus* (MSSA) and *methicillin-resistant S.*

aureus MRSA [94], [95].

Alongside its potential against *S. aureus*, curcumin has a remarkable action against

other bacteria including *Enterococcus faecalis, Bacillus, P. aeruginosa, E. coli,* and *K.*

pneumonia [96].

D.   Aims

General information about the two essential components; liposome and curcumin;

used in our research work, were introduced in Chapter I. Hence, our focusing will be on the

synthesis of liposomal curcumin and further establishing their properties and applications.

The synthesis of liposomes and liposomal curcumin is performed based on the thin

film method as it is described in Chapter II. Hence, two different liposomes are investigated

in our work; DAPC and DBPC liposomes.

 In Chapter III, we will highlight the effect of curcumin of the physical properties

of DAPC liposomes. Meaning that, curcumin will be used a fluorescence probe to check its

effect on the permeability of the liposomes membrane.

Furthermore, DBPC liposomes, having a longer chain than DAPC will be

investigated in our work. Initially, the physical properties of DBPC will be elaborated in

Chapter IV using curcumin as a fluorescence molecule. Phase transition temperature, quenching and partition coefficient will be studied.

An ionic liquid (IL) is a salt in the liquid state; Ionic liquids have many potential applications. In fact, they can alter the physical properties of the liposomes. For this reason, the effect of ionic liquid on the partition coefficient of DAPC and DBPC will be developed in Chapter V.

Moreover, curcumin and liposomes exhibit an anti-cancer activity. Hence, this activity can be enhanced when encapsulating curcumin into the liposomes with the addition of polymer. For this reason, in Chapter VI, the formed DAPC liposomal curcumin nanocapsules will be tested as anti-cancer agent against MCF-7 breast and Capan-1 pancreatic cancer cells in the presence and absence of polymer.
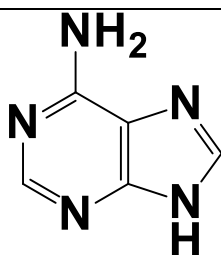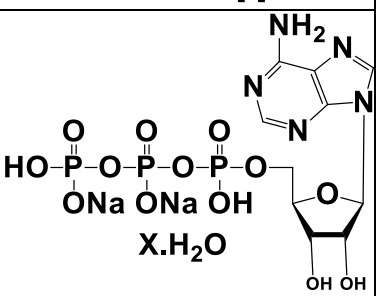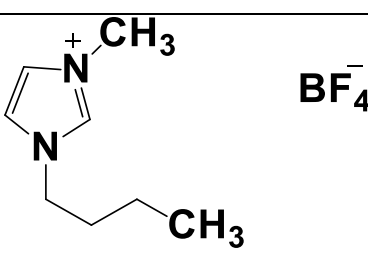
Ribonucleic acid (RNA) is a polymeric molecule indispensable in many biological fields as coding, decoding, regulation and expression of genes. RNA is constituted 4 nucleotides inducing nucleic acids. Along with lipids, proteins, and carbohydrates, nucleic acids constitute one of the four major macromolecules essential for all known forms of life. For this reason, in Chapter VII we will establish the effect of DBPC liposomal curcumin nanocapsules in the presence and absence of polymer as nanoprobe to detect RNA. The detection of RNA will be done using fluorescence emission intensity. The selectivity and the recovery of the method will be also investigated.
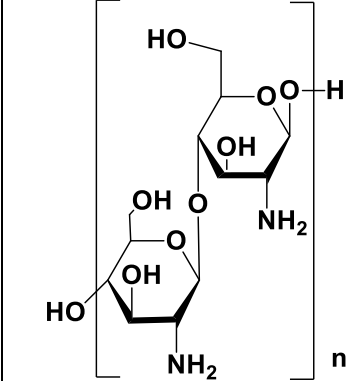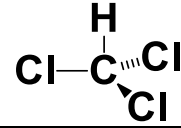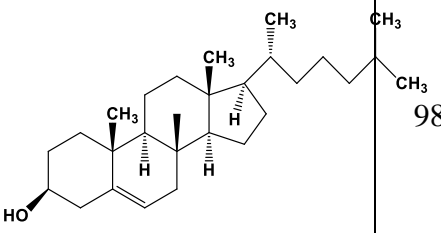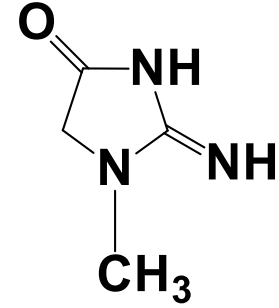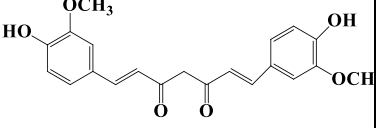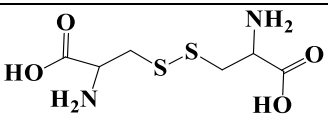
CHAPTER II
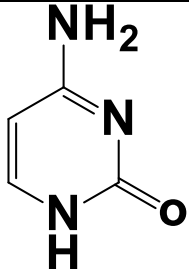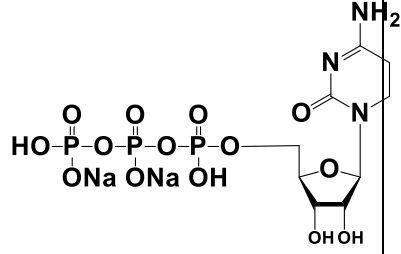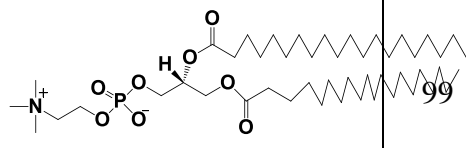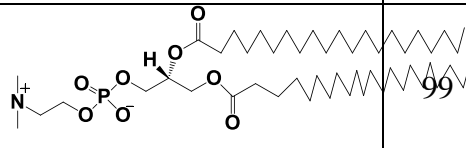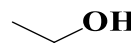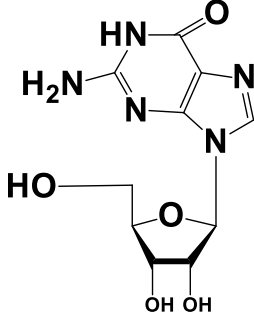
MATERIALS AND METHODS

A.   Materials

All the chemicals that were used in our research work are presented in Table 1

with their respective chemical formula, chemical structure, purity and source.

Nomenclature	Chemical formula	Chemical structure	Purity (%)	Source
Adenine	$C_5H_5N_5$		99	Sigma Aldrich
Adenosine 5′-triphosphate disodium salt hydrate	$C_{10}H_{14}N_5Na_2O_{13}P_3$ xH_2O		99	Sigma Aldrich
1-buytl-3-methyl imidazolium tetrafluoroborate	$C_8H_{15}BF_4N_2$		97	Sigma Aldrich

Chitosan oligosaccharide lactate	$C_{12}H_{24}N_2O_9$		98	Sigma Aldrich
Chloroform	$CHCl_3$		98	Merck
Cholesterol	$C_{27}H_{46}O$		98	Sigma Aldrich
Creatinine	$C_4H_7N_3O$		97	Merck
Curcumin	$C_{21}H_{20}O_6$		99	Sigma Aldrich
Cystine	$C_6H_{12}N_2O_4S_2$		98%	Merck

Cytosine	$C_4H_5N_3O$		98	Sigma Aldrich
Cytidine 5′-triphosphate disodium salt hydrate	$C_9H_{14}N_3Na_2O_{14}P_3$			Sigma Aldrich
1,2-diarachidoyl-sn-glycero-3-phosphocholine (DAPC)	$C_{48}H_{96}NO_8P$		99	Avanti-Polar
1,2-dibehenoyl-sn-glycero-3-phosphocholine (DBPC)	$C_{52}H_{104}NO_8P$		99	Avanti-Polar
Ethanol	CH_3CH_2OH		99	Sigma Aldrich
Guanosine	$C_{10}H_{13}N_5O_5$		99	Sigma Aldrich

Guanosine 5′-triphosphate disodium salt hydrate	$C_{10}H_{16}N_5O_{14}P_{3.x}Na^+$		99	Sigma Aldrich
1-Hexadecylpyridinium bromide (CPB)	$C_{21}H_{38}BrN$		99	Acros
Potassium iodide	KI	$K{-}I$	98	Sigma Aldrich
Thiazolyl Blue Tetrazolium Bromide	$C_{18}H_{16}BrN_5S$		99	Sigma Aldrich
Thymidine 5′-triphosphate disodium salt hydrate	$C_{10}H_{17}N_2NaO_{14}P_3$		99	Sigma Aldrich
Thymine	$C_5H_6N_2O_2$		98	Acros
Uracil	$C_4H_4N_2O_2$		99	Sigma Aldrich
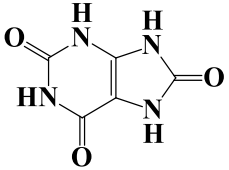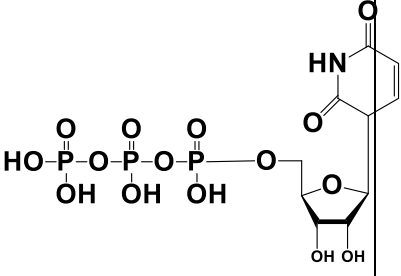
Uric acid	$C_5H_4N_4O_3$		98	Sigma Aldrich
Uridine 5′-triphosphate disodium salt hydrate	$C_9H_{15}N_2O_{15}P_3$		99	Sigma Aldrich

Table 1 List of chemicals used

B.   Sample preparation

The preparation of liposomes was done as described in Figure 3.

DAPC and DBPC liposomes' solutions were prepared by the classical solvent evaporation method. To obtain a 1 mM stock solution of each liposome, 4.231 mg of DAPC and 4.5 mg of DPBC were dissolved separately in a 5 mL chloroform/ethanol mixture with a 1:1 volume ratio. After vortex for few seconds, a rotary evaporator was used to evaporate the solvents at 35-40 ∘C. The thin films formed were dried under oven vacuum at 45∘C for 10 min. Then, 5 mL of phosphate buffer at pH = 7 was added to dissolve each film. During 5 min, the mixtures were alternatively vortexed for 30 s, and then heated for another 30 s at 75°C or 85°C for DAPC and DBPC respectively, 10°C above the phase transition temperature.

For some experiments, curcumin was incorporated into liposomes during its formation to obtain liposomal curcumin nanocapsules. For that purpose, after dissolving

0.184 mg of curcumin in 1:1 ratio of 1 mL ethanol/chloroform solution, the solution

obtained is mixed with the liposome's solution after vortex, and the organic solvents were

evaporated using Rotary evaporator similarly to the procedure explained above. A yellow

thin film is obtained which is then hydrated with 6 mL of the pH=7 phosphate buffer.

Likewise, the mixtures were dissolved at 10°C above the phase transition temperatures of

each liposome.
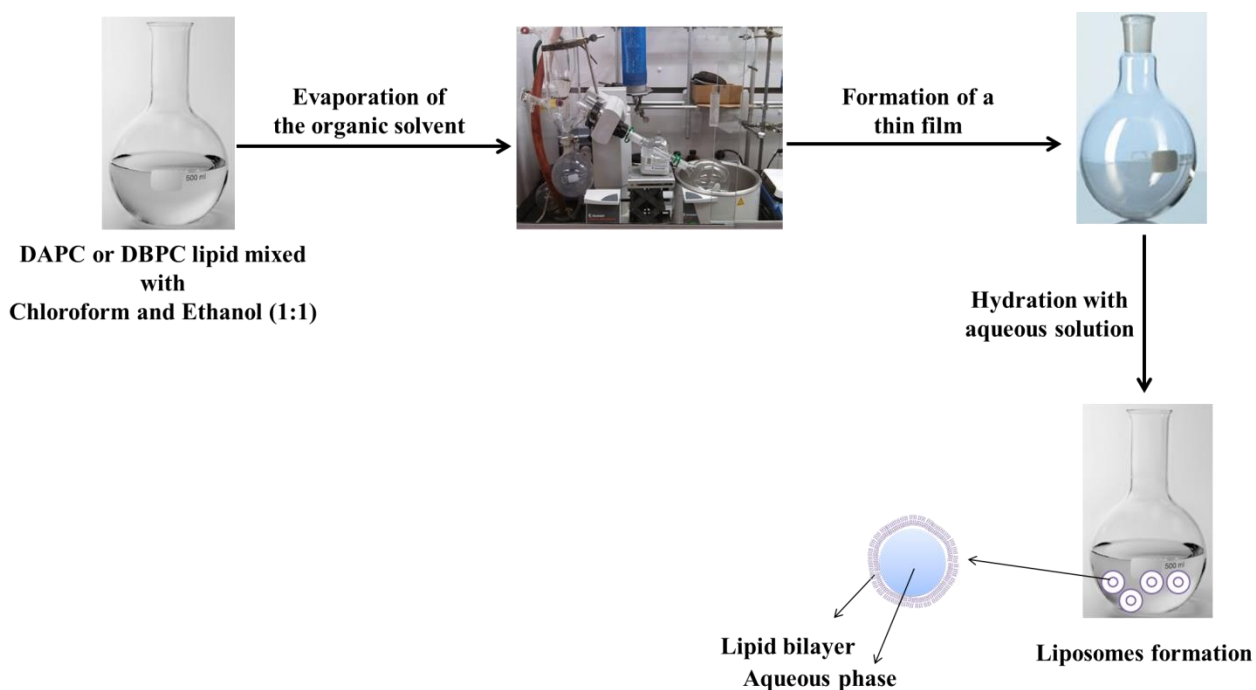
Figure 3 Schematic illustration of the liposome's preparation.

C.   Instrumentation

Scanning electron microscopy (SEM) analysis was done using a Tescan, Vega 3

LMU with an Oxford EDX detector (Inca XmaW20). The accelerating voltage was 5 kV

with a magnification of 500 nm. In short, few powder of liposomal curcumin nanocapsule

solution were deposited on an aluminum stub and coated with carbon conductive adhesive tape.

Zeta potential and dynamic light scattering value were measured using Particulate systems, NanoPlus Zeta Potential/Nano Particle analyzer.

The absorption spectra were recorded at room temperature using a JASCO V-570 UV-VIS-NIR spectrophotometer in the wavelength range of 200–800 nm in a 3 mL cuvette.

Fluorescence spectrum was measured using a Jobin-Yvon-Horiba Fluorolog III fluorometer and the FluorEssence program. The excitation source was a 100 W Xenon lamp, and the detector used was R-928 instrument operating at a voltage of 950 V by keeping the excitation and emission slits width at 5 nm.

The X-ray diffraction (XRD) data were collected using a Bruker d8 discover X-ray diffractometer equipped with Cu-Ka radiation ($\lambda = 1.5405$ Å). The monochromator used was a Johansson type monochromator.

Thermo gravimetric analysis (TGA) was performed using a Netzsch TGA 209 in the temperature range of 30 to 1000 °C with an increase of 10 °C. min^{-1} under N_2 atmosphere.

D.   Application of liposomal curcumin nanoparticles

Liposomal curcumin systems have taken much importance in the biomedical field. These nanocapsules have been used essentially in drug delivery, as anti-cancer, anti-inflammatory, in sensing applications, etc. In our research work, two main applications

were carried out to inspect the efficiency and suitability of these nanocapsules. These 2 applications are:

- Anti-cancer activity of DAPC-Cur nanocapsules coated with chitosan against MCF-7 and Capan-1 cancerous cell.

- The use DBPC-Cur coated with chitosan as nanoprobes for the detection of RNA.

It is important to mention that for each application, the sample preparation is developed in its specific chapter.

CHAPTER III

INTERACTION OF CURCUMIN WITH DAPC LIPOSOMES: CHITOSAN PROTECTS DAPC LIPOSOMES WITHOUT CHANGING PHASE TRANSITION TEMPERATURE BUT IMPACTING MEMBRANE PERMEABILITY

A.   Introduction

Designed by self-association of amphiphilic lipids, liposomes form a unique spherical structure which allow them to encapsulate both hydrophilic and hydrophobic drugs [97]. Hence, they can envelop poorly soluble molecules, like curcumin, enhancing thus its solubility together with protecting it from degradation or metabolic processes [98].

The main building blocks of liposomes are phospholipids. Among all the various categories, phosphatidylcholine (PC) is the most common lipid in cell membrane and the most abundant ingredient of pulmonary surfactant, the reason why PC liposomes are widely used as a model.

1,2-diarachidoyl-sn-glycero-3-phosphocholine (DAPC), is one of the phospholipids that is present in numerous biological systems. It is a fully saturated PC lipid consisting of 20 CH_2 groups in the acyl tail [99]. Despite its biological significance most of the reported study concentrated on DPPC (1,2-Dipalmitoyl-sn-glycero-3-phosphocholine) and DMPC (1,2-dimyristoyl-sn-glycero-3-phosphocholine) liposomes, and not much work is reported on DAPC.

The use of liposomes is still restricted because they can undergo hydrolysis which results in the loss of the loaded molecules, can be oxidized and they have a short circulation half-life [100]. Coating liposomes surface with polymers, such as chitosan, was suggested as an effective approach to protect and stabilize the liposomal curcumin system.

Chitosan possesses physiochemical and biological properties which make it a promising tool for drug delivery. Being a natural hydrophilic cationic polymer derived from shellfish, chitosan possesses interesting characteristics such as pH sensitivity, biocompatibility and low toxicity. It forms a protective polyelectrolyte layer around anionic liposomes established on the electrostatic interactions, without any chemical linkage between the two components. Moreover, chitosan is considered to be biodegradable since it is metabolized by human enzymes [100],[101].

There are many reports on interaction of chitosan with DMPC/DPPC liposomes for various applications [101],[102] but to our knowledge there is no report on interaction of DAPC and chitosan oligosaccharide lactate.

Liposomal curcumin formulation has been used in many applications. It was reported that incorporating curcumin into liposomes vesicles has many advantages such as enhancing the gastrointestinal absorption and increasing the plasma antioxidant activity of curcumin [103] , having an inhibitory effect on cancer cell growth along with antiangiogenic effects [104] and boosting the loading grade in cells [105].

The fluorescence spectrum of curcumin shifts to lower wavelength by increasing its fluorescence intensity while getting incorporated into liposomes and as a molecular probe can sense phase transition temperature of liposomes. For the best of our

47

knowledge, the physical properties of different liposomes as DPPC, DMPC, DSPC etc. are widely developed and published. Nevertheless, no studies have been published and elaborated for DAPC liposomes using curcumin and effect of chitosan on DAPC liposomes.

The main aim of current work was to use curcumin as a molecular probe to investigate DAPC liposomes. DAPC has a longer hydrocarbon chain length and higher phase transition temperature compared to DMPC, DPPC and DSPC liposomes, thus, its behavior needs to be understood. This was done by observing the fluorescence intensity changes of curcumin, based on the fact that its photophysical properties depends strongly on the polarity and viscosity of its environment [105]. Moreover, the influence of chitosan on the physical properties of the liposome was also assessed.

B.   Methods of preparation

1. *Sample preparation for phase transition experiment*

For phase transition temperature study, the temperature was varied from 50℃ to 75℃. Liposome concentration in a cuvette (3 mL) was kept 100 µM with 1 µM of curcumin (See Figure 4). The volume of the solution was completed to 3 mL with buffer solution (pH = 7).

Emission spectra at λex=425 nm

100 μM with 1 μM of curcumin

Variation of the temperature between 50-75°C
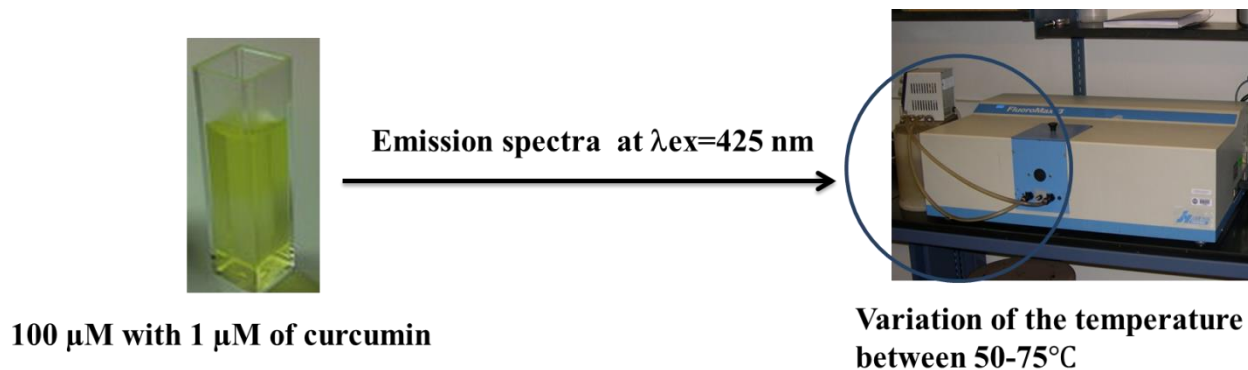
Figure 4 Sample preparation of phase transition temperature study.

In order to establish the effect of curcumin concentration, several experiments were done in the curcumin concentration of 1, 10, 15, 20 and 25 μM. The total volume was completed with a 10 mM pH = 7 buffer solution.

Moreover, the effect of chitosan was also investigated. For this purpose, 0.5 mg/mL of chitosan were added by withdrawing 300 μL from a 5 mg/mL stock solution.

2. *Sample preparation for quenching experiment*

For quenching study liposome and curcumin concentration were constant and kept at 100 μM and 1 μM respectively in all quenching studies, whereas CPB final concentration was varied from 0, 25, 50, 100, 150, 200, 250 to 300 μM in the samples.

Similarly, KI final concentration was varied from 0, 0.1, 0,2, 0.3, 0.5, 1 to 4 M (See Figure 5).

25 µM of CPB
Or
0.1 M of KI

100 µM of CPB
Or
0.3 M of KI

200 µM of CPB
Or
1 M of KI

300 µM of CPB
Or
4 M of KI

0 µM of CPB
Or
0 M of KI

50 µM of CPB
Or
0.2 M of KI

150 µM of CPB
Or
0.5 M of KI

250 µM of CPB
Or
2 M of KI

Keep undisturbed for
20 minutes

Emission spectra
at λ_{ex}=425 nm

100 µM with 1 µM of curcumin +
pH buffer solution
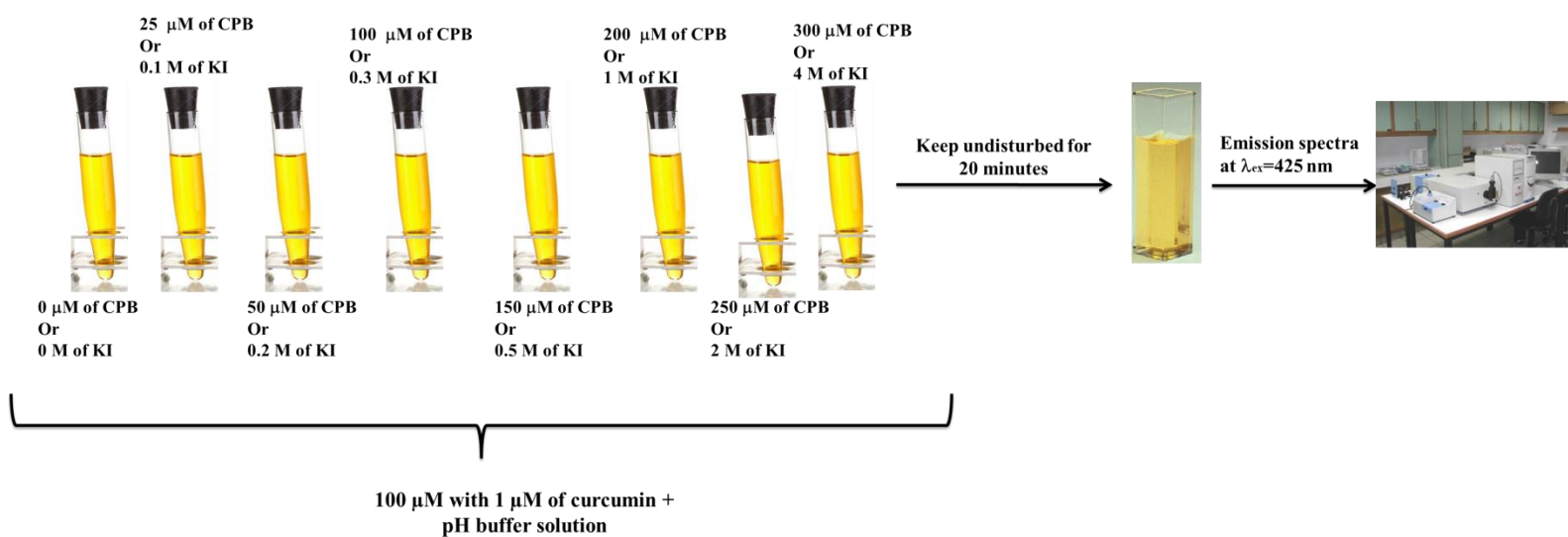
Figure 5 Sample preparation for quenching study.

For quenching study in the presence of chitosan oligosaccharide lactate, the final concentration of chitosan oligosaccharide lactate used was 0.5 mg/mL.

During measurement, the total volume was completed to 3 mL with a 10 mM pH equal to 7 buffer solution.

3. *Sample preparation for partition coefficient experiment*

For partition coefficient measurement, curcumin concentration was 1 µM in all trials. Liposomes concentration was varied from 0, 10, 20, 50, 100, 150, 200 to 250 mM. The total volume in these samples was completed to 3 mL with a 10 mM pH = 7 buffer solution (See Figure 6).
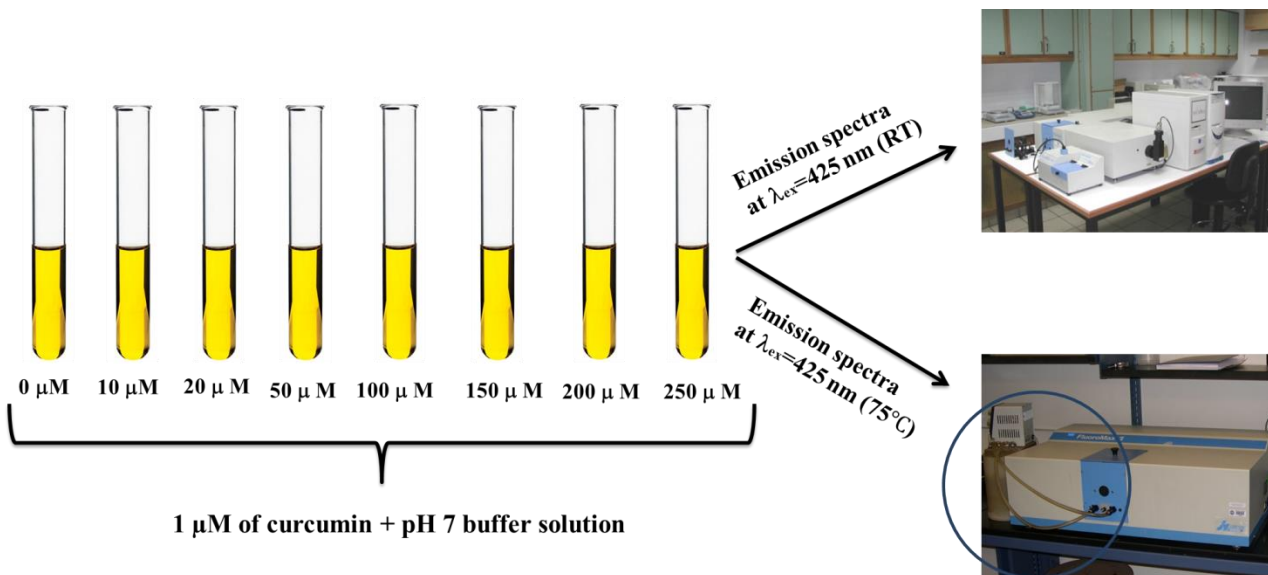
Figure 6 Sample preparation for partition coefficient analysis.

When chitosan oligosaccharide lactate was added, its concentration was also kept constant at 0.5mg/mL.

C.   Results and discussion

1. *Phase transition temperature*

The phase transition temperature (Tm) is defined as the temperature required to induce a change from the ordered gel phase to the lipid physical state. In the former, the hydrocarbon chains are fully extended and closely packed, while in the second state, the hydrocarbon chains are disordered, randomly oriented and fluid. This is due to the melting of the acyl chains in the hydrophobic core of the membrane.

For DAPC liposomes, this change occurs at around 66°C, as mentioned in Avanti Polar sheet where it's coded as 20:0 PC. (https://avantilipids.com/tech-support/physical-properties/phase-transition-temps).

In order to evaluate the effect of coating with a polymer like chitosan, the phase transition temperature was monitored in the presence and absence of chitosan.

Experimentally, the Tm was determined by adding curcumin to the liposome's solution or to the liposomes-chitosan solution, and measuring the fluorescence emission spectrum of the resulting mixture with increasing of the temperature.

a) Effect of curcumin concentration

The phase transition temperature for DAPC is not yet established. However, a normal phase transition experiment starts with an increasing in the emission intensity, until it reaches a maximum, then it decreases again. Hence, the maximum obtained reveals the Tm temperature of the liposome [99], [106].

Figure 7A shows the change in the fluorescence emission intensity of 1 μM curcumin in DAPC liposomes as a function of temperature. Obviously, the fluorescence emission intensity increased with temperature to a maximum at the phase transition temperature, then after Tm, the intensity decreased continuously.
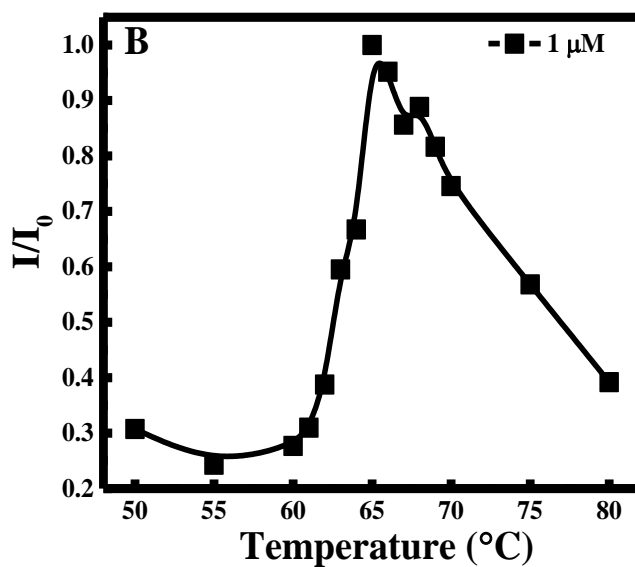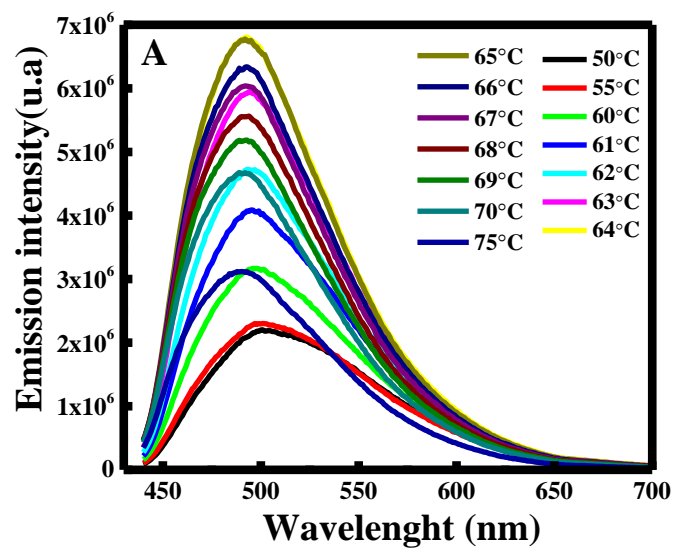
Figure 7 (A) Fluorescence emission spectra of 1 µM curcumin in DAPC membrane at various temperatures and (B) Normalized fluorescence emission intensity of 1 µM curcumin in DAPC membrane.

This change in the emission intensity is easily observed in Figure 7B when plotting I/I_0 ratio versus the temperature. Hence, as depicted in Figure 7B, the phase transition temperature measured for DAPC liposomes is in this case 65 °C, which is very close to the value reported in Avanti Polar.

This observation can be associated to two factors running against each other: the changes in the permeability of the DAPC liposomes and the viscosity of the solvent. Below the Tm, the system is shifting from the dense solid-gel phase to the more fluid liquid crystalline phase, thus, curcumin can penetrate more the hydrophobic phase in DAPC membrane. As a result, the fluorescence intensity of curcumin increases. If permeability was the only factor to be considered, the fluorescence intensity would have continuously increased after reaching the phase transition temperature until saturation. This was not the case in our experiments.

Furthermore, as the temperature is increased, a blue shift occurred from 505 nm to 495 nm, which confirms the incorporation of curcumin into the membrane. This happens because the emission transition is a π to π* emission which is blue shifted when going from non-polar to a polar medium. This relation between polarity of the solvent and emission wavelength of curcumin was proved in a study where it the wavelength of the maximum emission of curcumin shifts from 439 nm in hexane, 518 nm in DMSO to 536 nm in N-butyronitrile [107]. On the other hand, above the Tm, the viscosity of the solvent becomes the dominant factor. Hence, as the medium becomes less viscous at higher temperature, the emission intensity of curcumin decreases continuously due to the fact that the emission intensity of a fluorophore is directly proportional to the viscosity of the medium.

Accordingly, the fluorescence of curcumin was controlled by the permeability factor prior to the Tm and by the viscosity factor after reaching phase transition temperature [108].

Furthermore, the effect of molar concentration of curcumin on the Tm of DAPC liposomes was also studied and the results are displayed in Figure 8.

Therefore, the concentration of curcumin was increased, and the phase transition was measured at 1, 10, 15, 20 and 25 µM of curcumin. It's well noted that a shift in the Tm from 65°C for 1 µM curcumin to 63, 62, 62 and 61 °C for 10, 15, 20 and 25 µM respectively.
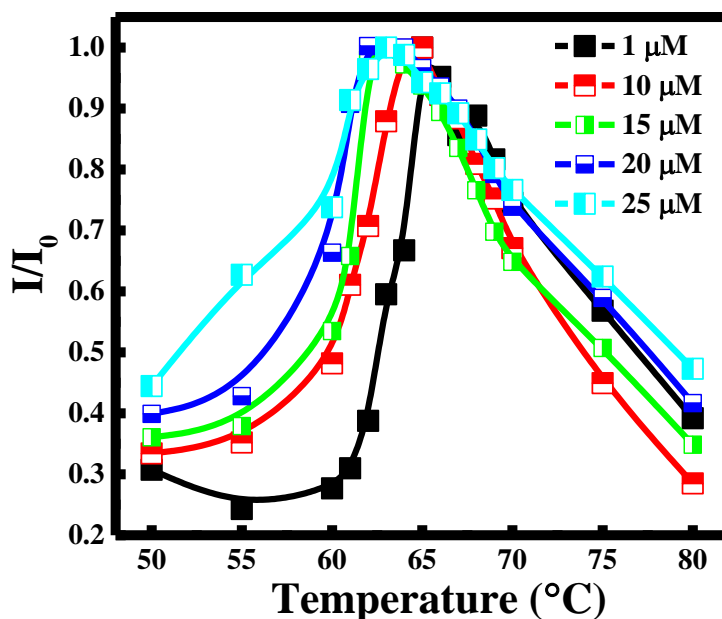
Figure 8 Profile of temperature–fluorescence intensity of curcumin at various molar ratio of curcumin concentration in DAPC liposomes.

This can be linked to the fact that as the population of curcumin is increasing, more curcumin molecules are intercalating between the acyl chains of the DAPC membrane. Hence, Van Der Waals interactions become weaker, which require less energy to disrupt the ordered packing, thus the Tm decreases.

Interestingly, another effect of the increase in the molar concentration of curcumin is the red shift in the fluorescence emission maximum. It was observed to shift from 495 nm for 1 µM to 502, 513, 517 and 520 nm for 10, 15, 20 and 25 µM of curcumin respectively. This observation suggests that at high concentration, a larger population of curcumin is exposed to aqueous medium as the penetration of curcumin gets saturated [106].

b) <u>Effect of chitosan oligosaccharide lactate</u>

As chitosan can protect the membrane layer, its effect was investigated. Figure 9 presents the variation of the emission intensity at different temperatures for 1 µM curcumin, after the addition of 0.5 mg/mL of chitosan. It is clear that same trend was obtained, where it reached a maximum at Tm=65°C. Hence Figure 9B displayed the variation of emission intensity with temperature for 1 µM curcumin concentration, without and with chitosan.

It's clear that the addition of chitosan had no significant effect on the Tm, but it affected the emission intensity which increased. This effect of chitosan is based on its location as it forms a coating layer on the DAPC membrane, thus enhancing the encapsulation of curcumin in the DAPC membrane.
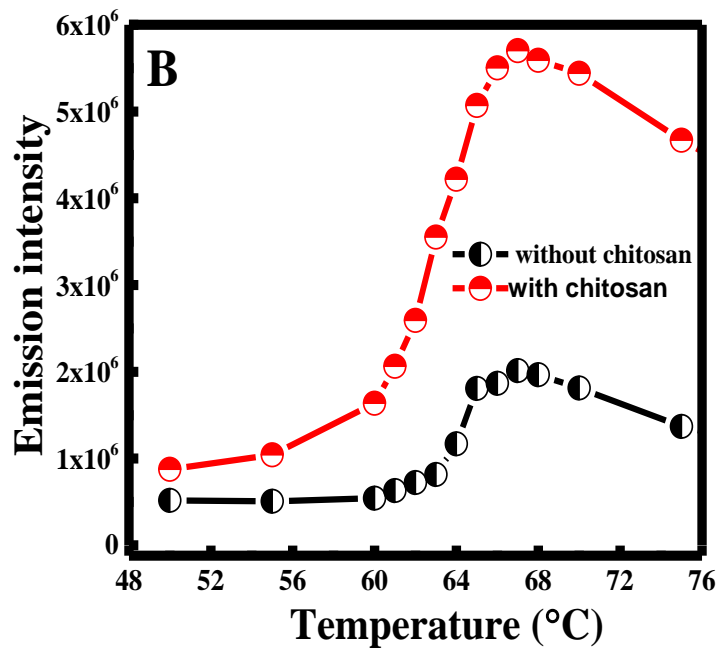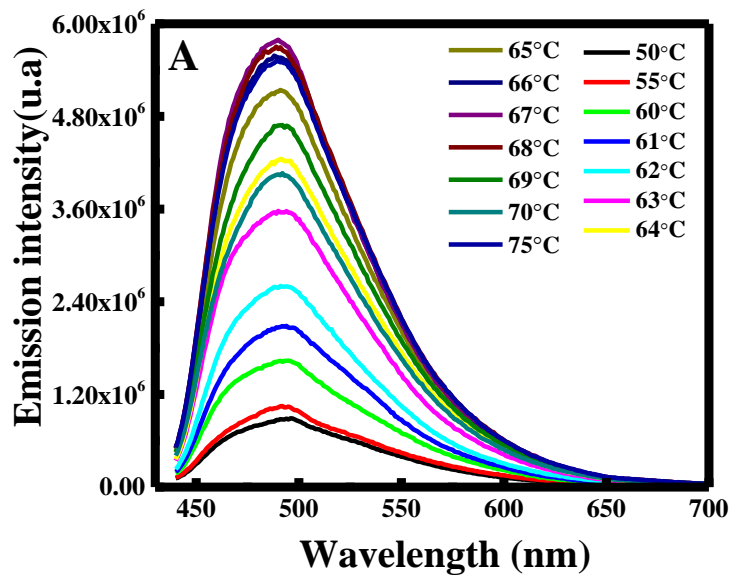
Figure 9 (A) Fluorescence emission spectra of 1 µM curcumin in DAPC membrane at various temperatures, in the presence of chitosan oligosaccharide lactate and (B) Comparative graphs for the variation of fluorescence emission intensity of 1 µM curcumin in DAPC membrane at various temperatures, with and without chitosan oligosaccharide lactate.

2. *Membrane permeability*

Lipophilicity is considered as one of the important property of liposomes. To study it, membrane permeability is usually anticipated, since they are both strongly related.

The permeability of a membrane is correlated with the ease at which a molecule can intercalate into it through passive transport. One way to investigate this property is by following the rate constant (Ksv) of a quenching reaction happening between a probe molecule located in the hydrophobic cavity of the liposome and a quencher, bearing in mind that Ksv is directly proportional to the quenching effect, which means that the higher it gets, the more quenching is happening, the more the quencher is in contact with the probe molecule [106].

Under steady state conditions the relationship derived by Stern and Volmer describes quenching as $F_0/F = 1 + K_{SV} [Q]$, where F_0 and F are the fluorescence intensities in the absence and presence of different quencher concentration ([Q]) respectively, and Ksv is the Stern-Volmer quenching constant, which is the slope of the linear equation.

a) Quenching study with CPB

CPB is a cationic surfactant that intercalates within the hydrophobic part of the liposome membrane with its charged moiety exposed at the surface, thus, if permeable enough, liposome will encourage contact between CPB and hydrophobic probe like curcumin (See Figure 10).
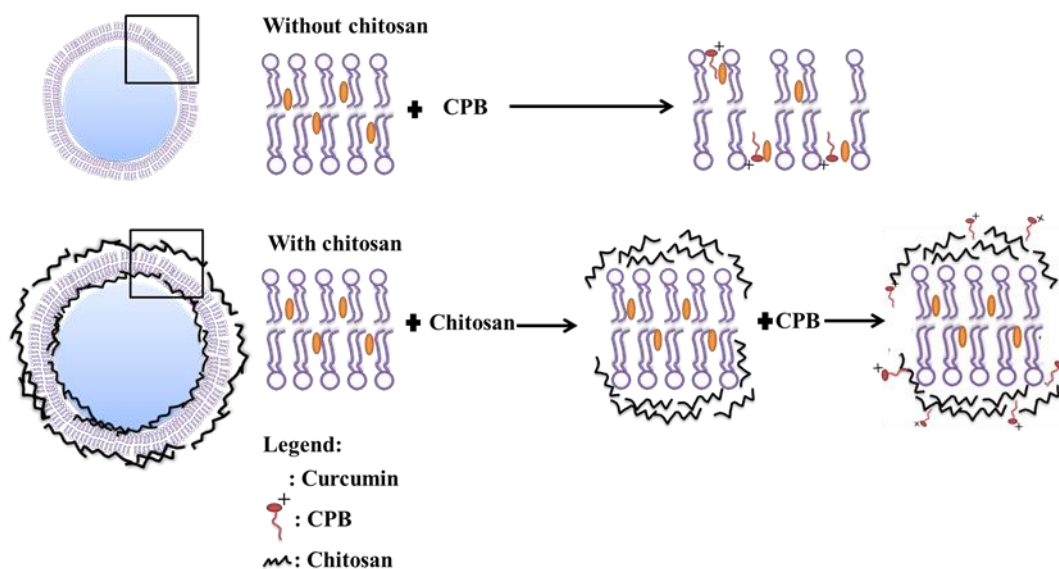
Figure 10 Quenching effect of CPB in the absence and presence of chitosan oligosaccharide lactate (chitosan).

The results are shown in Figure 11A&B in the presence and absence of chitosan respectively. The experimental data in Figure 11A reveals that the fluorescence intensity of curcumin was quenched by CPB since it decreases as concentration of CPB increases in the absence of chitosan, while when adding chitosan, the emission intensity remained approximately constant.
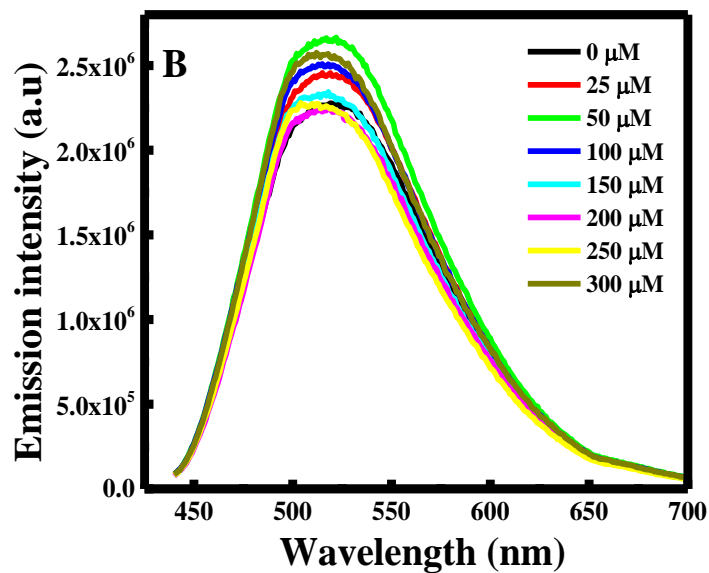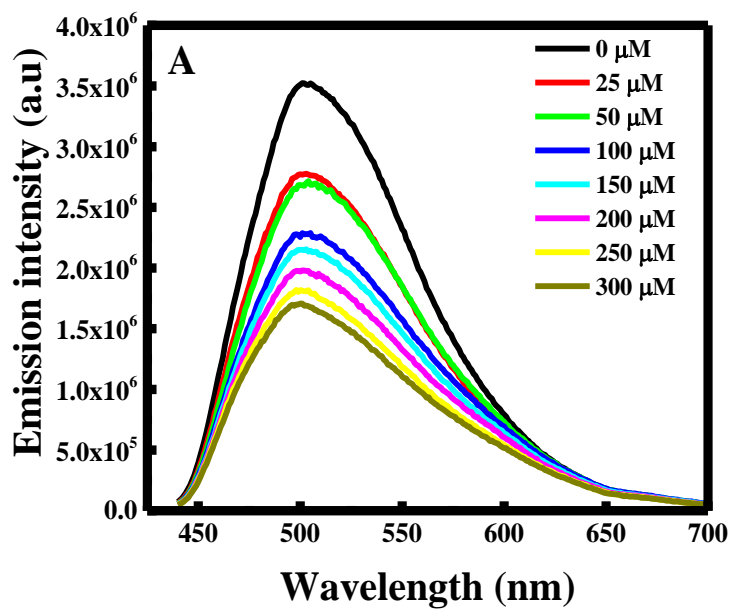
Figure 11 (A) Fluorescence emission spectra of curcumin in DAPC membrane at various
CPB concentration in the absence of chitosan; (B) Fluorescence emission spectra of
curcumin in DAPC membrane at various CPB concentration in the presence of chitosan
oligosaccharide lactate.

The ratio of F_0/F in both cases was plotted and illustrated in Figure 12. Graph Figure 12 clearly indicates that the addition of chitosan inhibits the quenching effect of CPB. The Stern-Volmer plot for fluorescence quenching of curcumin by CPB in DAPC liposomes was found to be linear, increasing without chitosan, and approximately constant after addition of chitosan.
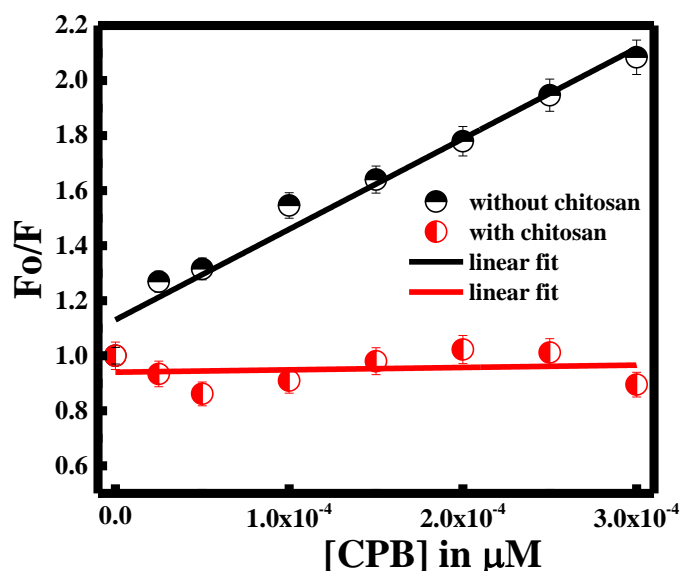
Figure 12 Comparative graphs for the normalized emission spectra of curcumin if DAPC membrane at various CPB concentrations, without and with chitosan oligosaccharide lactates.

The Ksv value, which is the slope of the increasing plot, was found to be high and equal to 3291.03 with linear regression $r^2 = 0.96$. The obtained result indicate that DAPC membrane is permeable to CPB, since quenching occurred. However, the addition of chitosan obstructs CPB from entering into the liposome, forbidding by such the interaction between CPB and curcumin.

The mechanism by which CPB quenches fluorescence of curcumin is suggested to be by electron transfer process, similar to pyrene. When curcumin absorbs the appropriate radiation and get excited, electron in the excited state is transferred from its aromatic ring to electron deficient N-atom of CPB [109]. For that, being a cationic polymer, chitosan repels CPB which is also cationic, forbidding by such the electron transfer between CPB and curcumin.

b) Quenching study with KI

KI is a water-soluble chemical compound. I⁻ ions will therefore remain in the aqueous environment around the liposomal-curcumin system. Therefore, no quenching will occur when using KI at low concentration [106]. Hence, to confirm this statement quenching experiment was done using KI in the presence or absence of chitosan. Figure 13 A&B represent the quenching without chitosan and with chitosan respectively.
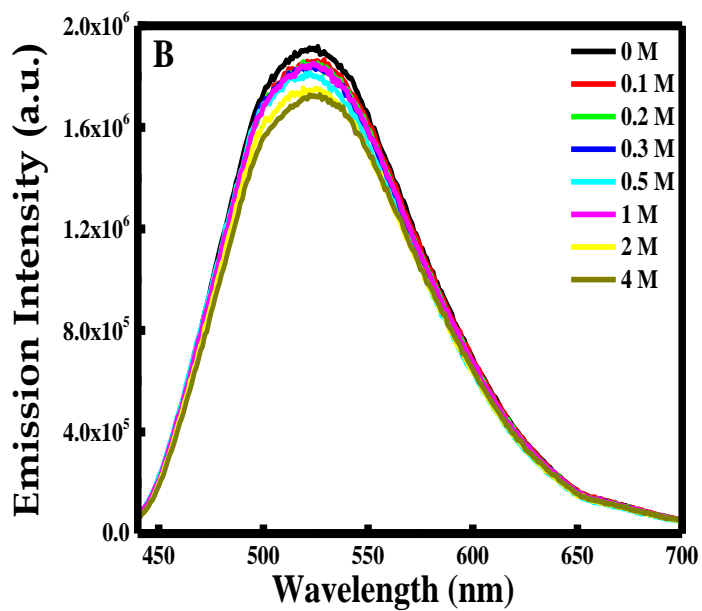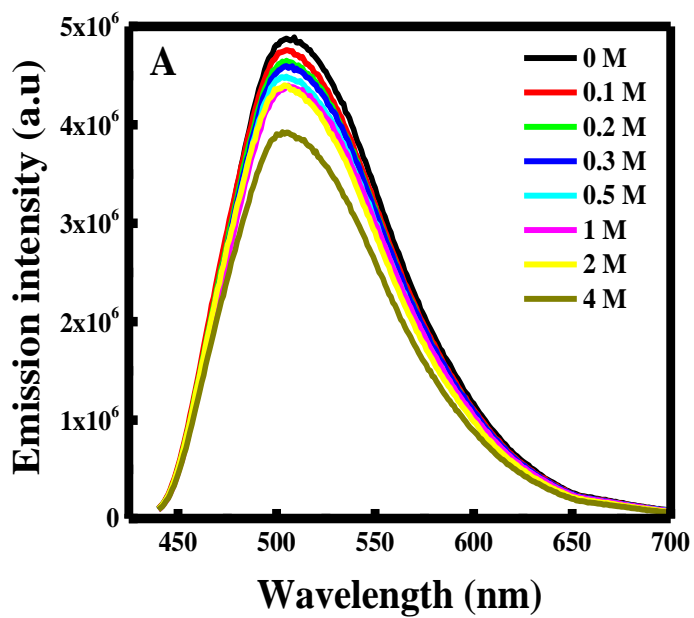
Figure 13 (A) Fluorescence emission spectra of curcumin in DAPC membrane at various KI concentration in the absence of chitosan; (B) Fluorescence emission spectra of curcumin in DAPC membrane at various KI concentration in the presence of chitosan.

The experimental data obtained in both cases show clearly that no quenching has

occurred which is reflected by an almost constant fluorescence emission intensity as KI

concentration was increased.
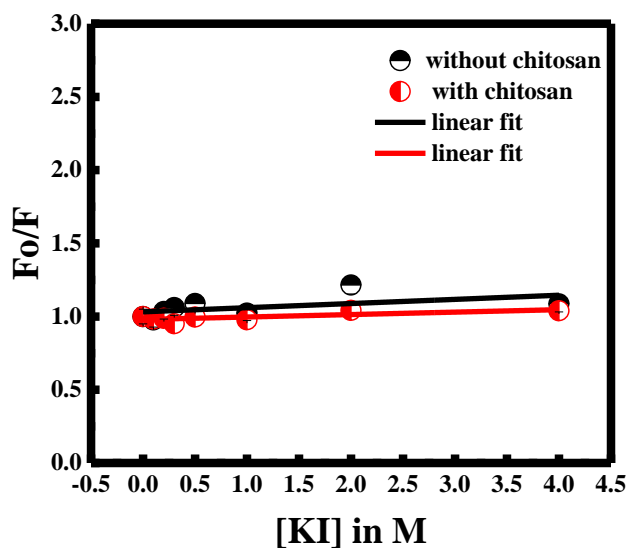
Figure 14 Comparative graphs for the normalized emission spectra of curcumin of DAPC
membrane at various KI concentration, without and with chitosan.

This is confirmed as well in graph (Figure 14) where Fo/F remain approximately

constant in both cases.

These results reflect the fact that there is no contact between curcumin which is largely

present in the hydrophobic environment of the liposomes, and I⁻ ions present in the

aqueous environment.

3. *Partition coefficient*

Partition coefficient (Kp) is measured to evaluate the lipophilicty of a compound. K_p gives information about the portion associated of the compound with the lipid. Fluorescence spectroscopy can be used to estimate the K_p value of any fluorescent molecule under a condition that the fluorescence intensity of the portioning molecule is different when it is in aqueous phase and when incorporated in the lipid membrane (See Figure 15).
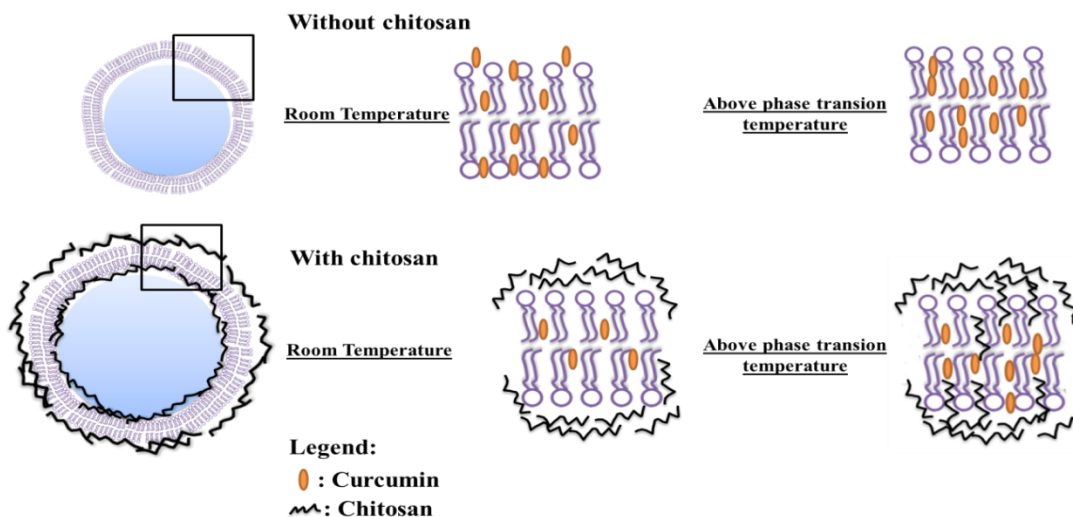
Figure 15 Partition of curcumin in the absence and presence of chitosan oligosaccharide lactate.

In the present case, the fluorescence intensity of curcumin was adopted as a framework to provide the partition coefficient of curcumin into DAPC liposome, without and after coating the liposome with chitosan. Kp is determined from the slope and intercept of the linear plot of 1/F against 1/[DAPC], using the following equation:

$1/F = [55.6/Kp*F_\#)]*(1/Lipid) + (1/F_\#)$

where F is fluorescence at a given liposome concentration and $F_\#$ is the fluorescence

obtained from total curcumin incorporated into the liposomes.

DAPC liposome has a phase transition temperature near 65°C. Below this

temperature, the liposome exists in the solid gel phase and above it, it exists in the liquid

crystalline phase. The partition coefficients at room temperature and at 75°C were

measured while increasing the liposome concentration with and without chitosan.

a) <u>At room temperature</u>

Figure 16 A&B represents the partition coefficient without chitosan and in the presence

of chitosan respectively. In both cases, the observed increase in fluorescence intensity of

curcumin as the concentration of DAPC liposomes is increasing confirms incorporation

of curcumin into the membrane.
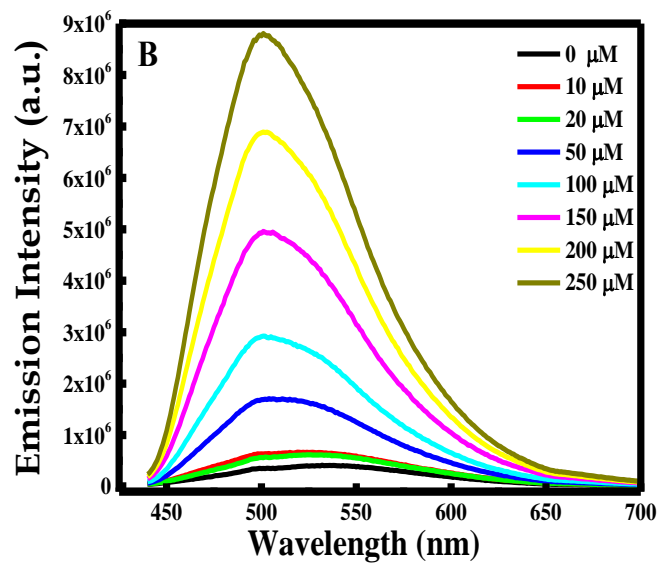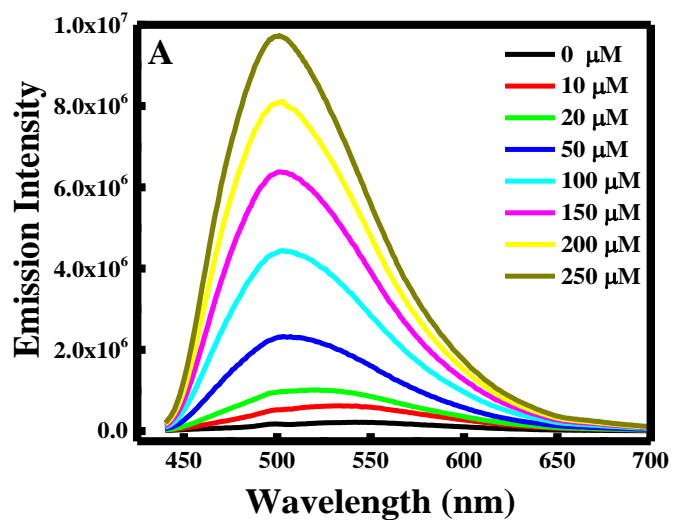
Figure 16 Fluorescence emission spectra of curcumin in various concentrations of DAPC liposomes (A) at RT without chitosan and (B) at RT with chitosan.

In addition, in both cases a blue shift was observed (See Table 2) confirming that curcumin is able to penetrate into the lipid bilayer of DAPC liposomes as it becomes more hindered from the aqueous media.

Concentration	Without chitosan	With chitosan
0 µM	535 nm	540 nm
250 µM	500 nm	510 nm

Table 2 Maximum emission wavelength values at RT, with and without chitosan.

Hence Figure 17 represents the linear plots of 1/F vs 1/[DAPC].
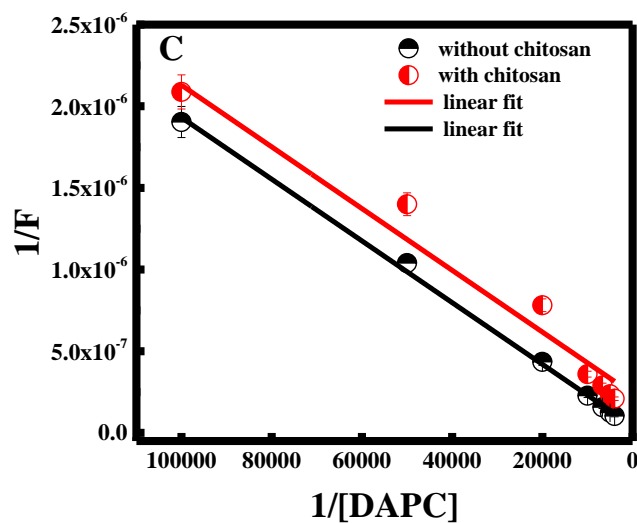
Figure 17 comparative Plot of 1/F vs 1/[DAPC] in at RT, with and without chitosan.

Using Stern-Volmer equation and the values of slope and intercept summarized in Table 3, Kp was calculated. As obtained, Kp without chitosan was much smaller than with chitosan which is equal to 7.047×10^5.

Without chitosan			With chitosan		
Slope	Intercept	Kp	Slope	Intercept	Kp
2.65443×10^{-11}	1.6767×10^{-7}	1.236×10^5	2.21431×10^{-11}	2.36252×10^{-7}	7.047×10^5

Table 3 slope and intercept values for the 1/F vs 1/[DAPC] plots, without and with chitosan at RT°C.

These results confirm that at RT, chitosan enhance the encapsulation of curcumin into DAPC membrane. Thus, chitosan represents a protective layer for the liposomal-curcumin system.

b) Above phase transition temperature

Same results were obtained when heating the solution above its phase transition temperature. Hence, when increasing the liposome concentration, the emission intensity increases proportionally. This increase was obtained in the presence and absence of chitosan (See Figure 18 A&B).
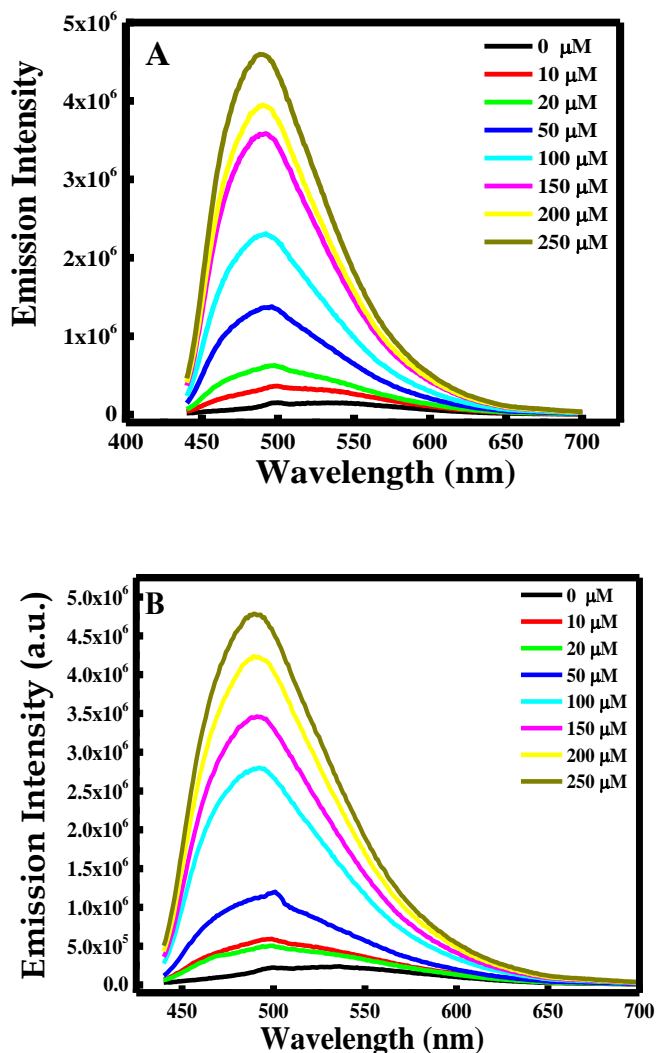
Figure 18 (A) Fluorescence emission spectra of curcumin in various concentration of DAPC liposomes at 75°C without chitosan; (B) Fluorescence emission spectra of curcumin in various concentration of DAPC liposomes at 75°C with chitosan.

Moreover, the increase in the intensity was conjugated to a blue shift of the peak (See Table 4) indicating thereby the penetration of curcumin into the lipid membrane.

Concentration	Without chitosan	With chitosan
0 microM	525 nm	550 nm
250 microM	490 nm	500 nm

Table 4 Maximum emission wavelength values at 75°C, with and without chitosan.

Moreover, in order to get Kp value, the plot between 1/F and 1/[DAPC] was illustrated (See Figure 19).
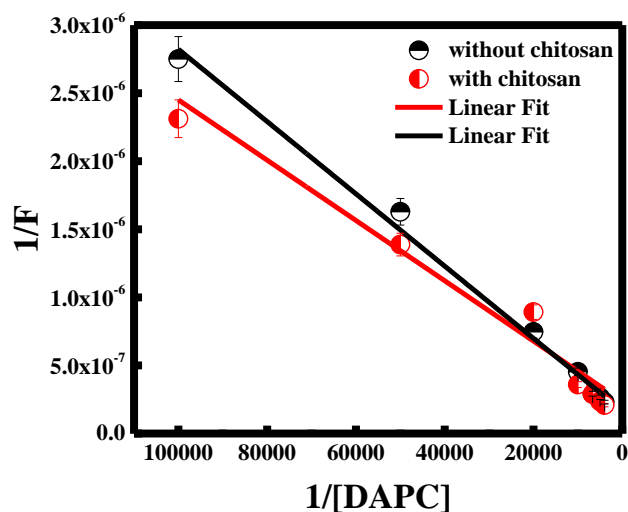
Figure 19 comparative Plot of 1/F vs 1/[DAPC] in at 75°C, with and without chitosan.

Hence, the value of the slope and intercept are summarized in Table 5. Similar results were obtained as the study done at room temperature were Kp value without chitosan was smaller than that obtained when using chitosan. This is in accordance with the results at RT, which reflects that chitosan forms a protective layer for the liposomal-curcumin system.

Without chitosan			With chitosan		
Slope	Intercept	Kp	Slope	Intercept	Kp
2.65443×10^{-11}	1.6767×10^{-7}	3.512×10^{5}	2.21431×10^{-11}	2.36252×10^{-7}	5.93214×10^{5}

Table 5 slope and intercept values for the 1/F vs 1/[DAPC] plots, without and with chitosan at 75°C.

c) Room temperature vs 75°C

It is found that the partition coefficient value of curcumin in DAPC liposome is ca 2.8-fold higher without chitosan, at the liquid crystalline phase compared to that in solid gel phase. Higher value of Kp at the liquid crystalline phase in comparison to the solid gel phase is judicious because the liquid crystalline phase is more fluid and flexible, whereas the solid gel phase is known to be more firm and compact [110].

This founding confirms the results of previous reports for other membrane systems and probe molecules [111],[112]. A lower K_p is obtained for the solid gel state compared with liquid crystalline phase due to the fact that as the temperature increases, the membrane permeability is enhanced which facilitates the incorporation of curcumin in the membrane.

However, this result was not the same when a chitosan layer was added. It's observed in Table 6 that the Kp value slightly decreases. This can reflect the fact that at high temperature, chitosan can penetrate more into the liquid crystalline state of the bilayer, which blocks the passage of curcumin inside the membrane.

	Partition Coefficients	
	Without Chitosan	**With Chitosan**
RT (solid gel phase)	1.236×10^5	7.047×10^5
75°C (liquid crystalline phase)	3.512×10^5	5.93214×10^5

Table 6 Partition coefficients of curcumin into DAPC phospholipids liposome.

D.   Conclusion

This study has shown that curcumin, a potential medicinal drug, can bind effectively to a liposome membrane. By monitoring the fluorescence emission intensity of this fluorophore, the phase transition temperature of DAPC liposomes was determined along with exploring the effect of adding a coating polymer layer such as chitosan which had no effect on the Tm, but only increased the emission intensity.

However, increasing curcumin concentration displayed a slight decrease in the Tm. Furthermore, quenching studies displayed the permeability of DAPC membranes to the hydrophobic CPB molecule which was reflected by the decrease in the fluorescence emission intensity of curcumin, and that curcumin is located in the hydrophobic core of the liposome since the aqueous KI did not affect its emission intensity.

Nevertheless, curcumin remarkably intercalated with DAPC liposomes and the partitioning of curcumin showed dependence on the temperature, and on the presence of chitosan. Chitosan did not change phase transition temperature of DAPC liposomes but it changes membrane permeability depending on solid gel or liquid crystalline phase.

CHAPTER IV

EFFECT OF CURCUMIN AND CHITOSAN OLIGOSACCHARIDE LACTATE ON DBPC LIPOSOMES PROPERTIES STUDIED BY CURCUMIN FLUORESCENCE

A.   Introduction

Recently, researches have proven the therapeutic effects of curcumin on several diseases including pulmonary, cancer, diseases of the nervous system, chronic kidney disorders, cardiovascular disease, metabolic disease, and other inflammatory diseases [113], [114].

In spite of its very promising practices, there are some limitations that hinder the usage of curcumin as a health-promoting agent. As a free drug, curcumin is rapidly metabolized by the liver which reduces its plasma half-life. Also, it has a limited bioavailability due to the fact that it's a hydrophobic compound, poorly water-soluble, <0.125 mg/L, and readily prone to enzymatic degradation in the blood [115].

Hence, to improve its therapeutic potential as a chemotherapeutic drug, drug delivery systems can be used to address the above-mentioned issues. Encapsulating curcumin into liposomes vesicles was proposed as a solution [104]. When being enclosed into liposomes, the compound is stabilized and shielded from its environment which increases its solubility in aqueous media.

In fact, Phosphatidylcholine (PC) liposomes are widely used as a model for the cell membrane, which is mainly composed of phosphatidylcholine [116].

Nevertheless, liposomes have a short circulation half-life and they are prone to hydrolysis and oxidation which make their usage restrained by the possibility of losing the loaded molecule inside.

Hence, protecting the liposomal-curcumin system is essential to improve the vesicle stability. Coating the surface with polymers was shown to be a possible successful way [117], [118]. Chitosan oligosaccharide lactate, with the linear formula $(C_{12}H_{24}N_2O_9)_n$ is one natural, widely used polymers for this purpose. It's a polycationic biopolymer possessing physiochemical and biological properties that make it a well-recognized promising material for drug delivery. Hence, being both a biocompatible and biodegradable polysaccharide, chitosan provides a protective layer for drug formulations [119].

The success of the polymeric layer in prolonging the retention time of liposomes coated with chitosan has been proven in several studies [120], [121].

In this work, curcumin was used as a molecular probe to study some physical properties of 1,2-dibehenoyl-sn-glycero-3-phosphocholine (DBPC) liposome with the molecular formula $C_{52}H_{104}NO_8P$. DBPC has a longer hydrocarbon chain length and higher phase transition temperature compared to DMPC, DPPC and DSPC liposomes, thus, its behavior needs to be understood.

This was achieved by monitoring the fluorescence intensity changes of curcumin, which depends on the polarity and viscosity of its environment [122]. Moreover, the influence of chitosan on the physical properties of the liposome was also assessed. However, to our knowledge there is no report on interaction of DBPC and chitosan oligosaccharide lactate and DBPC with curcumin.

B. Method of preparation

1. *Sample preparation for phase transition experiment*

For phase transition temperature study, the temperature was varied from 65℃ to 80°C. Liposome concentration in a cuvette (3 mL) was kept 100 µM with 1 µM of curcumin. The volume of the solution was completed to 3 mL with buffer solution (pH = 7).

In order to establish the effect of curcumin concentration, several experiments were done in the curcumin concentration of 1, 10, 15, 20 and 25 µM. The total volume was completed with a 10 mM pH = 7 buffer solution.

Moreover, the effect of chitosan was also investigated. For this purpose, 0.5 mg/mL of chitosan were added by withdrawing 300 µL from a 5 mg/mL stock solution.

2. *Sample preparation for quenching experiment*

For quenching study liposome and curcumin concentration were constant and kept at 100 µM and 1 µM respectively in all quenching studies, whereas CPB final concentration was varied from 0, 25, 50, 100, 150, 200, 250 to 300 µM in the samples.

Similarly, KI final concentration was varied from 0, 0.1, 0,2, 0.3, 0.5, 1 to 2 M.

For quenching study in the presence of chitosan oligosaccharide lactate, the final concentration of chitosan oligosaccharide lactate used was 0.5 mg/mL.

During measurement, the total volume was completed to 3 mL with a 10 mM pH equal to 7 buffer solution.

3. *Sample preparation for partition coefficient experiment*

For partition coefficient measurement, curcumin concentration was 1 µM in all trials.

When chitosan oligosaccharide lactate was added, its concentration was also kept constant at 0.5mg/mL.

Liposomes concentration was varied from 0, 10, 20, 50, 100, 150, 200 to 250 mM. The total volume in these samples was completed to 3 mL with a 10 mM pH = 7 buffer solution.

C. Results and discussion

1. *Phase transition temperature*

For DBPC liposomes, the phase transition temperature is equal to 75°C, as mentioned in Avanti Polar sheet where it's coded as 22:0 PC. (https://avantilipids.com/tech-support/physical-properties/phase-transition-temps).

a) Effect of curcumin concentration

Determination of Tm can be done by the fluorescence method [123], [124], which complement DSC measurements.

In the present study, the emission intensity changes of curcumin were observed to inspect the Tm of DBPC liposome. As shown in Figure 20, the fluorescence emission intensity increased with temperature to a maximum, defined to be the phase transition temperature, then after Tm, the intensity decreased continuously, in the presence of 1 µM curcumin.
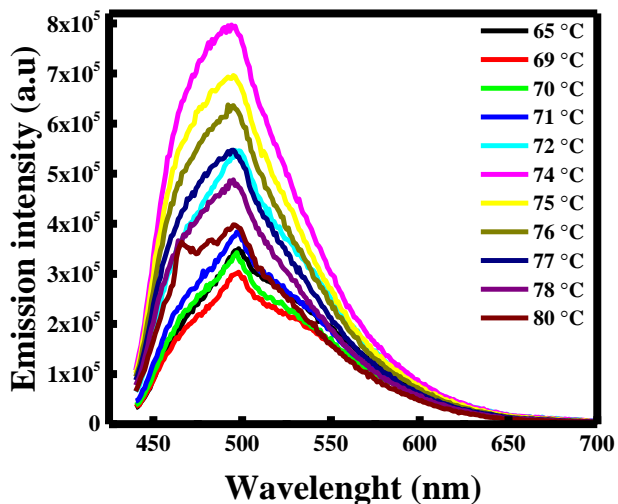
Figure 20 Fluorescence emission spectra of 1 µM curcumin in DBPC membrane at various temperatures.

This change in the intensity before and after the phase transition temperature is interpreted as such: In the first place, before reaching the Tm, the bilayer is transforming from the dense solid-gel phase to the fluid liquid crystalline phase, thus, curcumin can penetrate more the hydrophobic phase in DBPC membrane where it gets more dissolved, experiencing a nonpolar environment by binding to the hydrophobic regions of PC liposomes, resulting in an increase in the fluorescence intensity.

Furthermore, the blue shift from 498 nm to 481 nm, as the temperature increases confirms the incorporation of curcumin into the liposome membranes. When the temperature reaches higher than the Tm, the emission intensity of curcumin becomes affected by the viscosity of the solvent which decreases, resulting in a decrease in the emission intensity of curcumin decreases due to the fact that the emission intensity of a fluorophore is directly proportional to the viscosity of the medium.

Therefore, before the Tm, the increase in the permeability of the membrane controls the fluorescence of curcumin while after the Tm, the viscosity of the medium is the controlling factor [104].

Accordingly, the phase transition temperature can be easily obtained when plotting the I/I_0 ratio versus the temperature in the range of 60-80 °C in the presence of 1 µM curcumin (See Figure 21). Hence, the phase transition temperature measured for DBPC liposomes is in this case is equal to 74 °C, which is very close to the value reported in Avanti Polar.
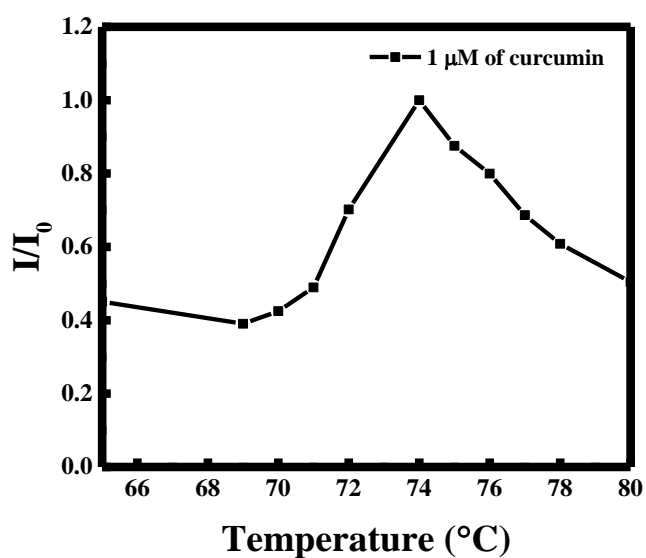
Figure 21 I/I_0 of 1 µM curcumin in DBPC liposomes at various temperatures.

As curcumin was used as a fluorophore molecule, the effect of its molar concentration was also investigated, as displayed in Figure 22. For that, the concentration of curcumin was increased and the phase transition was measured at 1, 10, 15, and 20 µM of curcumin. A depression in the Tm was observed from 74°C for 1 µM curcumin to 71

°C for 10, 15 and 20 µM. This is due to the fact that the more the curcumin population is increased, the higher is the proportion of curcumin entering the hydrophobic core of the liposomes which weaken the Van Der Waals interactions between the ordered packing, which require less energy, and thus the Tm decreases. In addition, a red shift in the fluorescence emission maximum was also noted from 498 nm to 501, 505 and 508 nm, as the molar concentration of curcumin increases. This shift suggests that as curcumin concentration increases, its penetration into the liposome gets saturated, thus a larger population becomes exposed to the aqueous polar medium which decreases the energy band gap of the non-polar π to π* transition resulting in a red shift [103].
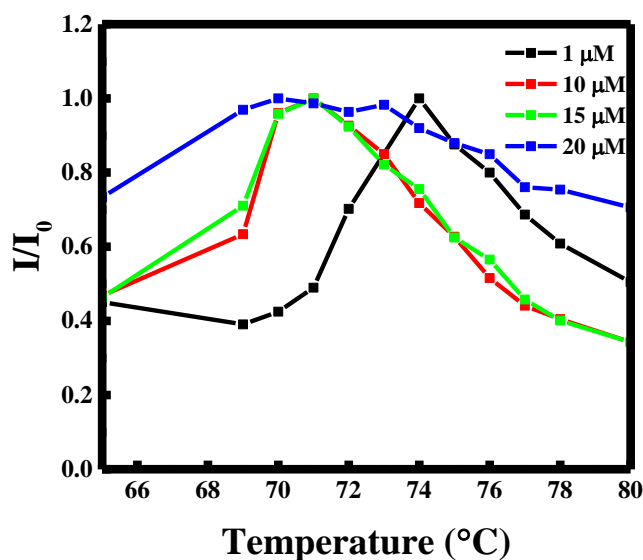
Figure 22 Profile of temperature fluorescence intensity of curcumin at various molar ratio of curcumin concentration in DBPC liposomes.

b) <u>With chitosan oligosaccharides</u>

Additionally, to observe the effect of coating with a polymer layer, 0.5 mg/mL of chitosan oligosaccharide lactate was added to the solution containing 1 µM curcumin, and the corresponding variation in the emission intensity at different temperature was observed and plotted in Figure 23.
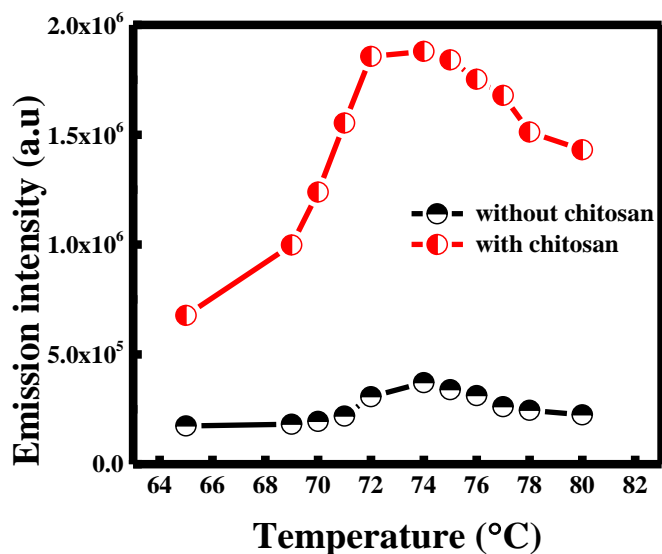
Figure 23 Comparative graphs for the variation of fluorescence emission intensity of 1 µM curcumin in DBPC membrane at various temperatures, with and without chitosan oligosaccharide lactate.

It was found that the addition of chitosan oligosaccharide lactate did not change the Tm which is remained equal to 74 °C, but only induced an increase in the emission intensity. This enhancement is due to the protective role that chitosan oligosaccharide lactate layer plays by enhancing the encapsulation of curcumin inside the DBPC membrane. This role of chitosan oligosaccharide lactate is achieved by the electrostatic

interactions between the cationic polymer and the negatively charged surface of the nanocapsule [125].

2. *Membrane permeability*

a) Quenching with CPB

The effect of CPB molecule on the emission intensity of curcumin is depicted in Figure 24 A&B in the absence and presence of chitosan respectively.
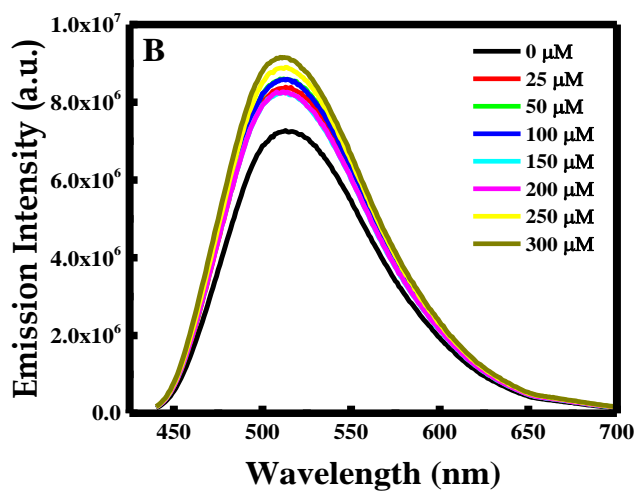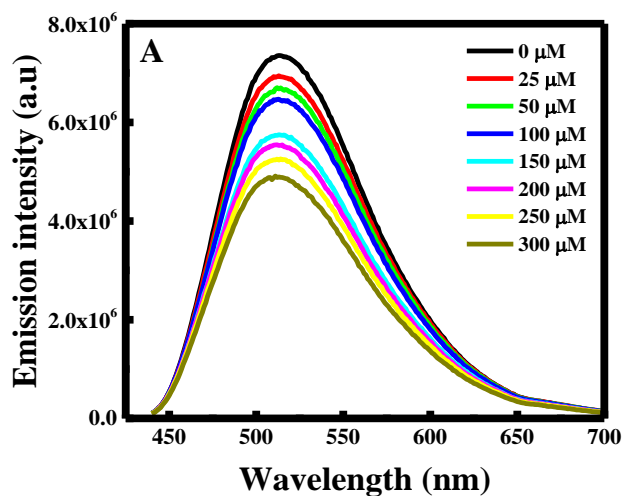
Figure 24 (A) Fluorescence emission spectra of curcumin in DBPC membrane at various CPB concentration in the absence of chitosan oligosaccharide lactate.; (B) Fluorescence emission spectra of curcumin in DBPC membrane at various CPB concentration in the presence of chitosan oligosaccharide lactate.

It is obvious that, without chitosan, the emission intensity decreases with the increase of CPB concentration, indicating that CPB quenches the fluorescence emission of curcumin, whereas the fluorescence emission did not vary much when chitosan was added.

Quantitatively, F0/F was plotted against CPB concentration for both cases (See Figure 25). The almost horizontal plot obtained with chitosan indicates that the addition of chitosan inhibits the quenching effect of CPB on curcumin fluorescence by forbidding CPB from approaching towards the liposome's surface and interacting with curcumin.
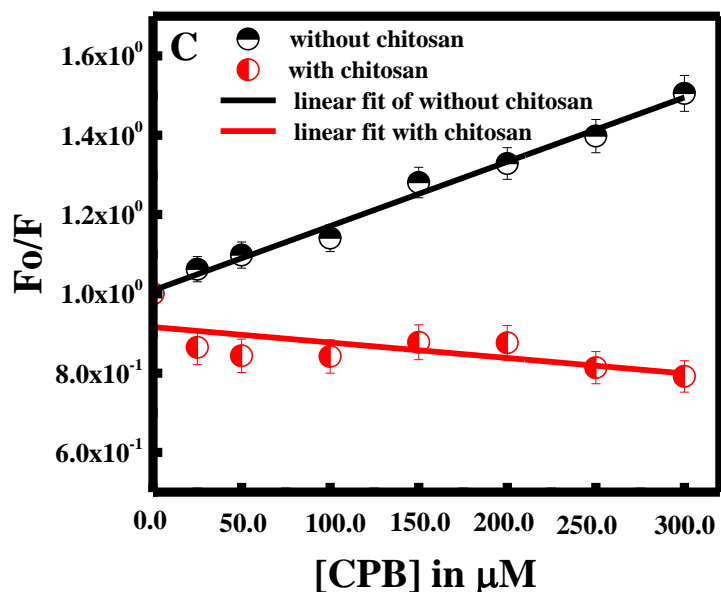
Figure 25 comparative graphs for the normalized emission spectra of curcumin if DBPC membrane at various CPB concentrations, without and with chitosan oligosaccharide lactates.

The Stern-Volmer quenching constant, which is the slope of the linear plot, was found to be equal to 1622.26 M^{-1} in the absence of chitosan before it drops to be negligible when chitosan was added. This considerable difference in the Ksv values has to do with the presence of the liposome layer around liposomal-curcumin system. Hence, being cationic, chitosan repels CPB which is also cationic; forbidding it by such from approaching the liposome's surface and interacting with curcumin.

As for the mechanism by which CPB quenches fluorescence of curcumin, it is suggested to be by electron transfer process, similar to the way pyrene fluorescence was proved to be quenched by CPB. Accordingly, after curcumin gets excited when absorbing the proper radiation, electron in its excited state is transferred from its aromatic ring to electron deficient N-atom of CPB [109].

Furthermore, this result proves that curcumin is located in the hydrophobic cavity of the liposome sphere.

b) Quenching study with KI

On the other hand, the emission intensity was not altered when high concentration of KI was used as a quencher in the presence and absence of chitosan (See Figure 26 A&B).
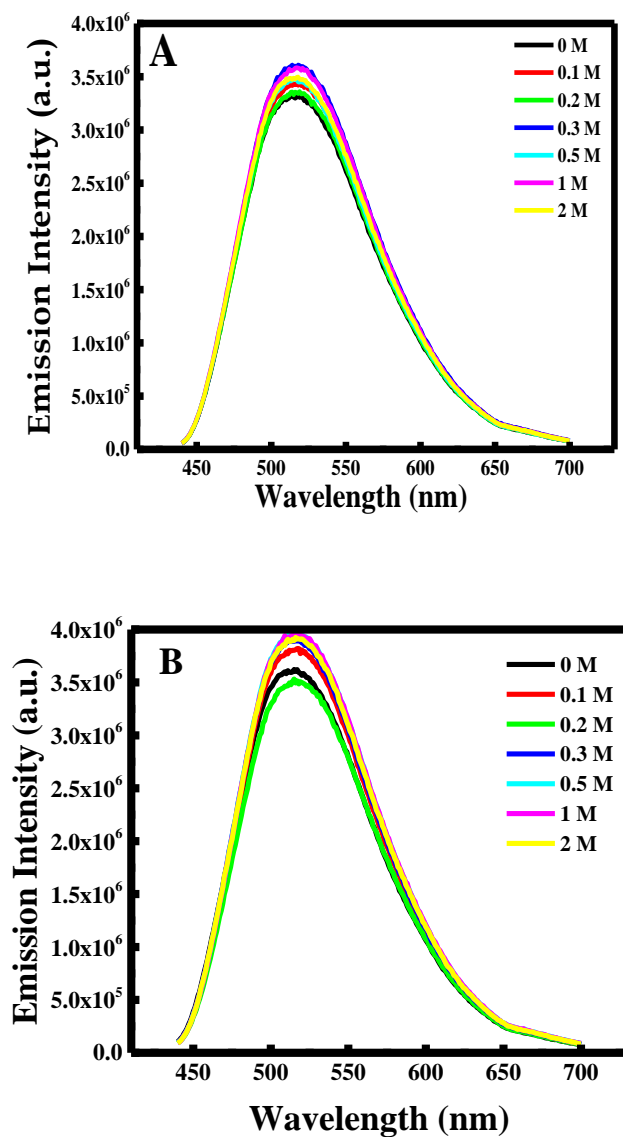
Figure 26 Fluorescence emission spectra of curcumin in DBPC membrane at various KI concentrations (A) in the absence of chitosan oligosaccharide lactate and (B) in the presence of chitosan oligosaccharide lactate.

The obtained Stern-Volmer horizontal plots represented in Figure 27 confirm that KI does not quench the fluorescence emission of curcumin. This indicates that no contact took place between curcumin molecules and the I^- ions. Moreover, this supports

the fact that curcumin, a hydrophobic molecule, is located in the deep bilayer of the

liposome and is far away from any contact between itself and an aqueous quencher.
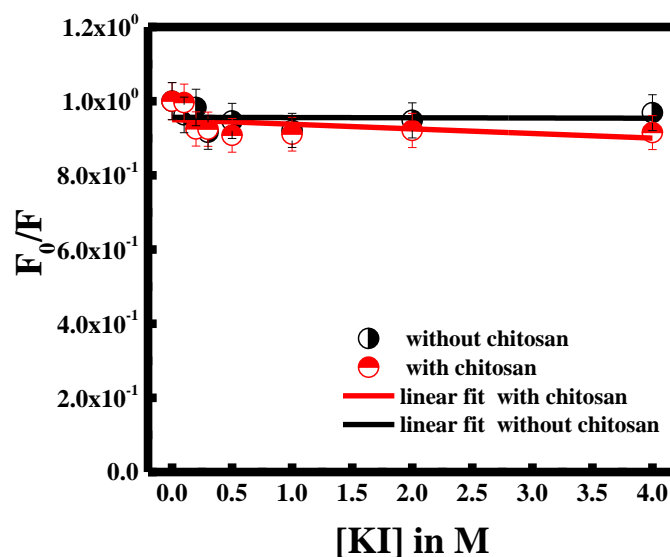
Figure 27 Comparative graphs for the normalized emission spectra of curcumin if DBPC
membrane at various KI concentrations, without and with chitosan oligosaccharide lactates.

3. Partition coefficient

The phase transition temperature of DBPC liposome is reported in Avanti Polar near 75°C.

Below this temperature, the liposome exists in the solid gel phase. However, above the

phase transition temperature, it exists in the liquid crystalline phase. The partition

coefficients at room temperature and at 85°C were measured while increasing the liposome

concentration with and without chitosan oligosaccharide lactate respectively.

a) <u>Without chitosan oligosaccharide lactate</u>

Figure 28 A&B represents the partition coefficient without chitosan at RT and at 85°C respectively. It's well observed that when liposomes concentration is increased, the emission intensity of curcumin also increases, conjugated with a blue shift. This blue shift confirms the penetration of curcumin from the aqueous media into DBPC membranes as it becomes hindered from the polar medium.
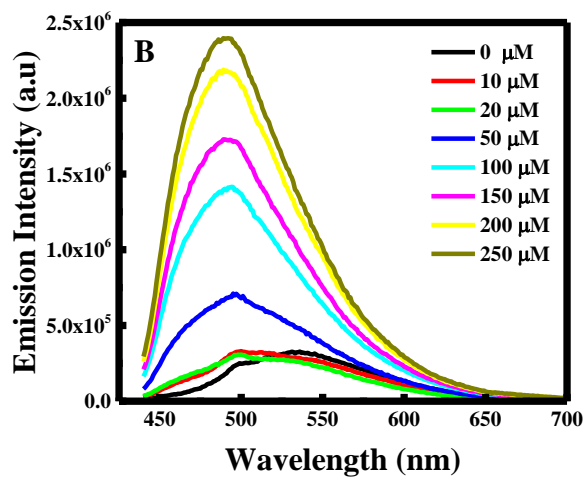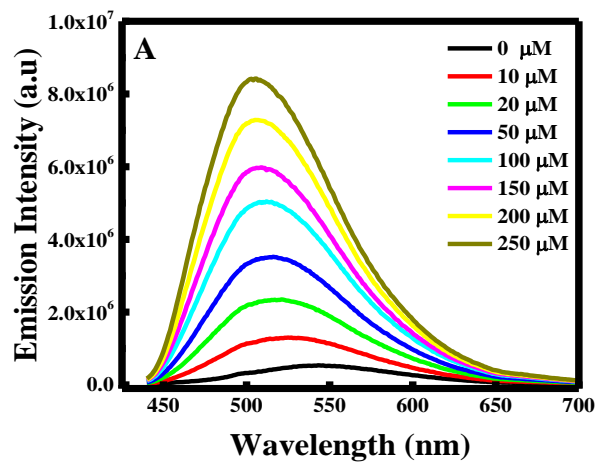
Figure 28 Fluorescence emission spectra in the absence of chitosan oligosaccharide lactate. of (A) curcumin in various concentration of DBPC liposomes at RT; (B) of curcumin in various concentration of DBPC liposomes at 85℃.

In order to calculate the Kp value, 1/F vs 1/[DBPC] was plotted and displayed in figure 29.
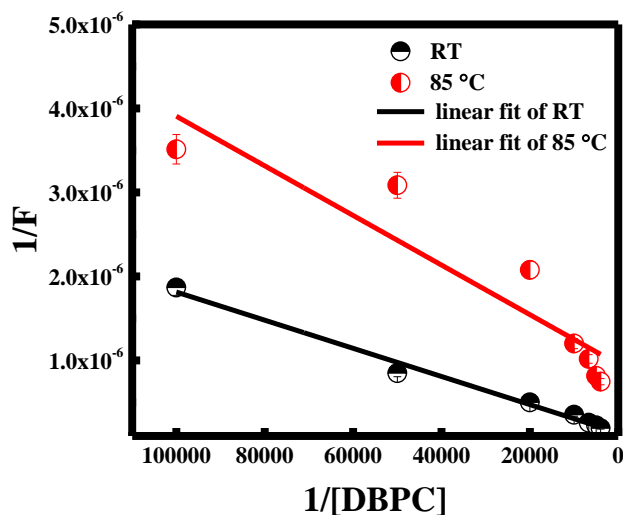
Figure 29 comparative Plot of 1/F vs 1/[DBPC] at RT and 85℃.

It was found that a high value of Kp was obtained when the experiment is performed at 85°C 1.797 x10^6 while at room temperature it was equal to 0.4583x10^6. As a matter of fact, it's reasonable to get a higher value of Kp at a temperature above the phase transition temperature since at this temperature, the liposome is in the disordered liquid crystalline phase, meaning that more curcumin can intercalate between its acyl chains. This result is in accordance with previous studies done for different membranes system using different probe molecules [111], [112].

b) Effect of chitosan oligosaccharide lactate

The effect of coating the liposomal membrane with a chitosan oligosaccharide lactate layer was also assessed. It was obvious that similar results were obtained in both cases in the absence and presence of chitosan oligosaccharide lactate.

Likewise, as the concentration of DBPC increases, a blue shift is observed coupled with an increase in the fluorescence emission intensity of curcumin, which reflects curcumin penetration into the hydrophobic cavity of DBPC (See Figure 30 A&B).
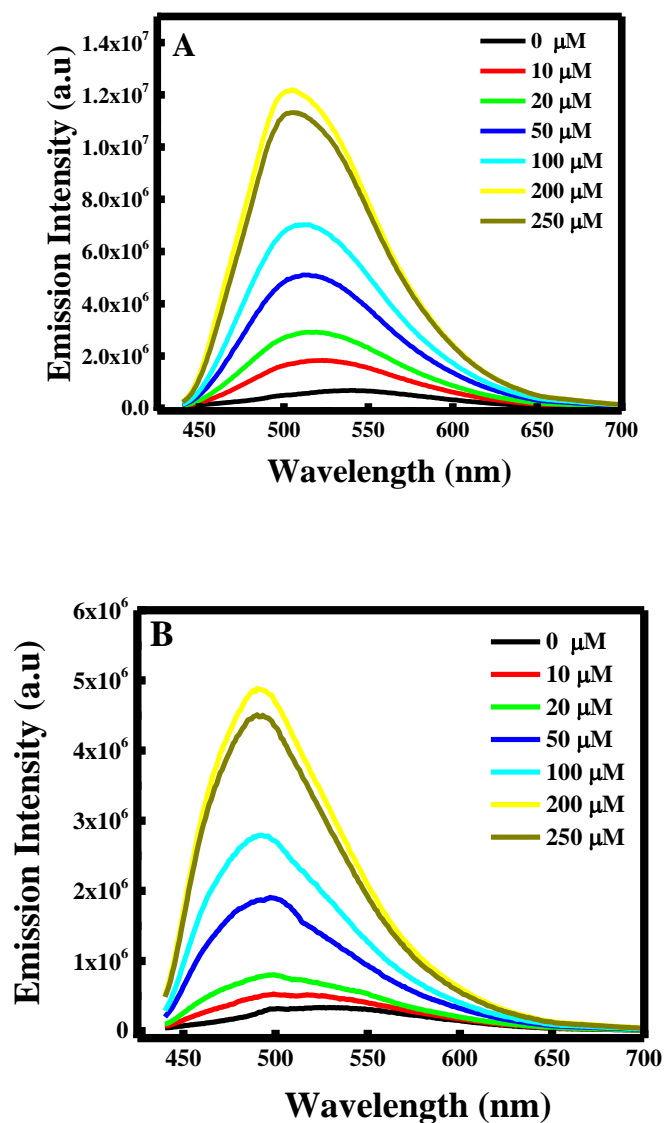
Figure 30 Fluorescence emission spectra in the presence of chitosan oligosaccharide lactate of (A) curcumin in various concentration of DBPC liposomes at RT; (B) of curcumin in various concentration of DBPC liposomes at 85°C.

Moreover, 1/F vs 1/[DBPC] was presented in Figure 31 in order to find kp values.
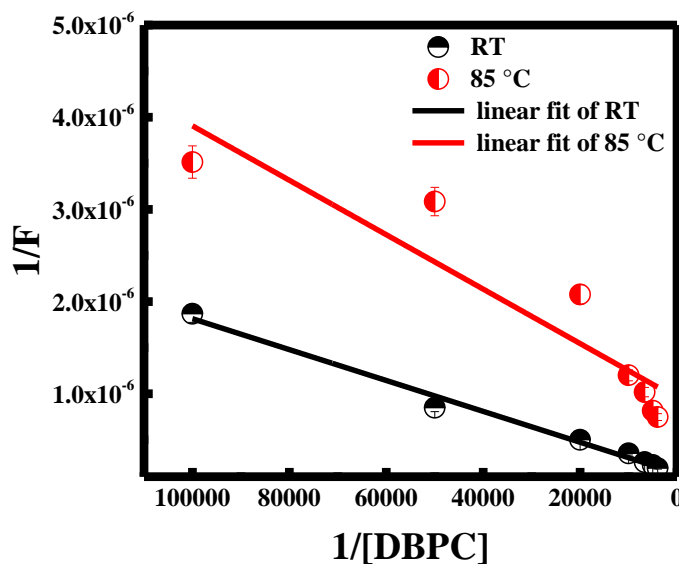
Figure 31 comparative Plot of 1/F vs 1/[DBPC] at RT and 85℃ in the presence of chitosan oligosaccharide lactate.

However, in contrast to the results obtained without chitosan oligosaccharide lactate, the Kp value slightly decreased above the phase transition temperature (See Table 7).

	Partition coefficient	
	Without chitosan	**With chitosan**
Solid gel phase (RT)	0.4583×10^6	1.226×10^6
Liquid crystalline phase (85℃)	1.797×10^6	0.8943×10^6

Table 7 Different Kp values of curcumin in the absence and the presence of chitosan at RT and 85℃.

This variation might be due to the possibility that as the temperature increases, chitosan oligosaccharide lactate layer coating the liposome approaches closer to the vicinity of its surface blocking by such the passage of curcumin molecules from the aqueous media inside the liposome. Hence, chitosan oligosaccharide lactate forms a barrier which disables a bigger number of curcumin molecules to enter the liposome as its bilayers become more permeable.

D.   Conclusion

To sum up, the interaction of curcumin and DBPC liposomes was highlighted for the first time in this work. The partition of curcumin was proved to be temperature dependent and was affected by the addition of a chitosan layer.

By observing the fluorescence emission intensity variation of curcumin, the phase transition temperature was concluded along with realizing the neutral effect of chitosan on its value but only affected the emission intensity fold. However, curcumin concentration caused a slight decrease in the Tm.

The permeability of DBPC membranes to the hydrophobic CPB molecule was noticed by the decrease in the fluorescence emission intensity of curcumin, which confirmed that curcumin is located in the hydrophobic core of the liposome. This was supported by the fact that the aqueous KI did not affect the emission intensity of curcumin. Chitosan did alter the phase transition temperature of DBPC liposomes but only changes membrane permeability depending on solid gel or liquid crystalline phase.

CHAPTER V

EFFECT OF IONIC LIQUID ON THE PARTITION OF DAPC AND DBPC LIPOSOMES

A. Introduction

In 1914, Paul Walden discovered a new type of solvents which he named as ionic liquids (ILs), and since then, their research field has been gradually increasing. ILs are liquid salts comprised entirely of poorly coordinating ions and are commonly defined as being liquid below 100°C because they have low melting points [126].

Hence, ILs are distinguished from other salts, such as table salt sodium chloride, essentially by their melting point as sodium chloride salts are molten at very high temperatures (>800°C) owing to their firmly packed assembly. Whereas the ions that constitute ILs have a bulky and asymmetrical structure [127].

Composed by highly polar but noncoordinating ions, ILs were found to be immiscible with some organic solvents thus offering a polar but non aqueous alternative for systems having two phases [128]–[130]. Moreover, they possess a low vapor pressure which made them be considered as green solvents as they have a low level of atmospheric pollutions and additionally, they demonstrated to have outstanding properties such as being chemically and thermally stable and having high ionic conductivity [131], [132].

In 2003, ILs were trademarked as "solvents of the future" owing to their interesting range of applications, most importantly as substitutes for conventional solvents in industry which were sometimes toxic, high volatile and flammable [133].

Above and beyond their utility as solvents, ILs were also used as diluents in polymeric membranes to sustain enough conductivities for different applications including solar cells [132], [134], [135], electromechanical transducers [136]–[138] and lithium batteries [139], [140].

The effect of ILs on human health and their toxicity profile is crucial after their progressive widespread use. In a study conducted previously in our lab, it was concluded that the insertion of ILs with micellar systems influences curcumin's binding properties. Moreover, it was found that ILs reduced the critical micellar concentration of charged surfactants which encourages their formation, whereas the effect was not similar to the micelle formed of non-ionic TX100 which was discouraged [141]. The goal of this study is to inspect the effect of ionic liquids on the modulation of DBPC and DAPC liposomes membranes properties by monitoring the fluorescence of curcumin, as a molecular probe, and to compare the results with our previous studies on DMPC and DPPC [99], [142].

DBPC (1,2-dibehenoyl-sn-glycero-3-phosphocholine) and DAPC (1,2-diarachidoyl-sn-glycero-3-phosphocholine) are two phosphatidylcholine (PC) liposomes that can be used as a model for the cell membrane, which is mainly composed of phosphatidylcholine. DBPC has a longer carbon chain than DAPC liposomes. It is very crucial to study the interaction of liposomes with drug/ guest molecules and to understand what factors or additives can alter its physiochemical properties because they illustrate the pharmacokinetic behavior and pharmacological response of the system [143]–[145].

Curcumin, a yellow polyphenol extracted from the roots of Curcuma longa, is well known appreciated to its bio-pharmaceutical activities as well as to its strong fluorescence enabling it to be a biocompatible probe for bio-imaging and sensing applications as well as

for determining membrane properties [146]. As a matter of fact, Nagahama et al prepared

nanoparticle of dextran-curcumin conjugate which was effectively used for delivery into

cancer cell where it exhibited strong fluorescence response for live-cell imaging [147].

Mondal et al used curcumin as a probe to determine the critical micelle concentration for

surfactants by measuring its absorption and fluorescence profiles [148]. In another study,

curcumin was used as a sensor for cyanide ions in aqueous media and living cells based on

the fact that its fluorescence emission is quenched in the presence of cyanide [149].

In chapters III and IV, it was proved that curcumin is being encapsulated inside

DAPC and DBPC liposomes bilayers along with studying its effect on membrane's

properties. The aim of this chapter is to determine the partition coefficient of curcumin into

both liposomes in the presence of different concentrations of bmit (1-buytl-3-methyl

imidazolium tetrafluoroborate), a short chain IL by monitoring the fluorescence emission of

curcumin.

B.   Sample preparation

Because of poor solubility, the stock solution of curcumin was made in spectroscopic grade

methanol. The final concentration of methanol was negligible in the measurement sample,

to avoid affecting the sample (Less than 0.1%).

A stock solution, ~7.89 mM, of bmit IL was prepared by dissolving 3.5 mg of bmit in 2 mL

of chloroform/ethanol with a 1:1 ratio.

The solutions of the analyzed samples were prepared first by heating the liposomes'

solutions to a temperature above the phase transition temperature of each (75°C for DAPC

and 85°C for DBPC), then adding 150 μL of curcumin solution, the desired volume of the

liposomes and finally adding the desired volume of IL of the required concentration (5, 10 or 25 μ from the stock. The solutions were equilibrated for 30 min before analysis (See Figure 32).
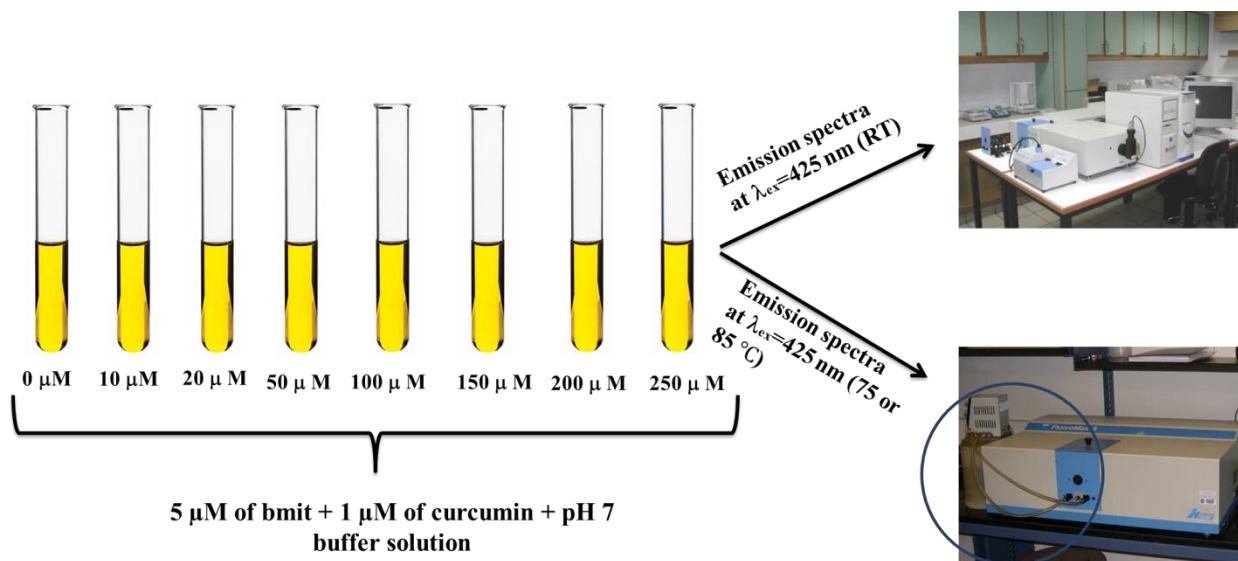
Figure 32 Scheme illustrating the preparation of the samples for ionic liquid effect.

C.   Results and discussion

The lipophilicity of a compound can be estimated by obtaining the partition coefficient Kp. The value of Kp gives information about the portion of the compound associated with the lipid. Fluorescence spectroscopy is the technique used when the compound is fluorophore and its emission intensity depends on the polarity of its environment.

In the presence of different concentrations of bmit IL, Kp was estimated from the slope and intercept of the double-reciprocal plot of 1/F vs 1/[DAPC] and 1/[DBPC] following the equation $\frac{1}{F} = \frac{55.6}{KpFo} \times \frac{1}{[liposome]} + \frac{1}{Fo}$

The phase transition temperature for DAPC and DBPC were determined in chapters III and IV where their values were found to be 64°C and 74°C respectively, below which the bilayers of the liposomes are tightly packed and order and above which they are more fluid and random.

Accordingly, the partition coefficients for curcumin in both liposomes and after adding bmit IL were successively measure at RT, at 75 °C for DAPC and at 85°C for DBPC. The concentration of curcumin was kept 1 µM in all trials, less than 2 molar percentages of the phospholipid concentration, or at a molar ratio 1:50, to minimize the effect of curcumin on liposomes as per previous chapters.

The double-reciprocal plots in all trial for 1/F vs 1/[liposome] were found to be linear.

The results obtained were similar to the results obtained in absence of bmit. That is, the fluorescence emission intensity for curcumin increased as the concentrations of DAPC and DBPC increased.

1. *DBPC liposomes in the presence of IL*

The fluorescence emission spectra of curcumin in the presence of 5 µM bmit at various DBPC concentrations in both phases are given in Figures 33 A&B respectively. As the results indicate, in the presence of bmit, curcumin can still penetrate into the hydrophobic core of the membrane.
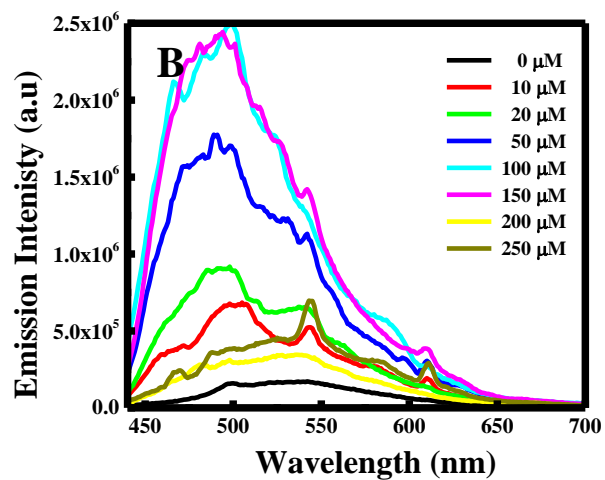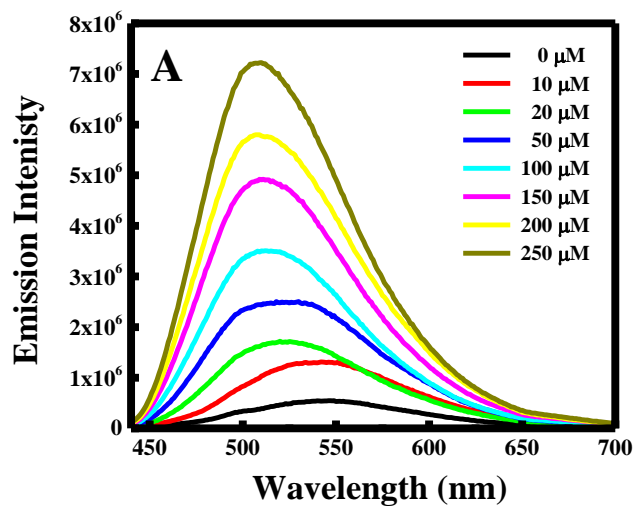
Figure 33 Fluorescence emission spectra in the presence of 5 μM bmit of (A) curcumin in various concentrations of DBPC liposomes at RT; (B) of curcumin in various concentrations of DBPC liposomes at 85℃.

To further investigate the modulating effect of bmit on the membrane as an external additive, the partition coefficient of curcumin in DBPC membrane in the presence

of different concentration of bmit in both phases is established. The corresponding

representative plots are given in Figure 34A&B.
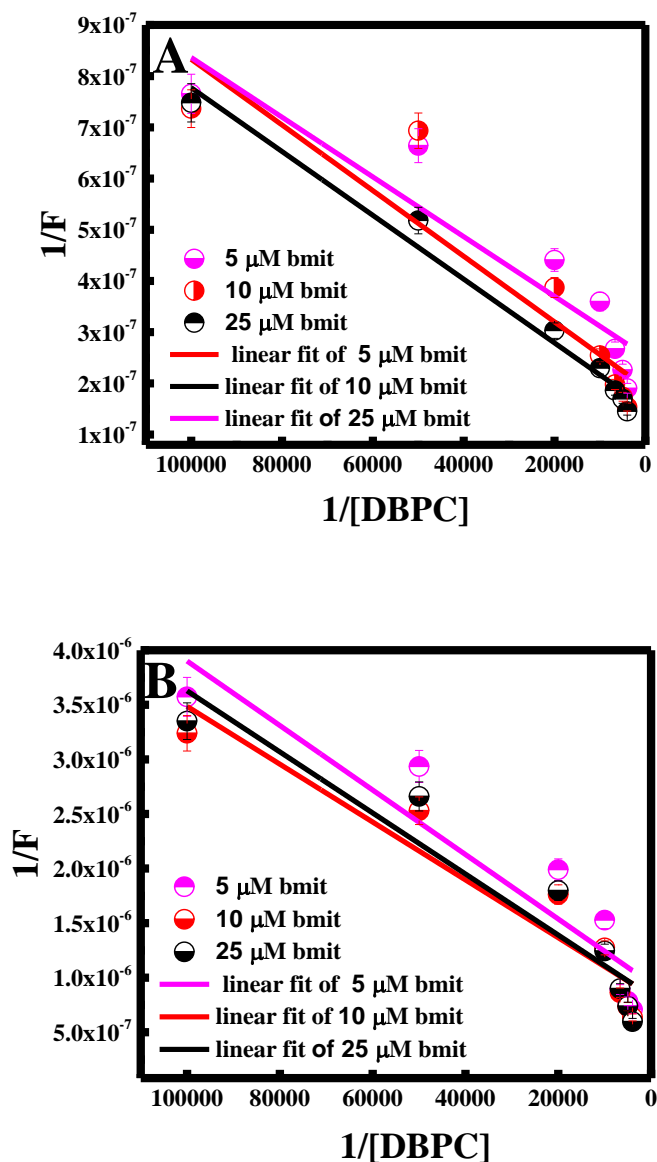
Figure 34 Comparative Plot of 1/F vs 1/[DBPC] in the presence of different bmit
concentration of (A) curcumin in various concentrations of DBPC liposomes at RT; (B) of
curcumin in various concentrations of DBPC liposomes at 85℃.

The partition coefficient values of curcumin into DBPC in the presence of bmit are summarized in Table 8. In the solid gel phase, the partition coefficient of curcumin increased 5-folds compared to that in the absence of bmit. However, further increase of bmit concentration to 10 μM appreciably decreased the Kp values and continued to decrease with increasing bmit concentration.

	Solid gel Phase (x10^6)	Liquid crystalline phase (x10^6)
Buffer Ph=7	0.46	1.80
5 μM bmit	2.42	1.78
10 μM bmit	1.66	1.74
25 μM bmit	1.38	1.65

Table 8 Different Kp values of curcumin in the absence and presence of different bmit concentration at RT and 85℃.

This result can be explained by the fact that there are two interactive forces of bmit running against each other: the bulky head group of bmit which needs to be accommodated around the negative phosphate head group of the liposome and the hydrophobic effect of the butyl group that can favorably interact with hydrophobic tail of liposomes. That being said, at low bmit concentration, steric hindrance between the head group of IL and polar head groups of liposomes dominates which keep bmit near the head group of the liposome making it possible for curcumin to penetrate inside the membrane.

However, when bmit concentrations was increased to 10 and 25 μM, the increase in concentration helps hydrophobic butyl group overcomes the steric hindrance and get buried more deeply in the membrane producing a kind of order to the more fluid liposome which make it less flexible and obstruct the passage of curcumin by not leaving for it a space to be introduced away from water, the reason why its partition coefficient decreased.

On the other hand, in the liquid crystalline phase, the addition of bmit did not appreciably changed the partition of curcumin and a slight decrease in the Kp values as the concentration of bmit increases was observed.

2. *DAPC in the presence of IL*

The same trend regarding the Kp values in the solid gel phase was obtained when the modulation of membrane properties by bmit on DAPC was studied. The fluorescence emission spectra of curcumin in the presence of 5 μM bmit at various DAPC concentrations in both phases are given in Figures 35 A&B respectively.
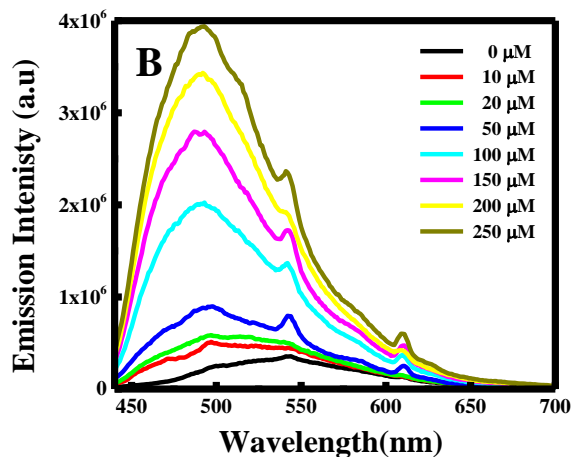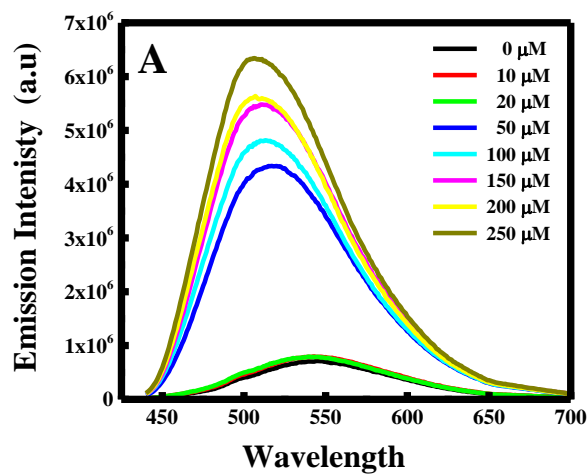
Figure 35 Fluorescence emission spectra in the prsence of 5 μM bmit of (A) curcumin in various concentrations of DAPC liposomes at RT; (B) of curcumin in various concentrations of DAPC liposomes at 75℃.

The corresponding representative plots representing the partition coefficient of curcumin in DAPC membrane in the presence of different concentration of bmit are given in Figure 36A&B.
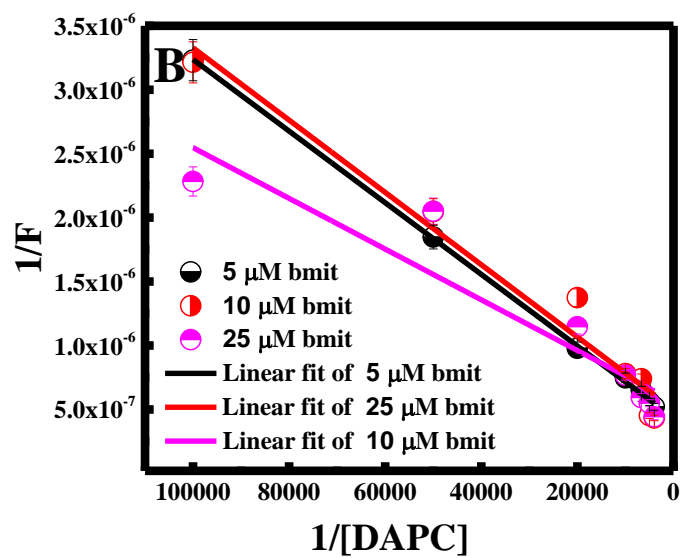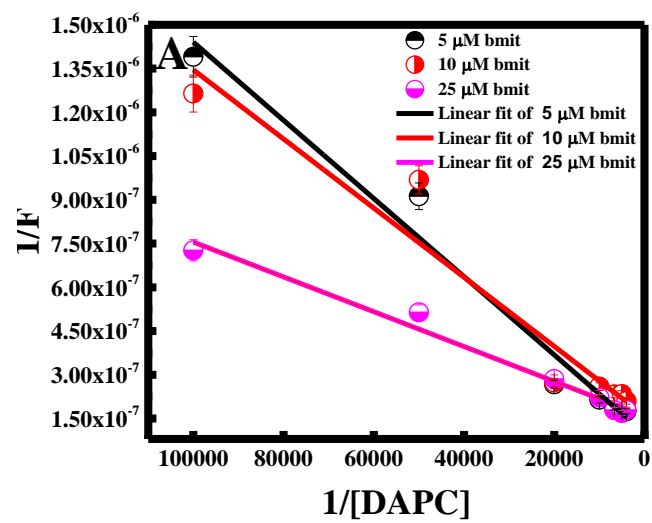
Figure 36 Comparative Plot of 1/F vs 1/[DAPC] in the presence of different bmit concentration of (A) curcumin in various concentrations of DAPC liposomes at RT; (B) of curcumin in various concentrations of DAPC liposomes at 75℃.

However, when DAPC is in its liquid crystalline phase, Kp initially increased for 5 µM of bmit and then decreased by not varying much as the bmit concentration was increased (See Table 9).

This can be explained by the fact that for the longer chain DBPC, the hydrophobic interactions are stronger and thus bmit can intercalate more between the acyl chains. However, DAPC is shorter and at a low bmit concentration, bulky steric hindrance forces are still more dominant and bmit will remain at the surface causing more curcumin to penetrate initially until raising the concentration.

	Solid gel Phase (x10^6)	Liquid crystalline phase (x10^6)
Buffer Ph=7	0.12	0.35
5 µM bmit	1.47	1.58
10 µM bmit	0.75	0.99
25 µM bmit	0.42	0..87

Table 9 Different Kp values of curcumin in the absence and presence of different bmit concentration at RT and 85℃.

3. Comparative study between DAPC and DBPC liposomes

Interestingly, it was also noticed that in all trials, Kp values obtained for DBPC were higher than DAPC values. This is owed to the longer carbon chain that DBPC has which will permeate the higher encapsulation of curcumin inside its hydrophobic core as it can get more deeply buried.

The role of IL as well as its behavior of the short butyl bmit IL is in accordance with the results obtained in our previous studies with where bmit incorporation into the membrane showed a dependence on the type of the dominant interactions [99], [142].

D.   Conclusion

ILs, which are being widely used in various disciplines in chemistry, are shown to modulate the partition of the powerful molecular probe curcumin into liposomes membranes.

1-buytl-3-methyl imadazolium tetrafluoroborate (bmit) IL was shown to affect the permeability and fluidity of DAPC and DBPC liposomes.

The partition coefficient of curcumin in the liposomes membrane depends on the temperature as it varies between the two different states, solid gel phase and liquid crystalline phase. In the solid gel phase and for both liposomes, the partition coefficient of curcumin increased remarkably for low bmit concentrations and then decreased as the bmit concentration increases whereas in the liquid crystalline phase, it did not show an important variation as saturation occurs. The influence of carbon length chain was noticed where the longest chain liposomes DBPC has higher Kp values in all trials.

CHAPTER VI

CHARACTERISATION AND ANTI CANCER ACTIVITY OF LIPOSOMAL CURCUMIN AGAINST BREAST AND PANCREATIC CANCER CELL LINES

A.   Introduction

Worldwide, cancer is considered the second cause of death. Based on the cancer statistics done Siegel et al. in 2014, only in the United States 1,665,540 people suffered from cancer, where 585,720 of them died due to this disease [150]. Therefore, cancer is one of the serious harms that alter the human health in all societies.

The principal percentage of cancer types that occurs in men, are found in the prostate, pancreas, lung and bronchus, urinary bladder. Hence, in women, cancer prevalence is highest in the breast, pancreas, lung and bronchus, thyroid [151] . These facts shows that pancreatic and breast cancer constitute a main type of cancer in men and women, respectively [152] .

For several years, breast cancer has had the maximum rate of all cancers in women worldwide [153], [154]. Breast cancer is a gathering of diverse malignancies that exhibits in the mammary glands [155] . Initially, nicotine stimulates breast cancer metastasis by stimulating N_2 neutrophils and generating pre-metastatic niche in lung [156] . Several human breast cancer cell lines recognized from metastatic breast cancer specimens are presented. The most deliberate is MCF-7, an estrogen receptor (ER)-positive cell line derived from a pleural effusion in a patient with breast cancer [156].

Yet, pancreatic adenocarcinoma (PA) is a violent disease that grows in a comparatively symptom-free way and is frequently advanced at the time of diagnosis [157]. As is common in epithelial tumors, carcinogenesis develops over a growth of transmutations and genetic lesions inducing an activation of oncogenes and inactivation of tumor suppressor genes [158]. Pancreatic cancer usually occurs in the age of 70s and rarely occurs before the age of 40 [159]. The main causes for pancreatic cancer include tobacco smoking [160], and obesity [161]. An important cell line of the pancreatic disease is Capan-1 cell lines. Capan-1 is a human pancreatic ductal adenocarcinoma cell line. These cells grow in adherent tissue culture and spectacle epithelial morphology [157].

However, cancer can be cured by surgery, chemotherapy, radiation or hormonal therapy. Yet, these operations suffer from the lack of propensity of cancers to attack contiguous tissue or to spread to distant sites by microscopic metastasis [162]. Moreover, chemotherapy and radiotherapy can have an undesirable consequence on normal cells [163]. For this reason, it was necessary to develop treatments with negligible effects.

Consequently, nanotechnology has been used as an adequate alternative for cancer therapy [164]. Indeed, nanotechnology possesses the potential to enhance the selectivity and strength of chemical, physical, and biological methodologies for stimulating cancer cell death. This is effective while diminishing collateral toxicity to nonmalignant cells. Hence, materials on the nanoscale are progressively being targeted to treat cancer cells with abundant specificity over both active and passive targeting [165].

Liposomes are on one of the most used nanomaterials for cancer treatment. Liposomes are spheres in the range of 10-100 nm, composed either from natural or synthetic phospholipid bilayer membrane and water phase cores [166]. Based on the

amphiphilicity of phospholipids, hydrophobic drugs can be easily incorporated in the bilayer membrane [167].

Curcumin, defined as the active ingredient of the Curcuma longa plant, has expected great devotion over the past two decades as an antioxidant, anti-inflammatory, and anticancer agent [168].

Curcumin alone inhibits the proliferation of different cell lines. For example curcumin has anti-tumor effect on human cervical carcinoma HeLa cells [169], MCF-7 cell lines [170], Capan-1 cell lines [171], colorectal cancer [172], etc.

This yellow compound aches from its low oral bioavailability which obstructs its application as therapeutic agent [173]. Accordingly, the encapsulation of curcumin into the liposomes stabilizes the loaded curcumin proportionally to its content and increases its solubility [174]. Frequently, curcumin is being encapsulated into DMPC, DPPC, DSPC liposomes in order to enhance its anti-cancer activity [81], [175].

In this work, curcumin will be encapsulated for the first time in diarachidonyl phosphatidyl choline (DAPC) liposomes, enhancing therefore its anti-cancer activity against MCF-7 breast cancer cell lines and Capan-1 pancreatic cancer cell lines.

B.   Methods of preparation

1. Culture of MCF-7 and Capan-1 cancer cells

MCF-7 and Capan-1 cells were cultured in a completed DMEM high glucose media, where 10% FBS, 1% penicillin/streptomycin were added to free DMEM high glucose. MCF-7 and Capan-1 cells were cultured in a 10 mm petri dish and kept at 37°C in

an incubator with a humidified atmosphere containing 95% O_2 and 5% CO_2 until they reached 80-90% confluency.

2. *Cytotoxicity study by MTT proliferation Assay*

The cytotoxicity study is summarized in Figure 37. After treating the cells with curcumin, chitosan, DAPC, DAPC-Cur NCs, and DAPC-Cur-Chi NCs; MTT assay was used to measure the cell activity. MCF-7 and Capan-1 cells were seeded at a density of 5000 cells per well in 96-well plates. At 30% confluence, cells were subject to a concentration equal to 22 μM for the different treatment. After 48 and 72, hours, 1mg/mL of MTT was added to the cells and kept for 1 hour incubated at 37°C. Later on, the media with the MTT were eliminating from the 96-well plate and DMSO was added in order to solubilize the formazan crystals. ELISA microplate reader, Thermo/LabSystems 352 Multiskan MS, was used to read the plates at a wavelength of 595 nm.

The cells were seeded in 96 well-plate and treated with different analytes
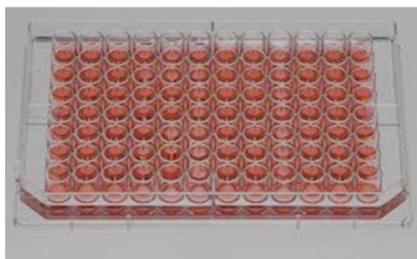
1-The cells were incubated for 48 and 72 hours

2- Addition of MTT

Formation of Formazan crystals

Addition of DMSO
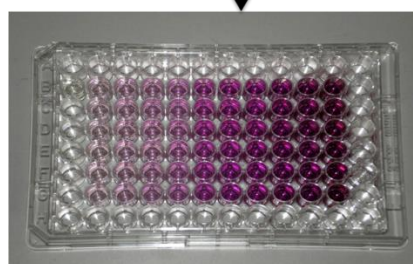
ELISA analysis

Figure 37 Schematic illustration of the cytotoxicity study by MTT proliferation study.

C.   Results and discussion

1. Synthesis and characterization of the synthesized DAPC-Cur NCs with and without chitosan

The preparation of liposomal curcumin was carried out based on the thin film hydration method. This method is considered one of the simplest ways to prepare liposomes. This method includes the formation of a thin lipid film in a vial after the evaporation of the organic solvents. Afterwards, the addition of dispersion medium, heterogeneous liposomes is formed [176]. The encapsulation of curcumin into the DAPC

111

membrane was verified initially through UV-Visible and fluorescence emission analysis respectively.

As shown in Figure 38, curcumin showed a broad maximum absorption band at wavelength $\lambda = 425$ nm. This maximum absorption wavelength is due to the electronic dipole allowed π-π* type excitation [177]. This absorption wavelength is red shifted to reach a maximum at $\lambda = 462$ nm.
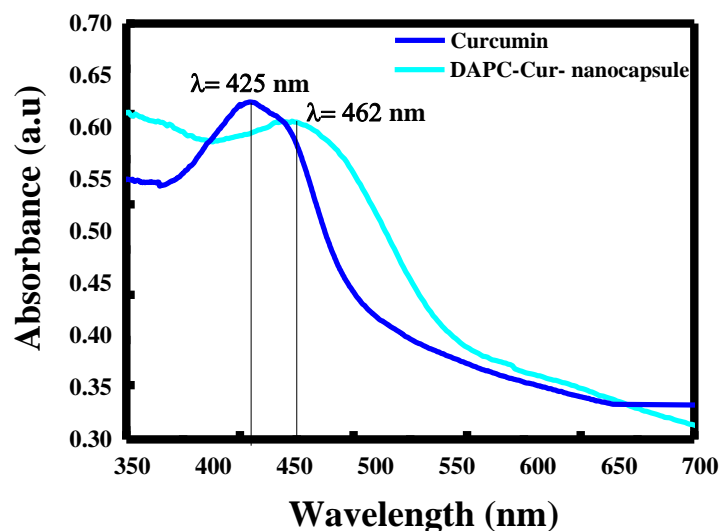
Figure 38 Uv-Visible spectrum and of pure curcumin and DAPC-Cur nanocapsules.

This shift confirms that curcumin got buried into DAPC membrane where it becomes deprotonated. This bonding, is also verified in the fluorescence emission spectrum, where the emission wavelength is blue shifted from 555 nm to 516 nm (See Figure 39). This shift indicates that curcumin is strongly portioning into the vesicle of the liposomes. This is due to the transfer of curcumin from polar to less polar environment.

Same results were obtained with Kunwar et al. [177] and El Khoury et al. [178] when

encapsulating curcumin into DMPC and DPPC liposomes.
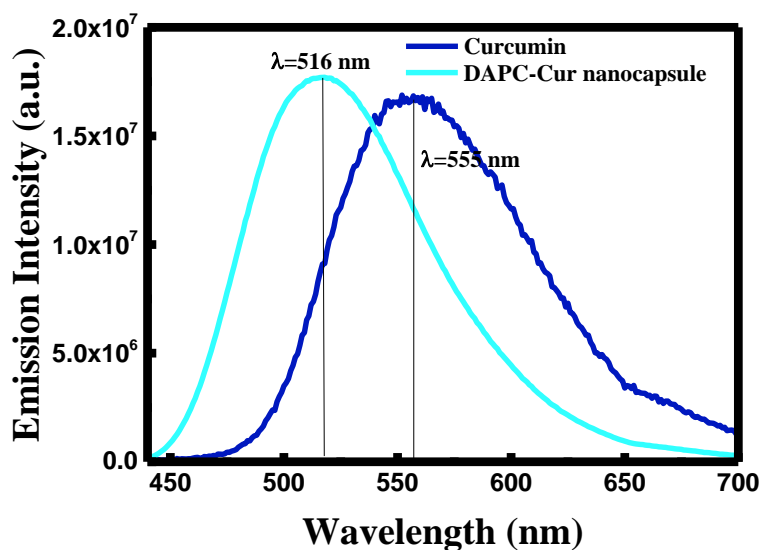
Figure 39 Fluorescence emission spectrum of pure curcumin and DAPC-Cur nanocapsules.

Moreover, SEM was established to confirm the spherical shape of the prepared

NCs. According to Athira et al., curcumin exhibit a flat rod like structure [179].
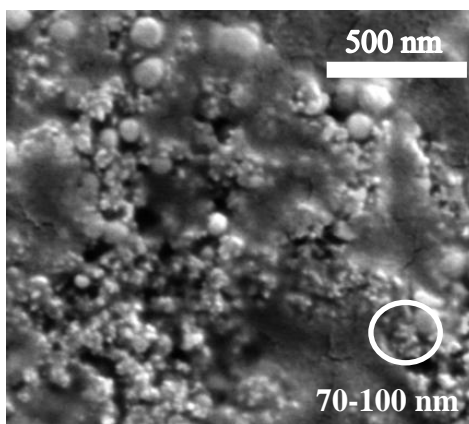
Figure 40 SEM image of DAPC-Cur nanocapsules.

However, as depicted in Figure 40, the formed nanoparticles are presented in a spherical shape. The difference in the shape, identify the successful encapsulation of curcumin into the liposome membrane.

Furthermore, X-Ray diffraction analysis was done and the results are depicted in Figure 41. As clearly observed, curcumin diffraction peak are available in the range of the 2θ 10°–30°. These diffraction peaks reveal the high crystallinity nature of the curcumin, where the crystallinity degree was equal to 87%. However, these peaks were totally absence in the X-Ray pattern of the DAPC-Cur nanocapsule showing an amorphous structure. The crystallinity degree of the nanocapsule was equal to 20.54%. This decrease in the crystallinity degree demonstrates the total entrapment of curcumin into the liposome membrane.
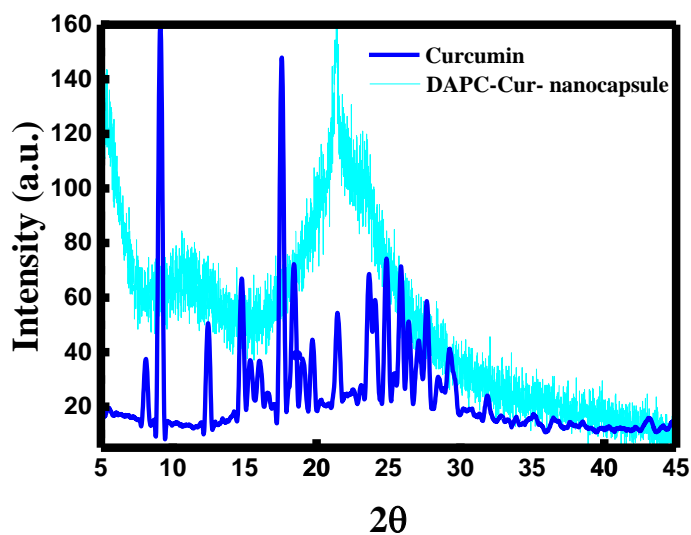
Figure 41 X-Ray diffractogram of pure curcumin and DAPC-Cur nanocapsules.

Generally, liposomes ache from a short half-life and from the leakage and fusion of the encapsulated drug [180]. These drawbacks prompt the use of additional polymer to protect the encapsulate curcumin. For this reason, chitosan oligosaccharide was added as a coating layer on the surface on the liposomal curcumin.

The deposition of chitosan layer on the surface of the liposomal curcumin was verified through zeta potential analysis.
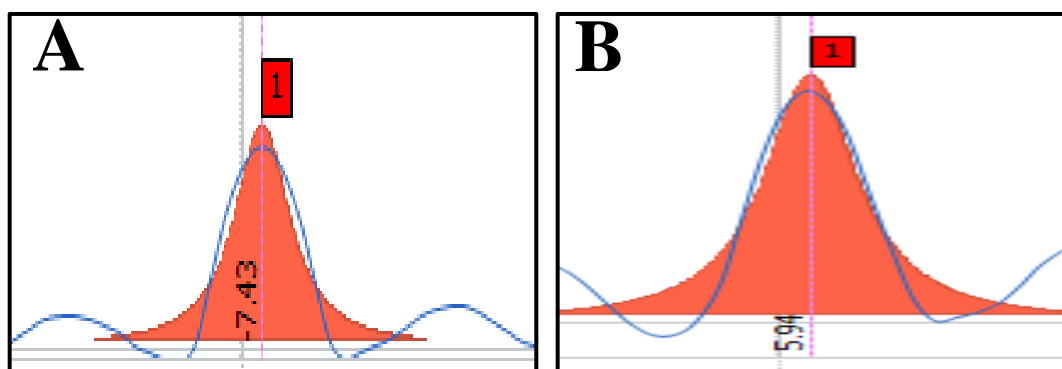
Figure 42 Zeta potential analysis of DAPC-Cur nanocapsule (A) in the absence of chitosan and (B) in the presence of chitosan.

It is obvious from Figure 42A, liposomal curcumin surface was negatively charged with a value equal to -7.43 mV. This is due to the location of the phosphate group of the liposomes towards the external aqueous component of the lipid bilayer. The zeta potential value became more positive in the presence of chitosan. Hence, liposomal curcumin coated with chitosan exhibits a positive surface charge equal to 5.94 mV (See Figure 42B). This variation in the surface charge is related to the presence of chitosan owing an amino group.

Indeed, the effectiveness of chitosan addition was evaluated through thermogravimetric analysis (See Figure 43). It is remarkable, that curcumin started to

degraded at 200℃, with a mass loss around 70%. As for DAPC-Cur NCs the mass loss

decreases to 40% due to the encapsulation of curcumin into the liposomes. The addition of

chitosan has reduced moreover the mass loss to 25%, generating more stable NCs.

Additionally; no mass loss was occurred around 100℃, revealing the formation of

dehydrated NCs.
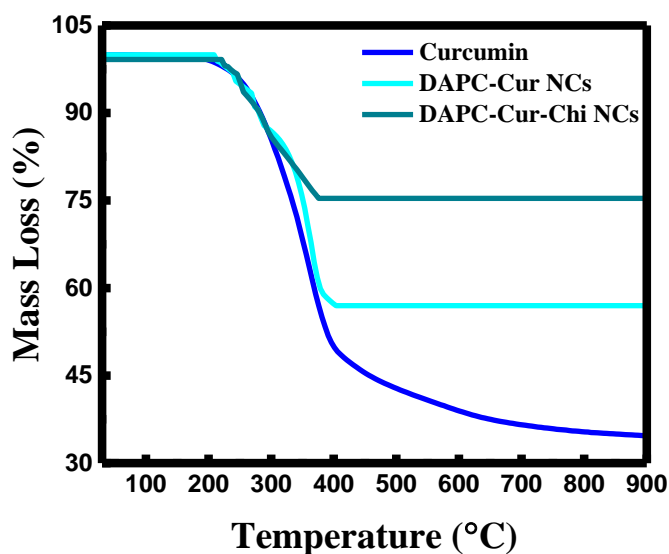
Figure 43 Thermogravimetric analysis of pure curcumin and DAPC-Cur nanocapsules
prepared in the presence and absence of chitosan.

2. *Cytotoxicity effect against cancerous cell*

a) Cytotoxicity effect of curcumin against MCF-7 and Capan-1 cell lines

The successful preparation of liposomal curcumin coated with chitosan was

proceeded by emerging their anticancer effect on MCF-7 and Capan-1 cell lines.

Actually, the cell cycle, organized in the subsequent stages, leads to the cell growth and division. First of all, in G1 stage, the cell propagates and chromosomes start to replicate. In the second phase which is the S phase, the DNA replicates and the chromosomes tend to be duplicated. In a third step, G2 phase occurs and represents the gap amongst DNA synthesis and mitosis. Finally, in the mitosis phase, nuclear and cytoplasmic division takes place, inducing the formation of two daughter cells [181].

Therefore, curcumin acting as anti-cancer agent inhibits the proliferation of cancerous cells. Yet, the mechanisms of act by which curcumin displays its distinctive anticancer activity comprise initially the apoptosis, the inhibition proliferation and the invasion of cancers by suppressing a variability of cellular signaling pathways [168].

The cancerous cell lines were exposed to several concentration of curcumin in the range of 0-30 μM for 48 hours, in order to get the IC_{50}. The half maximal inhibitory concentration (IC_{50}) is a quantity of the potency of a substance in inhibiting a precise biological or biochemical function. In other words, IC_{50} is a mathematical measure that postulates how much of a specific inhibitory material, as a drug, is required to inhibit 50% of a definite biological progress or biological element [182].

As shown in Figure 44, after 48 hours, 50% of the proliferation was inhibited when treated with curcumin. Therefore, the IC_{50} of curcumin was established to be equal to ~22 μM and ~20 μM for MCF-7 and Capan-1 respectively. These values were identical to the IC_{50} values found previously. In fact, after treatment for 48 hours, Mirakabad et al. have estimated the IC_{50} of curcumin to be equal to 21.32 μM for MCF-7 [183], and Sutaria et al. have exhibit the IC_{50} of curcumin to be equal to 19.6 μM for Capan-1 cells lines [184].
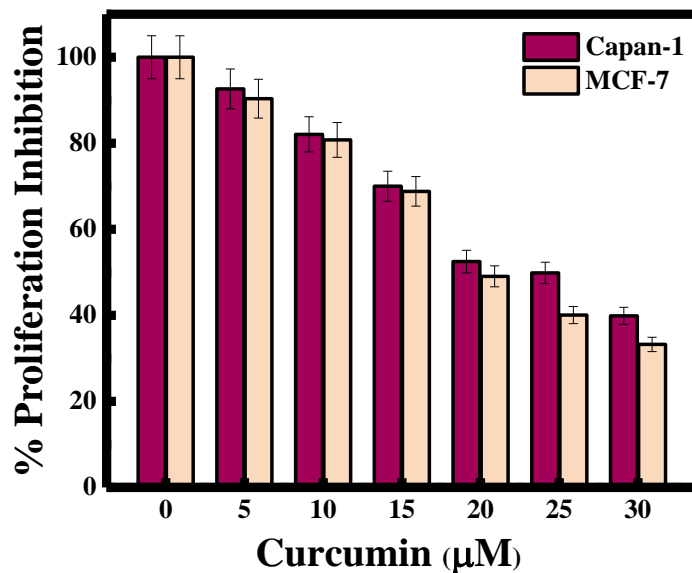
Figure 44 Curcumin cytotoxicity effect against MCF-7 and Capan-1 cell lines.

b) Cytotoxicity effect of DAPC-Cur-Chi against MCF-7 and Capan-1 cell lines

The activity of curcumin as anticancer reagent can be enhanced when encapsulated into liposomes. Hence, the use of liposomes in cancer treatment increases the activity of curcumin by releasing it to the specific target.

Based on the IC_{50} of curcumin, the cancerous cells were treated with the same concentration using DAPC, DAPC-Cur NCs, DAPC-Cur-Chi NCs, and chitosan alone. The treatment was done for 48 and 72 hours. As presented in Figure 45A&B, no remarkable effect was noticed when treated Capan-1 and MCF-7 cancerous cell line with chitosan and DAPC liposomes.
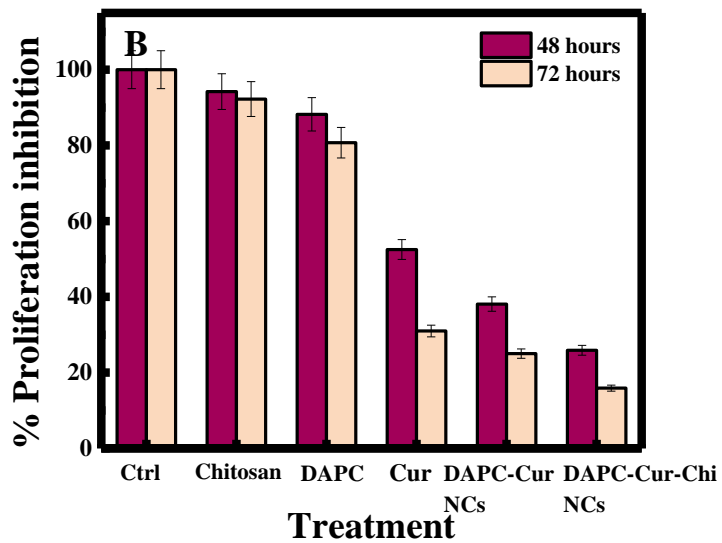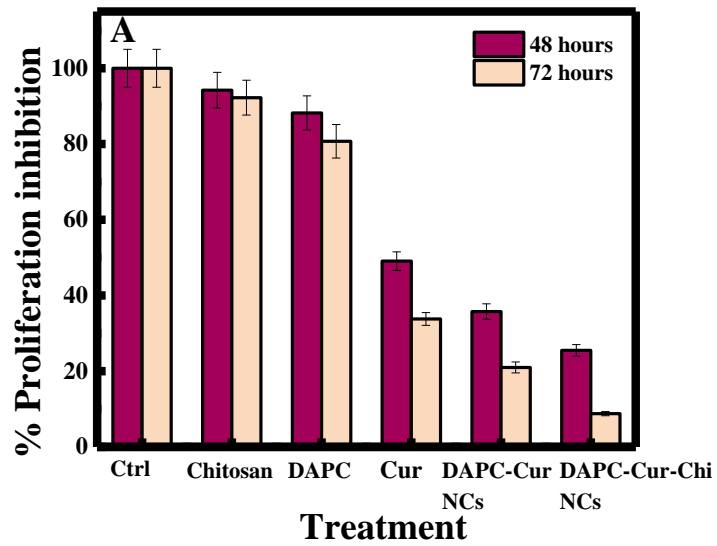
Figure 45 Cytotoxicity effect of different treatment against (A) Capan-1 and (B) MCF-7 cancerous cell lines respectively.

Thus, the use of DAPC-Cur NCs and DAPC-Cur-Chi NCs improves strongly the inhibition of Capan-1 cancer cells (Figure 45A). Hence, when treated with 20 μM (3

µg/mL) both nanocapsules, the inhibition proliferation was increased up to 65% after 48 hours.

Consequently, a remarkable inhibition proliferation was observed after 72 hours when treated with DAPC-Cur NCs, where ~75% inhibition was acquired. Meaning that, DAPC liposome enhances the anti-cancer activity of curcumin by specifying its target. Yet, after the same treatment duration using DAPC-Cur-Chi NCs, ~90% inhibition was determined. This difference in the value is linked to the presence of chitosan, where chitosan is acting as a protective layer and ensure the total entrapment of curcumin into DAPC liposomes, preventing its leakage.

Similarly, DAPC-Cur-Chi NCs have shown a good potential against MCF-7 cancerous cells (See Figure 45B). More than 70% of the cancerous cells were inhibited when using 3 µg/mL of DAPC-Cur-Chi NCs after 48 hours. Furthermore, 85% where inhibited after 72 hours.

Finally the efficiency of our nanoparticles was compared to different anti-cancer reagent used in the literature (See Table 10).

Cell Type	Anti-cancer agent	Concentration	% proliferation	Reference
MCF-7	Gold nanoparticles	20 µg/mL	50 %	[185]
	DSPC-Cur	10 µg/mL	65 %	[186]
	DAPC-Cur-Chi NCs	2 µg/mL	85 %	Our work
Capan-1	GA-MNP-Fe$_3$O$_4$ NPs	20 µg/mL	60 %	[187]
	DPPC-Cur	10 µg/mL	75 %	[188]
	DAPC-Cur-Chi NCs	2 µg/mL	90 %	Our work

Table 10 Different anti-cancer reagent used for the treatment of MCF-7 and Capan-1 cell lines.

D.   Conclusion

To sum up, the activity of curcumin as anticancer agent was verified, were curcumin inhibits the proliferation of MCF-7 and Capan 1 cancerous cell line. The IC50 of curcumin was found to be equal to 22 and 19 µM for MCF-7 and Capan-1 rescpectively. However, for the same concentration the matrix liposomal curcumin coated with chitosan enhances the anti-cancer activity of curcumin where the percentage inhibition was equal to 85% and 90% for MCF-7 and Capan-1 cell lines.

CHAPTER VII

DBPC LIPOSOMAL CURCUMIN WITH CHITOSAN LAYER: A SELECTIVE NANOSENSOR FOR THE DETECTION OF RIBONUCLEIC ACID

A.   Introduction

Nanosensors, or nanotechnology-enabled sensors, are having impressive impact in providing alternative solutions in biological sensing. This permits advanced detection sensitivity and specificity for health assessments[189].

By definition, a sensor is a material that responds to a physical, chemical or biological specification and translates its response into an output or signal change [190]. The development of nanosensors have emerged due to many compelling drivers such as the dramatic increase of chronic diseases which cause mutations in RNAs which requires upgraded, low-cost, rapid preparation and easy detection sensors to identify early stage disease [191].

To establish an ideal detection of the abnormal expression of a certain disease, the nanosensor should not interfere with the tracked specific analyte. This is hardly achieved with the traditional sensors like the microelectrode or the fiber optical sensors, owing to their relatively large area and size which cause physical noise [192].

Fluorescent sensors have so far been exerting numerous applications in sensing, due to their fast response, sharp signal with the minimum background noise and interferences along with the very straightforward experimental procedure [193]. Badagu et al have published a study in which they used boronic acid containing fluorophores to

monitor tear glucose level [194]. In previous studies, curcumin was used as a probe to detect DNA when encapsulated in poly(diallylammonium chloride-co-sulfur dioxide) [195]. In addition, when curcumin was encapsulated into Poly(Ethylene Oxide)-Block-Poly(Propylene Oxide)-Block-Poly(Ethylene Oxide), the detection of both RNA and DNA was achieved [196].

Being a fluorescent transducer, curcumin is used in biomedical applications to detect RNA [197] . In fact, fluorescence probing provides more detailed information spanning the sensitivity to a single molecule, which is why this technique is more favored over the classical microscopy technique [198].

Biological benefit of curcumin encompasses anti-inflammatory, anticancer and anti-amyloid activities [199]–[203]. Additional benefit of curcumin is its use as a probe molecule to study the environment of solvents [107], micelle [141], liposomes [99] and proteins [204], [205]. Furthermore, curcumin possesses a compelling absorption and fluorescence profile, which has render it as a useful molecular probe for many sensing applications [206].

 Physiochemical properties of curcumin can be extremely improved after being encapsulated in liposomes. When it's incorporated inside the liposomes membrane, its solubility, bioavailability and biostability is enhanced which results in higher intensity of the fluorescence signal [207], [208].

In this study, curcumin was encapsulated inside DBPC liposomes, in the presence and absence of a chitosan coating layer. Moreover, the encapsulation efficiency and loading capacity, without and with chitosan, were obtained and compared in order to use the optimal system for the detection of RNA.

B. Methods of preparation

1. *Determination of Encapsulation Efficiency (EE) and Loading Capacity (LC)*

Encapsulation Efficiency and Loading Capacity were calculated for the prepared liposomal curcumin, in the absence and presence of chitosan layer. In both cases, liposomal curcumin solution was centrifuged at 15000 rpm for 20 minutes.

EE and LC were calculated based on measuring the absorbance of the supernatant after centrifugation, and based on the precipitate mass obtained after freeze dryer for 24 hours.

2. *Sample preparation for RNA detection*

A stock solution of RNA was prepared by dissolving 5 mg of RNA powder in 5 mL of double distilled water. From this solution, several samples were prepared in the concentration range of 0-500 µg/mL. Each time a definite volume was taken from RNA stock solution and was added to 0.2 mL of the nanocapsules. The volume was completed to 3 mL by adding double distilled water (See Figure 46).

Figure 46 Schematic illustration of RNA sensing sample.

Similarly, 50 µg/mL stock solutions of DNA, thymine, cholesterol, tryptophan, cystine, kreatinine, uric acid, GTP, UTP, CTP and TTP analytes were prepared for interference study.

C.   Results and discussion

1. *Determination of Encapsulation Efficiency (EE) and Loading Capacity (LC)*

Polymers are usually used as a protective layer for the drug and the nanocapsule. Hence, chitosan was used in order to enhance the encapsulation of curcumin into the liposome membrane, inhibiting therefore the release of the drug. The role of chitosan was verified when calculating the value of the encapsulation efficiency and loading capacity in the absence and presence of chitosan.

The calculations of the concentrations and the masses of un-encapsulated curcumin were obtained based on the calibration curve of curcumin in buffer pH = 7 (See Figure 47).
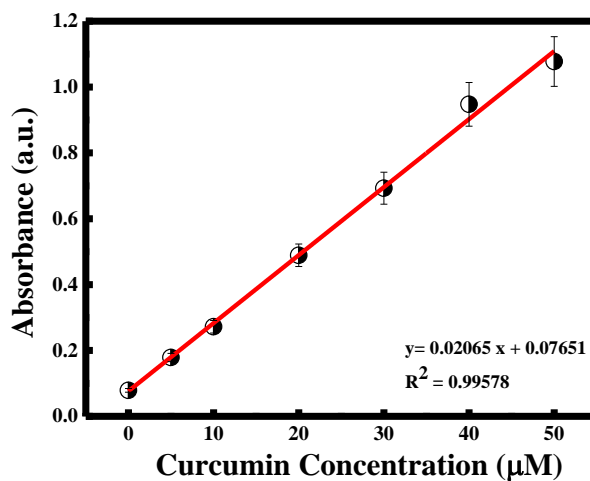
Figure 47 Calibration Curve of free Curcumin at pH 7.

The concentration of free curcumin in the supernatant was calculated using the Beer-Lambert law:

$A = \varepsilon \times C \times l$

where ε is molar extinction coefficient, C is the molar concentration of curcumin and l is the optical path length of the used cuvette (1cm).

The formulas used to calculate EE and LC are given below:

$$EE = \frac{mass\ of\ curcumin\ encapsulated\ in\ liposomes}{mass\ of\ curcumin\ initially\ introduced} \times 100$$

$$LC = \frac{mass\ of\ curcumin\ encapsulated\ in\ liposomes}{mass\ of\ dried\ nanocapsules} \times 100$$

where the mass of curcumin encapsulated in liposomes is the mass of free curcumin subtracted from the mass of curcumin initially introduced.

Hence, the drug loading content was found to be equal to 17.17% and 26.71% for the nanocapsules prepared without and with chitosan respectively. The encapsulation efficiency of the nanocapsule prepared without chitosan was equal to 91%. The high encapsulation efficiency obtained is due to the long chain of DBPC present ($C_{52}H_{104}NO_8P$).

Also, the encapsulation efficiency of curcumin in DBPC, was enhanced in the presence of chitosan, where it was found to be equal to 99.40%. This is expected as the drug loading percentage must increase with the addition of polymer layer.

This is in a good agreement with previous findings where it was clearly demonstrated that the drug loading and encapsulation efficiency of curcumin increased in the presence of a coating layer [209].

Hence, liposomal curcumin coated with a chitosan layer will be used in this study throughout the sensing application.

2. *Sensing of RNA molecule*

The encapsulated curcumin in DBPC liposomes coated with chitosan layer was used to detect RNA in aqueous solution. For this purpose, the fluorescence spectroscopic measurement of curcumin was investigated in the presence of different concentrations of RNA.

Figure 48 displayed the variation of the emission intensity of the nanocapsule with the increase of the RNA concentration. Interestingly, it was found that the addition of different concentrations of RNA has remarkably affected the emission spectrum with ~ 8 fold increase. Moreover, upon the addition of RNA, the position of the peak of the signal was slightly altered with a small shift towards lower wavelength region. The peak was blue shifted from 530 nm to 519 nm with the increase of the RNA concentration.
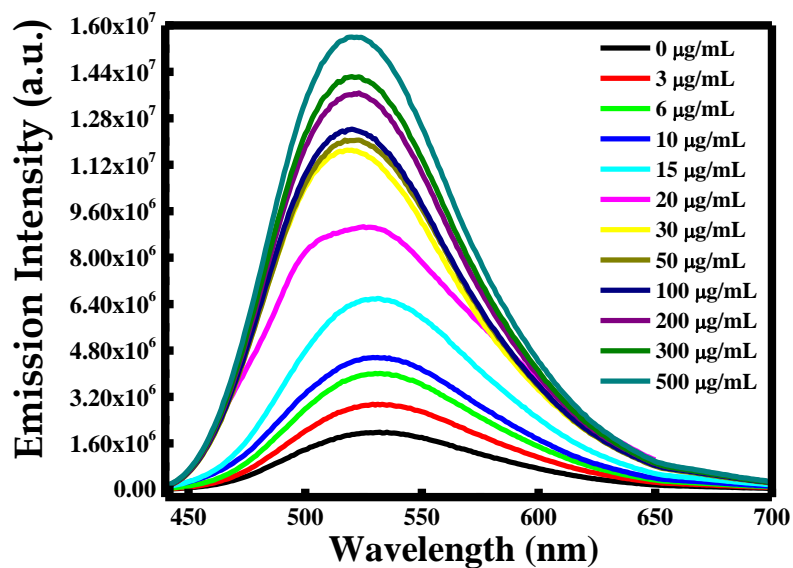
Figure 48 Variation of the emission intensity with the increase of RNA concentration.

a) Sensing mechanism

Logically, both the enhancement of the emission intensity and the shift in the wavelength has occurred as a result of the electrostatic interactions between the positively charged nanocapsules and the negatively charged RNA molecule.

Hence, this interaction promotes aggregation in the solution which further stabilizes the excited state of curcumin inside the liposomes-chitosan nano-capsules resulting in the boost of the emission intensity [195] .

Furthermore, the association of RNA with the nano-capsules shields the exposure curcumin to polar media by increasing the hydrophobic environment around curcumin, which shifts the emission maximum towards the blue region.

These results were verified by zeta potential analysis, where the surface charged of the nanocapsules, RNA and the mixture were equal to 8.87 mV, -9.39 mV and -2.63 respectively (See Figure 49 A-C). These results confirm the change of the surface charge of the mixture when adding RNA being more negative.
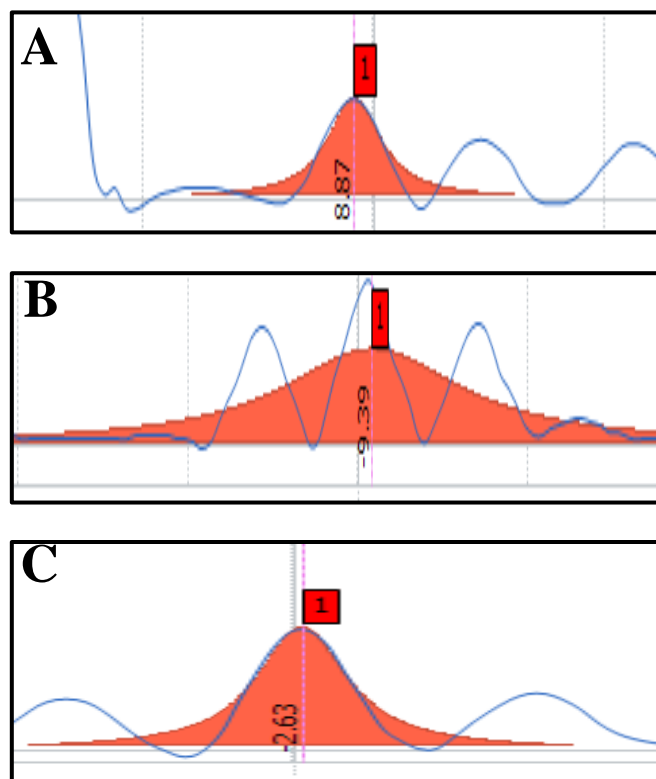
Figure 49 Zeta potential analysis of (A) nanocapsule; (B) RNA solution and (C) mixture of nanocapsule-RNA.

b) <u>Limit of detection (LOD)</u>

The linear correlation of emission intensity of encapsulated curcumin vs. RNA concentration in the range of 0-20 µg/mL and 30-500 µg/mL is plotted in Figure 50A&B.

The linear equations for the two concentration ranges are I= 0.17082x + 0.9275 with a correlation coefficient $R^2 = 0.99147$ and I = 0.00418x + 5.88588 a correlation coefficient $R^2 = 0.99536$, respectively.

Such a good correlation validates the applicability of this method to quantify unknowns RNA samples in the two given concentration ranges.

The limit of detection was found to be 36 ng/mL,

referring to $K \, x \, \dfrac{\sigma}{s}$ criteria, where σ is the standard deviation of the measurements and s is

the slope of the calibration curve.
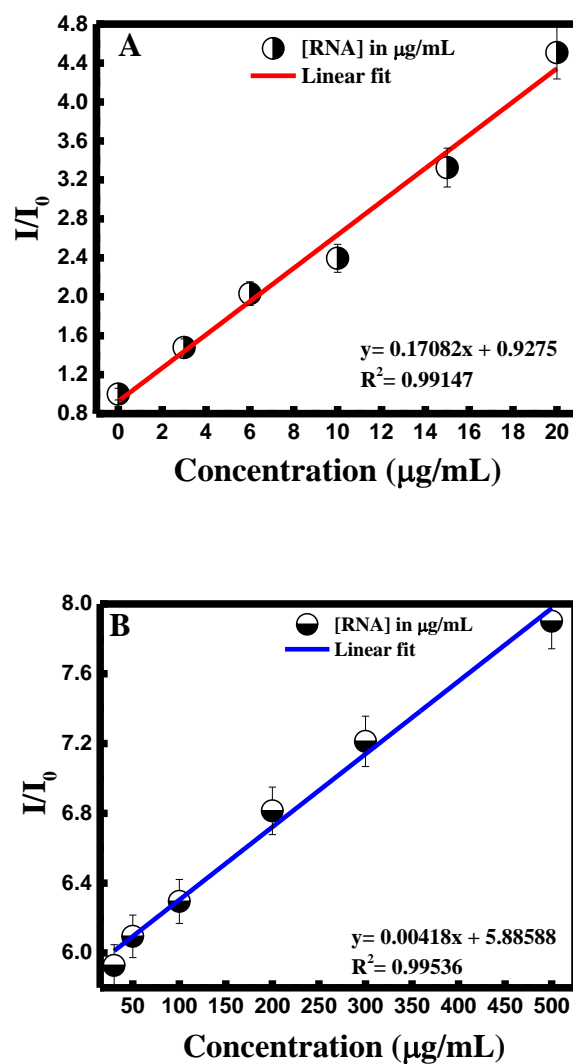
Figure 50 (A) and (B) Linear fit of the proposed method in the range 0 μg/mL-20 μg/mL
and 30 μg/mL-500 μg/mL respectively.

c) <u>Analysis of the interaction site in RNA molecule</u>

Ribonucleic acid (RNA) is a single stranded molecule made up of polynucleotides chains. There exist many types of RNA.

Each nucleotide consists of a phosphate group, a sugar group and a nitrogen base. The four types of nitrogen bases are adenine (A) which has an amino group (-NH2), uracil (U), guanine (G), and cytosine (C) belonging to pyrimidine bases.

In order to determine the specific site of interaction of RNA molecule with the nanocapsule, the fluorescence of the encapsulated curcumin with each of the 4 nitrogen bases was established.
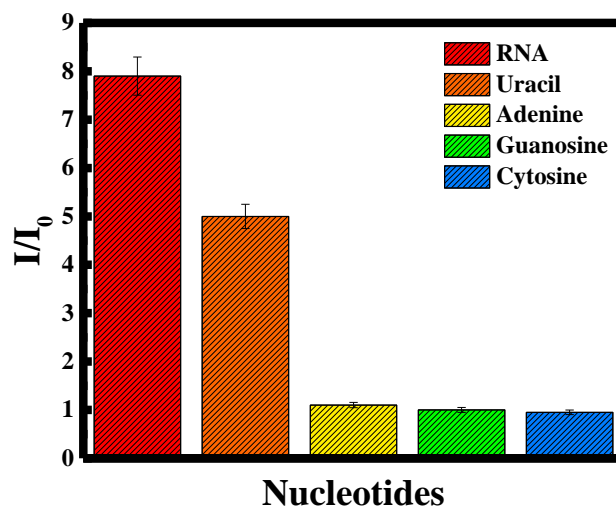
Figure 51 I/I_0 for RNA molecules and its nucleotides.

As it was noticed in Figure 51, only uracil altered the emission intensity of curcumin. This indicates that uracil is the actual site of interaction between RNA and the encapsulated curcumin. Hence, since uracil is the replacement of thymine in DNA molecule

and is present in RNA only, this clarifies the selectivity of the formed nanocapsules in the detection of RNA only.

d) Selectivity and pecificity towards the biosensor

Moreover, the evaluation of the specificity of DBPC-Cur-Chi nanocapsule toward RNA was achieved by measuring the fluorescence emission of DBPC-Cur-Chi nanocapsule in the presence of other interference molecules.

It is obvious from Figure 52 that no significant change in the fluorescence emission intensity of DBPC-Cur-Chi nanocapsule with other molecules has occurred, confirming the stronger interaction between DBPC-Cur-Chi nanocapsule and RNA molecule.
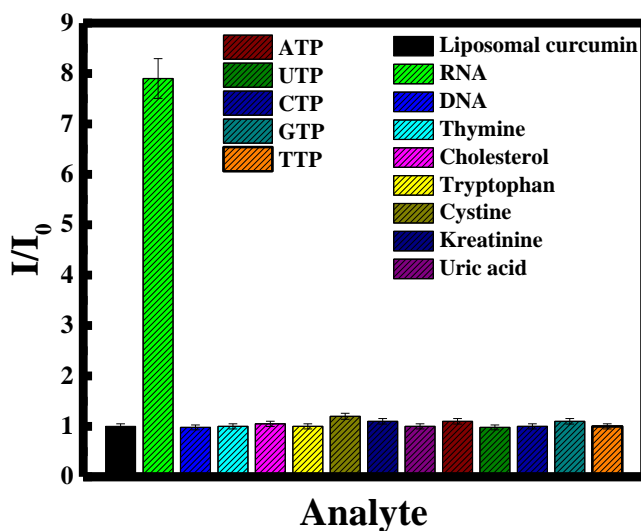
Figure 52 I/I_0 of DBPC-Cur-Chi nanocapsule alone and of DBPC-Cur-Chi nanocapsule with different analogues at C= 500 µg/mL.

The efficiency of our NCs was also compared to other probe used in the literature (See Table 11).

Methods	LOD	Concentration Range	References
Label free electrochemical method	0.14 ng.mL^{-1}	0.34-34 ng.mL^{-1}	[210]
RRS technique using AgNPs	38 µg.mL^{-1}	10-100µg.mL^{-1}	[211]
DBPC-Cur-Chi nanocapsules	36 ng.mL^{-1}	0-500 µg.mL^{-1}	Our work

Table 11 Different methods used for the detection of RNA

e) <u>Photo-stability of DBPC-Cur-Chi nanocapsule with/without RNA</u>

The photo-stability of DBPC-Cur-Chi nanocapsule in the absence and presence of RNA was elaborated and the results are illustrated in Figure 53.

It was notable, that the fluorescence emission intensity ratio, of DBPC-Cur-Chi with and without remained stable within one hour. The obtained result indicates that the sensor is fairly stable while performing the measurements.
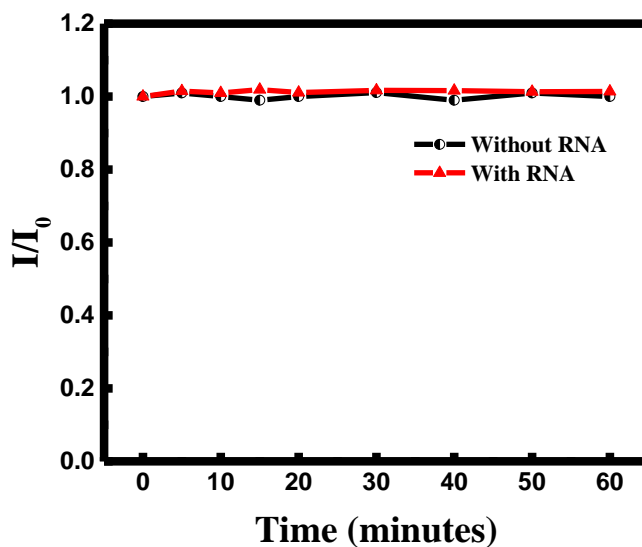
Figure 53 Plot of I/I$_0$ of DBPC-Cur-Chi nanocapsule with time in the absence and presence of RNA.

f) Recovery of the method

The examination of the method applicability was done by evaluating the analytical recovery of four unknown samples by using the obtained fitted calibration curves. Table 12 summarized the obtained results, where the percent of recovery of RNA was obtained to be between 99.5 and 100.33% (n=3).

	Theoretical Concentration (µg/mL)	Experimental concentration (µg/mL)	Recovery (%)
Unknown 1	8	7.98	99.75
Unknown 2	60	60.07	100.11
Unknown 3	150	149.32	99.5
Unknown 4	400	401.32	100.33

Table 12 Percentage recovery of the proposed method.

D.   Conclusion

To conclude, DBPC liposomal curcumin nanocapsule coated with chitosan were prepared using thin film method in order to compose a specific nanosensor for the detection of RNA. The detection of RNA molecule was ensued due to the presence of direct electrostatic interaction between the phosphate groups of the RNA molecule with the amino group of chitosan. However, no change in the emission intensity was observed when using liposomal curcumin and curcumin alone. The technique used was selective and sensitive towards the detection of RNA using DBPC-Cur-Chi nanocapsule against different interference molecule. The recovery of the method was found to be between 99.5 and 100.33 % and the limit of detection was found to be 36 ng/mL.

CHAPTER VIII

CONCLUSION

In the present thesis, curcumin was highlighted to be a potential candidate for probing membranes as well as being a good agent for analytical and therapeutical applications. The membranes studied, DAPC and DBPC, were further stabilized by coating their surface with chitosan oligosaccharide lactate. Hence, four nanocapsules were prepared: DAPC-cur; DAPC-cur-Chi; DBPC-cur; DBPC-cur-chi.

Spectroscopic measurements such as fluorescence were conducted to determine the phase transition temperatures (Tm) along with the permeability of the membrane, as well as to calculate the partition coefficients of curcumin inside DAPC and DBPC, without and with chitosan. The fluorescence intensity is maximized at Tm. The increase is due to the increase in the permeability of the bilayer before the Tm, and the decrease after the Tm is due to the decrease in the viscosity.

For DAPC, the Tm was found to be 65℃, as for DBPC it was 74℃, both values very close to the reported ones on Avanti Polar: 66℃ and 75 ℃ respectively. Furthermore, the effect of curcumin's concentration was also assessed and showed a slight decrease in the Tm values. As for the effect of chitosan oligosaccharide lactate, it was observed that it increases the fluorescence emission intensity with no effect on the Tm values.

Moving forward to determine the membrane permeability, this was done by following the quenching rate constants Ksv with two quenchers: hydrophilic KI and hydrophobic CPB. The results obtained confirmed the location of curcumin to be inside the

hydrophobic core by observing the quenching of the emission of curcumin with CPB in the absence of chitosan only. This experiment further justifies the role of chitosan to be a protective coating layer for the liposomes-curcumin systems.

Moreover, the partition of curcumin into the membranes was further verified by calculating the partition coefficients (Kp) of curcumin into the four nanocapsules. The values obtained clearly indicate that without chitosan, Kp increases in going from the solid gel phase to the liquid crystalline phase. This result is rational as the lipids are transforming to the more fluid state. Opposite results were obtained with the chitosan layer where Kp but decreases as moving into the liquid crystalline phase. This has to do with the chitosan chains that intercalates into the membrane at higher temperature.

To evaluate the importance of ionic liquids (IL), the short chain IL bmit was used which shows to increase the solubility of curcumin in the bilayers, reflected by the increase in the emission intensity as bmit concentration was increased. For DAPC liposomes, partition coefficient values increased at low concentrations. The same trend was observed for DBPC at the solid gel phase. As for the liquid crystalline phase, Kp remained approximately unaffected with the presence of bmit.
The obtained results were explained by the competitive interactions of the bmit polar head group and its hydrophobic butyl chain with the liposomes.

Indeed, DAPC liposomes have shown a great barrier to encapsulate curcumin. Hence, the successful encapsulation of curcumin into the liposomes membrane was verified based on UV-Visible, fluorescence emission analysis, X-ray Diffraction (XRD) and scanning electron microscopy (SEM). Moreover, the efficiency of chitosan oligosaccharide

as a protective layer was confirmed through zeta analysis using Dynamic Light Scattering (DLS) and thermogravimetric analysis (TGA).

Furthermore, the anti-cancer effect of DAPC-CUR/without and with chitosan was assessed for the inhibition of MCF-7 and Capan-1 cancer cells proliferation. The results obtained were in favor of the benefit of coating with chitosan where the percentage of the inhabitation proliferation observed for both cells lines was higher compared to without chitosan after 72 hours, for only 3 µg/mL of nanocapsules used, where the percentage inhibition was equal to 85% and 90% for MCF-7 and Capan-1 cell lines.

Finally, based on the high encapsulation efficiency obtained when coating the nanocapsule with chitosan, DBPC-Cur-Chi NPs were used as a nanoprobe to detect RNA, which was based on the fluorescence emission, an easy, low cost and selective technique. The prepared NPs showed a linear relationship in two ranges 0-20 and 30-500 µg/mL. The detection of RNA was based on electrostatic interactions between the positive charged chitosan and the negative charged RNA molecules which caused aggregation resulting in an increase in curcumin emission intensity.

REFERENCES

[1]   E. A. J. Bleeker *et al.*, "Considerations on the EU definition of a nanomaterial: Science to support policy making," *Regul. Toxicol. Pharmacol.*, vol. 65, no. 1, pp. 119–125, 2013, doi: 10.1016/j.yrtph.2012.11.007.

[2]   G. Lidén, "The European commission tries to define nanomaterials," *Ann. Occup. Hyg.*, vol. 55, no. 1, pp. 1–5, 2011, doi: 10.1093/annhyg/meq092.

[3]   M. Lungu, A. Neculae, M. Bunoiu, and C. Biris, "Nanoparticles' promises and risks: Characterization, manipulation, and potential hazards to humanity and the environment," *Nanoparticles' Promises Risks Charact. Manip. Potential Hazards to Humanit. Environ.*, no. 4, pp. 1–355, 2015, doi: 10.1007/978-3-319-11728-7.

[4]   N. Düzgüneş and G. Gregoriadis, "Introduction: The origins of liposomes: Alec Bangham at Babraham," *Methods Enzymol.*, vol. 391, no. SPEC. ISS., pp. 1–3, 2005, doi: 10.1016/S0076-6879(05)91029-X.

[5]   A. D. Bangham, M. M. Standish, and J. C. Watkins, "Diffusion of univalent ions across the lamellae of swollen phospholipids," *J. Mol. Biol.*, vol. 13, no. 1, pp. 238–252, 1965, doi: 10.1016/S0022-2836(65)80093-6.

[6]   P. Trucillo, R. Campardelli, and E. Reverchon, "Liposomes: From bangham to supercritical fluids," *Processes*, vol. 8, no. 9, pp. 1–15, 2020, doi: 10.3390/pr8091022.

[7]   N. Zafar, I. Bashir, N. Alvi, and M. I. Sajid, "Structural components of liposomes and characterization tools," *Indo Am. J. Pharm. Res.*, vol. 4, no. 08, pp. 3559–3567, 2014.

[8]   P. van Hoogevest and A. Wendel, "The use of natural and synthetic phospholipids as pharmaceutical excipients," *Eur. J. Lipid Sci. Technol.*, vol. 116, no. 9, pp. 1088–1107, 2014, doi: 10.1002/ejlt.201400219.

[9]   A. Elhissi, D. Phoenix, and W. Ahmed, *Some approaches to large-scale manufacturing of liposomes*, Second Edi. Elsevier Inc., 2014.

[10]   Y. Duan, Y. Liu, J. Li, H. Wang, and S. Wen, "Investigation on the nanomechanics of liposome adsorption on titanium alloys: Temperature and loading effects," *Polymers (Basel).*, vol. 10, no. 4, pp. 1–15, 2018, doi: 10.3390/polym10040383.

[11]   K. Simons and J. L. Sampaio, "Membrane organization and lipid rafts," *Cold Spring Harb. Perspect. Biol.*, vol. 3, no. 10, pp. 1–17, 2011, doi: 10.1101/cshperspect.a004697.

[12]   R. Koynova and B. Tenchov, "Transitions between lamellar and nonlamellar phases

in membrane lipids and their physiological roles," *OA Biochem.*, vol. 1, no. 1, 2013, doi: 10.13172/2052-9651-1-1-602.

[13]   J. Barauskas, M. Johnsson, and F. Tiberg, "Self-assembled lipid superstructures: Beyond vesicles and liposomes," *Nano Lett.*, vol. 5, no. 8, pp. 1615–1619, 2005, doi: 10.1021/nl050678i.

[14]   S. Šegota and D. urd ica Težak, "Spontaneous formation of vesicles," *Adv. Colloid Interface Sci.*, vol. 121, no. 1–3, pp. 51–75, 2006, doi: 10.1016/j.cis.2006.01.002.

[15]   R. Nagarajan, "Molecular packing parameter and surfactant self-assembly: The neglected role of the surfactant tail," *Langmuir*, vol. 18, no. 1, pp. 31–38, 2002, doi: 10.1021/la010831y.

[16]   J. N. Israelachvili, D. J. Mitchell, and B. W. Ninham, "Theory of self-assembly of lipid bilayers and vesicles," *BBA - Biomembr.*, vol. 470, no. 2, pp. 185–201, 1977, doi: 10.1016/0005-2736(77)90099-2.

[17]   J. Leng, S. U. Egelhaaf, and M. E. Cates, "Kinetics of the micelle-to-vesicle transition: Aqueous lecithin-bile salt mixtures," *Biophys. J.*, vol. 85, no. 3, pp. 1624–1646, 2003, doi: 10.1016/S0006-3495(03)74593-7.

[18]   S. Shailesh, S. Neelam, K. Sandeep, and G. Gd, "Liposomes : A review," vol. 2, no. 7, pp. 1163–1167, 2009.

[19]   P. J. R. S. Marripati, K. Umasankar, "A review on liposome," vol. 1, no. 2, pp. 159–169, 2014.

[20]   A. Akbarzadeh, R. Rezaei-sadabady, S. Davaran, S. W. Joo, and N. Zarghami, "Liposome : classification , preparation , and applications," pp. 1–9, 2013.

[21]   D. A. Balazs and W. Godbey, "Liposomes for Use in Gene Delivery," *J. Drug Deliv.*, vol. 2011, pp. 1–12, 2011, doi: 10.1155/2011/326497.

[22]   L. Cattel, M. Ceruti, and F. Dosio, "From conventional to stealth liposomes a new frontier in cancer chemotherapy," *Tumori*, vol. 89, no. 3, pp. 237–249, 2003, doi: 10.1177/030089160308900302.

[23]   A. L. Klibanov, K. Maruyama, V. P. Torchilin, and L. Huang, "Amphipathic polyethyleneglycols effectively prolong the circulation time of liposomes," *FEBS Lett.*, vol. 268, no. 1, pp. 235–237, 1990, doi: 10.1016/0014-5793(90)81016-H.

[24]   D. Elsser-gravesen and A. Elsser-gravesen, "Engineering Liposomes and Nanoparticles for Biological Targeting," no. November 2013, pp. 29–49, 2014, doi: 10.1007/10.

[25]   G. Krenning and M. C. Harmsen, "MicroRNAs in Tissue Engineering and Regenerative Medicine," *MicroRNA Regen. Med.*, pp. 1159–1200, 2015, doi:

10.1016/B978-0-12-405544-5.00044-7.

[26] J. Gabrielska, J. Sarapuk, and S. Przestalski, "Antioxidant Protection of Egg Lecithin Liposomes during Sonication," *Zeitschrift fur Naturforsch. - Sect. C J. Biosci.*, vol. 50, no. 7–8, pp. 561–564, 1995, doi: 10.1515/znc-1995-7-814.

[27] M. Grit and D. J. A. Crommelin, "Chemical-stability-of-liposomes-implications-for-their-physical-stability_1993_Chemistry-and-Physics-of-Lipids," *Chem. Phys. Lipids*, vol. 64, pp. 3–18, 1993.

[28] F. Csempesz and I. Puskás, "Controlling the Physical Stability of Liposomal Colloids," *Colloids Interface Sci. Ser.*, vol. 3, pp. 79–89, 2010, doi: 10.1002/9783527631193.ch29.

[29] B. Pradhan, N. Kumar, S. Saha, and A. Roy, "Liposome: method of preparation, advantages, evaluation and its application," *J. Appl. Pharm. Res.*, vol. 3, no. 3, pp. 1–8, 2016, [Online]. Available: http://www.japtronline.com/index.php/JOAPR/article/view/54%5Cnfile:///C:/Users/Lisa/Documents/Citavi 5/Projects/Liposome/Citavi Attachments/Pradhan, Kumar et al. 2016 - Liposome method of preparation.pdf TS - www.japtronline.com U6 - http://www.japtronl.

[30] K. Shashi, K. Satinder, and P. Bharat, "a Complete Review on: Liposomes," *Int. Res. J. Pharm.*, vol. 3, no. 7, pp. 10–16, 2012.

[31] G. Gregoriadis and R. E. B, "Liposomes as Carriers of Enzymes or Drugs: a New Approach to the Treatment of Storage Diseases," *Biochem. Soc.*, vol. 238, no. 6173, pp. 761–762, 2003.

[32] G. Betz, A. Aeppli, N. Menshutina, and H. Leuenberger, "In vivo comparison of various liposome formulations for cosmetic application," *Int. J. Pharm.*, vol. 296, no. 1–2, pp. 44–54, 2005, doi: 10.1016/j.ijpharm.2005.02.032.

[33] V. B. Patravale and S. D. Mandawgade, "Novel cosmetic delivery systems: An application update," *Int. J. Cosmet. Sci.*, vol. 30, no. 1, pp. 19–33, 2008, doi: 10.1111/j.1468-2494.2008.00416.x.

[34] Y. Barenholz, "Doxil® - The first FDA-approved nano-drug: Lessons learned," *J. Control. Release*, vol. 160, no. 2, pp. 117–134, 2012, doi: 10.1016/j.jconrel.2012.03.020.

[35] T. O. B. Olusanya, R. R. H. Ahmad, D. M. Ibegbu, J. R. Smith, and A. A. Elkordy, "Liposomal drug delivery systems and anticancer drugs," *Molecules*, vol. 23, no. 4, pp. 1–17, 2018, doi: 10.3390/molecules23040907.

[36] D. D. Verma, S. Verma, G. Blume, and A. Fahr, "Liposomes increase skin penetration of entrapped and non-entrapped hydrophilic substances into human skin: A skin penetration and confocal laser scanning microscopy study," *Eur. J. Pharm.*

Biopharm., vol. 55, no. 3, pp. 271–277, 2003, doi: 10.1016/S0939-6411(03)00021-3.

[37] D. D. Lasic, "Novel applications of liposomes," *Trends Biotechnol.*, vol. 16, no. 7, pp. 307–321, 1998, doi: 10.1016/S0167-7799(98)01220-7.

[38] J. Epstein, I. R. Sanderson, and T. T. MacDonald, "Curcumin as a therapeutic agent: The evidence from in vitro, animal and human studies," *Br. J. Nutr.*, vol. 103, no. 11, pp. 1545–1557, 2010, doi: 10.1017/S0007114509993667.

[39] B. B. Aggarwal, C. Sundaram, N. Malani, and H. Ichikawa, "Curcumin: The Indian solid gold," *Adv. Exp. Med. Biol.*, vol. 595, pp. 1–75, 2007, doi: 10.1007/978-0-387-46401-5_1.

[40] W. H. Lee, C. Y. Loo, P. M. Young, D. Traini, R. S. Mason, and R. Rohanizadeh, "Recent advances in curcumin nanoformulation for cancer therapy," *Expert Opin. Drug Deliv.*, vol. 11, no. 8, pp. 1183–1201, 2014, doi: 10.1517/17425247.2014.916686.

[41] S. C. Gupta, S. Patchva, W. Koh, and B. B. Aggarwal, "Discovery of curcumin, a component of golden spice, and its miraculous biological activities," *Clin. Exp. Pharmacol. Physiol.*, vol. 39, no. 3, pp. 283–299, 2012, doi: 10.1111/j.1440-1681.2011.05648.x.

[42] A. Shehzad, S. Khan, and Y. Sup Lee, "Curcumin molecular targets in obesity and obesity-related cancers," *Futur. Oncol.*, vol. 8, no. 2, pp. 179–190, 2012, doi: 10.2217/fon.11.145.

[43] Bhawana, R. K. Basniwal, H. S. Buttar, V. K. Jain, and N. Jain, "Curcumin nanoparticles: Preparation, characterization, and antimicrobial study," *J. Agric. Food Chem.*, vol. 59, no. 5, pp. 2056–2061, 2011, doi: 10.1021/jf104402t.

[44] S. D. Brinkevich, N. I. Ostrovskaya, M. E. Parkhach, S. N. Samovich, and O. I. Shadyro, "Effects of curcumin and related compounds on processes involving α-hydroxyethyl radicals," *Free Radic. Res.*, vol. 46, no. 3, pp. 295–302, 2012, doi: 10.3109/10715762.2011.653966.

[45] W.-H. Lee, C.-Y. Loo, M. Bebawy, F. Luk, R. Mason, and R. Rohanizadeh, "Curcumin and its Derivatives: Their Application in Neuropharmacology and Neuroscience in the 21st Century," *Curr. Neuropharmacol.*, vol. 11, no. 4, pp. 338–378, 2013, doi: 10.2174/1570159x11311040002.

[46] A. R. E. A.G.Perkin, "Natural organic colouring matters.," vol. I, no. 2587, p. 2587, 1919.

[47] C. J. Cooksey, "Turmeric: old spice, new spice," *Biotech. Histochem.*, vol. 92, no. 5, pp. 309–314, 2017, doi: 10.1080/10520295.2017.1310924.

[48] G. Grynkiewicz and P. Ślifirski, "Curcumin and curcuminoids in quest for medicinal

status," *Acta Biochim. Pol.*, vol. 59, no. 2, pp. 201–212, 2012, doi: 10.18388/abp.2012_2139.

[49] V. Lampe and J. Milobedzka, "Studien über Curcumin," *Berichte der Dtsch. Chem. Gesellschaft*, vol. 46, no. 2, pp. 2235–2240, 1913, doi: 10.1002/cber.191304602149.

[50] K. R. Srinivasan, "a Chromatographic Study of the Curcuminoids in Curcuma Longa, L," *J. Pharm. Pharmacol.*, vol. 5, no. 1, pp. 448–457, 1953, doi: 10.1111/j.2042-7158.1953.tb14007.x.

[51] National Library of Medicine, "Curcumin," *Pubchem*. .

[52] K. I. Priyadarsini, "The chemistry of curcumin: From extraction to therapeutic agent," *Molecules*, vol. 19, no. 12, pp. 20091–20112, 2014, doi: 10.3390/molecules191220091.

[53] M. L. A. D. Lestari and G. Indrayanto, *Curcumin*, vol. 39. 2014.

[54] Y. Manolova, V. Deneva, L. Antonov, E. Drakalska, D. Momekova, and N. Lambov, "The effect of the water on the curcumin tautomerism: A quantitative approach," *Spectrochim. Acta - Part A Mol. Biomol. Spectrosc.*, vol. 132, pp. 815–820, 2014, doi: 10.1016/j.saa.2014.05.096.

[55] T. M. Kolev, E. A. Velcheva, B. A. Stamboliyska, and M. Spiteller, "DFT and experimental studies of the structure and vibrational spectra of curcumin," *Int. J. Quantum Chem.*, vol. 102, no. 6, pp. 1069–1079, 2005, doi: 10.1002/qua.20469.

[56] P. Basnet and N. Skalko-Basnet, "Curcumin: An anti-inflammatory molecule from a curry spice on the path to cancer treatment," *Molecules*, vol. 16, no. 6, pp. 4567–4598, 2011, doi: 10.3390/molecules16064567.

[57] D. Yanagisawa *et al.*, "Relationship between the tautomeric structures of curcumin derivatives and their Aβ-binding activities in the context of therapies for Alzheimer's disease," *Biomaterials*, vol. 31, no. 14, pp. 4179–4185, 2010, doi: 10.1016/j.biomaterials.2010.01.142.

[58] M. Borsari, E. Ferrari, R. Grandi, and M. Saladini, "Curcuminoids as potential new iron-chelating agents: Spectroscopic, polarographic and potentiometric study on their Fe(III) complexing ability," *Inorganica Chim. Acta*, vol. 328, no. 1, pp. 61–68, 2002, doi: 10.1016/S0020-1693(01)00687-9.

[59] M. Bernabé-Pineda, M. T. Ramírez-Silva, M. Romero-Romo, E. González-Vergara, and A. Rojas-Hernández, "Determination of acidity constants of curcumin in aqueous solution and apparent rate constant of its decomposition," *Spectrochim. Acta - Part A Mol. Biomol. Spectrosc.*, vol. 60, no. 5, pp. 1091–1097, 2004, doi: 10.1016/S1386-1425(03)00342-1.

[60] M. Metzler, E. Pfeiffer, S. I. Schulz, and J. S. Dempe, "Curcumin uptake and

metabolism," *BioFactors*, vol. 39, no. 1, pp. 14–20, 2013, doi: 10.1002/biof.1042.

[61]   K. Indira Priyadarsini, "Chemical and Structural Features Influencing the Biological Activity of Curcumin," *Curr. Pharm. Des.*, vol. 19, no. 11, pp. 2093–2100, 2013, doi: 10.2174/1381612811319110010.

[62]   H. H. Tønnesen and J. Karlsen, "Studies on curcumin and curcuminoids - V. Alkaline Degradation of Curcumin," *Z. Lebensm. Unters. Forsch.*, vol. 180, no. 2, pp. 132–134, 1985, doi: 10.1007/BF01042637.

[63]   Y. J. Wang *et al.*, "Stability of curcumin in buffer solutions and characterization of its degradation products," *J. Pharm. Biomed. Anal.*, vol. 15, no. 12, pp. 1867–1876, 1997, doi: 10.1016/S0731-7085(96)02024-9.

[64]   S. Mondal, S. Ghosh, and S. P. Moulik, "Stability of curcumin in different solvent and solution media: UV–visible and steady-state fluorescence spectral study," *J. Photochem. Photobiol. B Biol.*, vol. 158, pp. 212–218, 2016, doi: 10.1016/j.jphotobiol.2016.03.004.

[65]   P. H. Bong, "Spectral and photophysical behaviors of curcumin and curcuminoids," *Bull. Korean Chem. Soc.*, vol. 21, no. 1, pp. 81–86, 2000.

[66]   S. M. Khopde, K. Indira Priyadarsini, D. K. Palit*, and T. Mukherjee, "Effect of Solvent on the Excited-state Photophysical Properties of Curcumin¶," *Photochem. Photobiol.*, vol. 72, no. 5, p. 625, 2000, doi: 10.1562/0031-8655(2000)072<0625:eosote>2.0.co;2.

[67]   C. T. Ho, "High Performance Liquid Chromatographic Analysis of Curcuminoids and Their Photo-Oxidative Decomposition Compounds in Curcuma Longal," *J. Liq. Chromatogr.*, vol. 11, no. 11, pp. 2295–2304, 1988, doi: 10.1080/01483918808067200.

[68]   L. Slika and D. Patra, "A short review on chemical properties, stability and nano-technological advances for curcumin delivery," *Expert Opin. Drug Deliv.*, vol. 17, no. 1, pp. 61–75, 2020, doi: 10.1080/17425247.2020.1702644.

[69]   B. Hirko, S. Abera, and H. Mitiku, "Effect of Curing and Drying Methods on the Physical Quality of Turmeric (Curcuma Longa L.) Rhizome Grown in South Western Ethiopia," *Int. J. Res. Stud. Agric. Sci.*, vol. 5, no. 11, pp. 1–8, 2019, doi: 10.20431/2454-6224.0511003.

[70]   B. Kocaadam and N. Şanlier, "Curcumin, an active component of turmeric (Curcuma longa), and its effects on health," *Crit. Rev. Food Sci. Nutr.*, vol. 57, no. 13, pp. 2889–2895, 2017, doi: 10.1080/10408398.2015.1077195.

[71]   C. D. Lao *et al.*, "Dose escalation of a curcuminoid formulation," *BMC Complement. Altern. Med.*, vol. 6, pp. 4–7, 2006, doi: 10.1186/1472-6882-6-10.

[72] V. Laura *et al.*, "Potential of curcumin in skin disorders," *Nutrients*, vol. 11, no. 9, 2019, doi: 10.3390/nu11092184.

[73] X. Cai, Z. Fang, J. Dou, A. Yu, and G. Zhai, "Bioavailability of Quercetin: Problems and Promises," *Curr. Med. Chem.*, vol. 20, no. 20, pp. 2572–2582, 2013, doi: 10.2174/09298673113209990120.

[74] E. Burgos-Morón, J. M. Calderón-Montaño, J. Salvador, A. Robles, and M. López-Lázaro, "The dark side of curcumin," *Int. J. Cancer*, vol. 126, no. 7, pp. 1771–1775, 2010, doi: 10.1002/ijc.24967.

[75] K. Maiti, K. Mukherjee, A. Gantait, B. P. Saha, and P. K. Mukherjee, "Curcumin-phospholipid complex: Preparation, therapeutic evaluation and pharmacokinetic study in rats," *Int. J. Pharm.*, vol. 330, no. 1–2, pp. 155–163, 2007, doi: 10.1016/j.ijpharm.2006.09.025.

[76] Z. Wang, M. H. M. Leung, T. W. Kee, and D. S. English, "The role of charge in the surfactant-assisted stabilization of the natural product curcumin," *Langmuir*, vol. 26, no. 8, pp. 5520–5526, 2010, doi: 10.1021/la903772e.

[77] S. Bisht *et al.*, "Polymeric nanoparticle-encapsulated curcumin ('nanocurcumin'): A novel strategy for human cancer therapy," *J. Nanobiotechnology*, vol. 5, pp. 1–18, 2007, doi: 10.1186/1477-3155-5-3.

[78] A. Safavy *et al.*, "Design and development of water-soluble curcumin conjugates as potential anticancer agents," *J. Med. Chem.*, vol. 50, no. 24, pp. 6284–6288, 2007, doi: 10.1021/jm700988f.

[79] H. H. Tønnesen, M. Másson, and T. Loftsson, "Studies of curcumin and curcuminoids. XXVII. Cyclodextrin complexation: Solubility, chemical and photochemical stability," *Int. J. Pharm.*, vol. 244, no. 1–2, pp. 127–135, 2002, doi: 10.1016/S0378-5173(02)00323-X.

[80] S. C. Gupta, S. Patchva, and B. B. Aggarwal, "Therapeutic roles of curcumin: Lessons learned from clinical trials," *AAPS J.*, vol. 15, no. 1, pp. 195–218, 2013, doi: 10.1208/s12248-012-9432-8.

[81] Y. Wei and R. J. Lee, "Liposomal curcumin and its application in cancer Physical property," pp. 6027–6044, 2017.

[82] R. Wilken, M. S. Veena, M. B. Wang, and E. S. Srivatsan, "Curcumin: A review of anti-cancer properties and therapeutic activity in head and neck squamous cell carcinoma," *Mol. Cancer*, vol. 10, no. 1, p. 12, 2011, doi: 10.1186/1476-4598-10-12.

[83] National Cancer Institute, "No Title." https://seer.cancer.gov/archive/csr/1975_2005/.

[84] L. Li, B. B. Aggarwal, S. Shishodia, J. Abbruzzese, and R. Kurzrock, "Nuclear

factor-κB and IκB are constitutively active in human pancreatic cells, and their down-regulation by curcumin (Diferuloylmethane) is associated with the suppression of proliferation and the induction of apoptosis," *Cancer*, vol. 101, no. 10, pp. 2351–2362, 2004, doi: 10.1002/cncr.20605.

[85] N. Dhillon *et al.*, "Phase II trial of curcumin in patients with advanced pancreatic cancer," *Clin. Cancer Res.*, vol. 14, no. 14, pp. 4491–4499, 2008, doi: 10.1158/1078-0432.CCR-08-0024.

[86] S. Hewlings and D. Kalman, "Curcumin: A Review of Its Effects on Human Health," *Foods*, vol. 6, no. 10, p. 92, 2017, doi: 10.3390/foods6100092.

[87] R. S. Ramsewak, D. L. DeWitt, and M. G. Nair, "Cytotoxicity, antioxidant and anti-inflammatory activities of curcumins I-III from Curcuma longa," *Phytomedicine*, vol. 7, no. 4, pp. 303–308, 2000, doi: 10.1016/S0944-7113(00)80048-3.

[88] I. Gülçin, "Antioxidant activity of food constituents: An overview," *Arch. Toxicol.*, vol. 86, no. 3, pp. 345–391, 2012, doi: 10.1007/s00204-011-0774-2.

[89] I. Batinić-Haberle, J. S. Rebouças, and I. Spasojević, "Superoxide dismutase mimics: Chemistry, pharmacology, and therapeutic potential," *Antioxidants Redox Signal.*, vol. 13, no. 6, pp. 877–918, 2010, doi: 10.1089/ars.2009.2876.

[90] Sankar.Palanisamy, "Effects of Nanoparticle-encapsulated curcumin on arsenic-induced liver toxicity in rats," *Far East. Entomol.*, vol. 165, no. April, p. 16, 2006, doi: 10.1002/tox.

[91] A. S. Jiménez-Osorio, A. Monroy, and S. Alavez, "Curcumin and insulin resistance—Molecular targets and clinical evidences," *BioFactors*, vol. 42, no. 6, pp. 561–580, 2016, doi: 10.1002/biof.1302.

[92] T. Kim, J. Davis, A. J. Zhang, X. He, and S. T. Mathews, "Curcumin activates AMPK and suppresses gluconeogenic gene expression in hepatoma cells," *Biochem. Biophys. Res. Commun.*, vol. 388, no. 2, pp. 377–382, 2009, doi: 10.1016/j.bbrc.2009.08.018.

[93] Z. Ran, Y. Zhang, X. Wen, and J. Ma, "Curcumin inhibits high glucose-induced inflammatory injury in human retinal pigment epithelial cells through the ROS-PI3K/AKT/mTOR signaling pathway," *Mol. Med. Rep.*, vol. 19, no. 2, pp. 1024–1031, 2019, doi: 10.3892/mmr.2018.9749.

[94] A. P. D. Ribeiro *et al.*, "Phototoxic effect of curcumin on methicillin-resistant Staphylococcus aureus and L929 fibroblasts," *Lasers Med. Sci.*, vol. 28, no. 2, pp. 391–398, 2013, doi: 10.1007/s10103-012-1064-9.

[95] J. Wang, X. Zhou, W. Li, X. Deng, Y. Deng, and X. Niu, "Curcumin protects mice from Staphylococcus aureus pneumonia by interfering with the self-Assembly process of α-hemolysin," *Sci. Rep.*, vol. 6, no. June, pp. 1–12, 2016, doi:

10.1038/srep28254.

[96] H. Gunes, D. Gulen, R. Mutlu, A. Gumus, T. Tas, and A. E. Topkaya, "Antibacterial effects of curcumin: An in vitro minimum inhibitory concentration study," *Toxicol. Ind. Health*, vol. 32, no. 2, pp. 246–250, 2016, doi: 10.1177/0748233713498458.

[97] S. S. Bansal, M. Goel, F. Aqil, M. V. Vadhanam, and R. C. Gupta, "Advanced drug delivery systems of curcumin for cancer chemoprevention," *Cancer Prev. Res.*, vol. 4, no. 8, pp. 1158–1171, 2011, doi: 10.1158/1940-6207.CAPR-10-0006.

[98] M. Kolter, M. Wittmann, M. Köll-Weber, and R. Süss, "The suitability of liposomes for the delivery of hydrophobic drugs – A case study with curcumin," *Eur. J. Pharm. Biopharm.*, vol. 140, pp. 20–28, 2019, doi: 10.1016/j.ejpb.2019.04.013.

[99] D. Patra, E. El Khoury, D. Ahmadieh, S. Darwish, and R. M. Tafech, "Effect of curcumin on liposome: Curcumin as a molecular probe for monitoring interaction of ionic liquids with 1,2-dipalmitoyl-sn-glycero-3- phosphocholine liposome," *Photochem. Photobiol.*, vol. 88, pp. 317–327, 2012, doi: 10.1111/j.1751-1097.2011.01067.x.

[100] F. Cuomo *et al.*, "In-vitro digestion of curcumin loaded chitosan-coated liposomes," *Colloids Surfaces B Biointerfaces*, vol. 168, pp. 29–34, 2018, doi: 10.1016/j.colsurfb.2017.11.047.

[101] F. Zhou *et al.*, "Chitosan-coated liposomes as delivery systems for improving the stability and oral bioavailability of acteoside," *Food Hydrocoll.*, vol. 83, pp. 17–24, 2018, doi: 10.1016/j.foodhyd.2018.04.040.

[102] W. Liu *et al.*, "Environmental stress stability of microencapsules based on liposomes decorated with chitosan and sodium alginate," *Food Chem.*, vol. 196, pp. 396–404, 2016, doi: 10.1016/j.foodchem.2015.09.050.

[103] M. Takahashi, S. Uechi, K. Takara, Y. Asikin, and K. Wada, "Evaluation of an oral carrier system in rats: Bioavailability and antioxidant properties of liposome-encapsulated curcumin," *J. Agric. Food Chem.*, vol. 57, no. 19, pp. 9141–9146, 2009, doi: 10.1021/jf9013923.

[104] L. Li, F. S. Braiteh, and R. Kurzrock, "Liposome-encapsulated curcumin: In vitro and in vivo effects on proliferation, apoptosis, signaling, and angiogenesis," *Cancer*, vol. 104, no. 6, pp. 1322–1331, 2005, doi: 10.1002/cncr.21300.

[105] C. Chignell, P. Bilski, J. K. Reszka, G. A. Motten, H. R. Sik, and T. Dahl, "Spectral and Photochemical properties of curcumin," vol. 59, no. 3, pp. 295–302, 1994.

[106] Z. Moussa, M. Chebl, and D. Patra, "Interaction of curcumin with 1,2-dioctadecanoyl-sn-glycero-3-phosphocholine liposomes: Intercalation of rhamnolipids enhances membrane fluidity, permeability and stability of drug molecule," *Colloids Surfaces B Biointerfaces*, vol. 149, pp. 30–37, 2017, doi:

10.1016/j.colsurfb.2016.10.002.

[107] D. Patra and C. Barakat, "Synchronous fluorescence spectroscopic study of solvatochromic curcumin dye," *Spectrochim. Acta - Part A Mol. Biomol. Spectrosc.*, vol. 79, no. 5, pp. 1034–1041, 2011, doi: 10.1016/j.saa.2011.04.016.

[108] E. D. El Khoury and D. Patra, "Ionic liquid expedites partition of curcumin into solid gel phase but discourages partition into liquid crystalline phase of 1,2-dimyristoyl-sn- glycero-3-phosphocholine liposomes," *J. Phys. Chem. B*, vol. 117, pp. 9699–9708, 2013, doi: 10.1021/jp4061413.

[109] D. K. Palit, A. V. Sapre, and J. P. Mittal, "Picosecond studies on the electron transfer from pyrene and perylene excited singlet states to N-hexadecyl pyridinium chloride," *Chem. Phys. Lett.*, vol. 269, no. 3–4, pp. 286–292, 1997, doi: 10.1016/S0009-2614(97)00278-9.

[110] J. Sujatha and A. K. Mishra, "Phase transitions in phospholipid vesicles: Excited state prototropism of 1-naphthol as a novel probe concept," *Langmuir*, vol. 14, no. 9, pp. 2256–2262, 1998, doi: 10.1021/la9702749.

[111] T. Shyamala and A. K. Mishra, "Ground- and Excited-state Proton Transfer Reaction of 3-Hydroxyflavone in Dimyristoylphosphatidylcholine Liposome Membrane¶," *Photochem. Photobiol.*, vol. 80, no. 2, p. 309, 2004, doi: 10.1562/2004-03-07-ra-104.1.

[112] A. P. Demchenko, Y. Mély, G. Duportail, and A. S. Klymchenko, "Monitoring biophysical properties of lipid membranes by environment-sensitive fluorescent probes," *Biophys. J.*, vol. 96, no. 9, pp. 3461–3470, 2009, doi: 10.1016/j.bpj.2009.02.012.

[113] B. B. Aggarwal and B. Sung, "Pharmacological basis for the role of curcumin in chronic diseases: an age-old spice with modern targets," *Trends Pharmacol. Sci.*, vol. 30, no. 2, pp. 85–94, 2009, doi: 10.1016/j.tips.2008.11.002.

[114] K. Ramaswamy, "Neuroprotection by Spice-Derived Nutraceuticals: You Are What You Eat!," *Bone*, vol. 23, no. 1, pp. 1–7, 2008, doi: 10.1007/s12035-011-8168-2.Neuroprotection.

[115] R. Jadia, J. Kydd, B. Piel, and P. Rai, "Liposomes Aid Curcumin's Combat with Cancer in a Breast Tumor Model," *Oncomedicine*, vol. 3, pp. 94–109, 2018, doi: 10.7150/oncm.27938.

[116] A. Karewicz, D. Bielska, B. Gzyl-Malcher, M. Kepczynski, R. Lach, and M. Nowakowska, "Interaction of curcumin with lipid monolayers and liposomal bilayers," *Colloids Surfaces B Biointerfaces*, vol. 88, no. 1, pp. 231–239, 2011, doi: 10.1016/j.colsurfb.2011.06.037.

[117] F. Cuomo, A. Ceglie, M. Piludu, M. G. Miguel, B. Lindman, and F. Lopez, "Loading

and protection of hydrophilic molecules into liposome-templated polyelectrolyte nanocapsules," *Langmuir*, vol. 30, no. 27, pp. 7993–7999, 2014, doi: 10.1021/la501978u.

[118] F. Cuomo, F. Lopez, M. G. Miguel, and B. Lindman, "Vesicle-templated layer-by-layer assembly for the production of nanocapsules," *Langmuir*, vol. 26, no. 13, pp. 10555–10560, 2010, doi: 10.1021/la100584b.

[119] M. Prabaharan and J. F. Mano, "Chitosan-based particles as controlled drug delivery systems," *Drug Deliv. J. Deliv. Target. Ther. Agents*, vol. 12, no. 1, pp. 41–57, 2005, doi: 10.1080/10717540590889781.

[120] J. Zhuang, Q. Ping, Y. Song, J. Qi, and Z. Cui, "Effects of chitosan coating on physical properties and pharmacokinetic behavior of mitoxantrone liposomes," *Int. J. Nanomedicine*, vol. 5, no. 1, pp. 407–416, 2010, doi: 10.2147/ijn.s10189.

[121] M. M. Mady and M. M. Darwish, "Effect of chitosan coating on the characteristics of DPPC liposomes," *J. Adv. Res.*, vol. 1, no. 3, pp. 187–191, 2010, doi: 10.1016/j.jare.2010.05.008.

[122] H. Sik, "SPECTRAL AND PHOTOCHEMICAL PROPERTIES OF CURCUMIN," vol. 59, no. 3, pp. 295–302, 1994.

[123] T. Inoue, Y. Muraoka, K. Fukushima, and R. Shimozawa, "Interaction of surfactants with vesicle membrane of dipalmitoylphosphatidylcholine: fluorescence depolarization study," *Chem. Phys. Lipids*, vol. 46, no. 2, pp. 107–115, 1988, doi: 10.1016/0009-3084(88)90120-X.

[124] M. Mohapatra and A. K. Mishra, "1-naphthol as a sensitive fluorescent molecular probe for monitoring the interaction of submicellar concentration of bile salt with a bilayer membrane of DPPC, a lung surfactant," *J. Phys. Chem. B*, vol. 114, no. 46, pp. 14934–14940, 2010, doi: 10.1021/jp103855q.

[125] A. Karewicz *et al.*, "Curcumin-containing liposomes stabilized by thin layers of chitosan derivatives," *Colloids Surfaces B Biointerfaces*, vol. 109, pp. 307–316, 2013, doi: 10.1016/j.colsurfb.2013.03.059.

[126] T. Welton, "Ionic liquids: a brief history," *Biophys. Rev.*, vol. 10, no. 3, pp. 691–706, 2018, doi: 10.1007/s12551-018-0419-2.

[127] M. J. Earle and K. R. Seddon, "Ionic liquids: Green solvents for the future," *ACS Symp. Ser.*, vol. 819, no. 7, pp. 10–25, 2002, doi: 10.1021/bk-2002-0819.ch002.

[128] A. M. Funston, T. A. Fadeeva, J. F. Wishart, and E. W. Castner, "Fluorescence probing of temperature-dependent dynamics and friction in ionic liquid local environments," *J. Phys. Chem. B*, vol. 111, no. 18, pp. 4963–4977, 2007, doi: 10.1021/jp068298o.

[129] J. L. Anderson, V. Pino, E. C. Hagberg, V. V. Sheares, and D. W. Armstrong, "Surfactant solvation effects and micelle formation in ionic liquids," *Chem. Commun.*, vol. 3, no. 19, pp. 2444–2445, 2003, doi: 10.1039/b307516h.

[130] K. A. Fletcher and S. Pandey, "Solvatochromic probe behavior within ternary room-temperature ionic liquid 1-butyl-3-methylimidazolium hexafluorophosphate + ethanol + water solutions," *J. Phys. Chem. B*, vol. 107, no. 48, pp. 13532–13539, 2003, doi: 10.1021/jp0276754.

[131] T. Welton, "Ionic liquids in Green Chemistry," *Green Chem.*, vol. 13, no. 2, p. 225, 2011, doi: 10.1039/c0gc90047h.

[132] J. Lu, F. Yan, and J. Texter, "Advanced applications of ionic liquids in polymer science," *Prog. Polym. Sci.*, vol. 34, no. 5, pp. 431–448, 2009, doi: 10.1016/j.progpolymsci.2008.12.001.

[133] R. D. Rogers and K. R. Seddon, "Ionic Liquids - Solvents of the Future?," *Science (80-.).*, vol. 302, no. 5646, pp. 792–793, 2003, doi: 10.1126/science.1090313.

[134] S. C. Yang, H. G. Yoon, S. S. Lee, and H. Lee, "Roles of layered titanates in ionic liquid electrolytes for quasi-solid state dye-sensitized solar cells," *Mater. Lett.*, vol. 63, no. 17, pp. 1465–1467, 2009, doi: 10.1016/j.matlet.2009.03.042.

[135] A. Mishra, M. K. R. Fischer, and P. Büuerle, "Metal-Free organic dyes for dye-Sensitized solar cells: From structure: Property relationships to design rules," *Angew. Chemie - Int. Ed.*, vol. 48, no. 14, pp. 2474–2499, 2009, doi: 10.1002/anie.200804709.

[136] M. D. Bennett, D. J. Leo, G. L. Wilkes, F. L. Beyer, and T. W. Pechar, "A model of charge transport and electromechanical transduction in ionic liquid-swollen Nafion membranes," *Polymer (Guildf).*, vol. 47, no. 19, pp. 6782–6796, 2006, doi: 10.1016/j.polymer.2006.07.061.

[137] A. J. Duncan, D. J. Leo, and T. E. Long, "Beyond nafion: Charged macromolecules tailored for performance as ionic polymer transducers," *Macromolecules*, vol. 41, no. 21, pp. 7766–7775, 2008, doi: 10.1021/ma800956v.

[138] J. Ding *et al.*, "Use of ionic liquids as electrolytes in electromechanical actuator systems based on inherently conducting polymers," *Chem. Mater.*, vol. 15, no. 12, pp. 2392–2398, 2003, doi: 10.1021/cm020918k.

[139] X. Y. Zhang, S. H. Fang, Z. X. Zhang, and L. Yang, "Li/LiFePO 4 battery performance with a guanidinium-based ionic liquid as the electrolyte," *Chinese Sci. Bull.*, vol. 56, no. 27, pp. 2906–2910, 2011, doi: 10.1007/s11434-011-4655-0.

[140] M. Galiński, A. Lewandowski, and I. Stepniak, "Ionic liquids as electrolytes," *Electrochim. Acta*, vol. 51, no. 26, pp. 5567–5580, 2006, doi: 10.1016/j.electacta.2006.03.016.

[141] D. Patra and C. Barakat, "Unique role of ionic liquid [bmin][BF 4] during curcumin-surfactant association and micellization of cationic, anionic and non-ionic surfactant solutions," *Spectrochim. Acta - Part A Mol. Biomol. Spectrosc.*, vol. 79, no. 5, pp. 1823–1828, 2011, doi: 10.1016/j.saa.2011.05.064.

[142] E. D. El Khoury and D. Patra, "Ionic liquid expedites partition of curcumin into solid gel phase but discourages partition into liquid crystalline phase of 1,2-dimyristoyl-sn- glycero-3-phosphocholine liposomes," *J. Phys. Chem. B*, vol. 117, no. 33, pp. 9699–9708, 2013, doi: 10.1021/jp4061413.

[143] J. Li *et al.*, "A review on phospholipids and their main applications in drug delivery systems," *Asian J. Pharm. Sci.*, vol. 10, no. 2, pp. 81–98, 2015, doi: 10.1016/j.ajps.2014.09.004.

[144] A. H. Thomas, Á. Catalá, and M. Vignoni, "Soybean phosphatidylcholine liposomes as model membranes to study lipid peroxidation photoinduced by pterin," *Biochim. Biophys. Acta - Biomembr.*, vol. 1858, no. 1, pp. 139–145, 2016, doi: 10.1016/j.bbamem.2015.11.002.

[145] H. I. Ingolfsson, R. E. Koeppe, and O. S. Andersen, "Curcumin is a modulator of bilayer material properties," *Biochemistry*, vol. 46, no. 36, pp. 10384–10391, 2007, doi: 10.1021/bi701013n.

[146] A. Kumar *et al.*, "Two-photon fluorescence properties of curcumin as a biocompatible marker for confocal imaging," *Appl. Phys. Lett.*, vol. 100, no. 20, 2012, doi: 10.1063/1.4717753.

[147] K. Nagahama, Y. Sano, and T. Kumano, "Anticancer drug-based multifunctional nanogels through self-assembly of dextran-curcumin conjugates toward cancer theranostics," *Bioorganic Med. Chem. Lett.*, vol. 25, no. 12, pp. 2519–2522, 2015, doi: 10.1016/j.bmcl.2015.04.062.

[148] S. Mondal and S. Ghosh, "Role of curcumin on the determination of the critical micellar concentration by absorbance, fluorescence and fluorescence anisotropy techniques," *J. Photochem. Photobiol. B Biol.*, vol. 115, pp. 9–15, 2012, doi: 10.1016/j.jphotobiol.2012.06.004.

[149] Y. M. Hijji *et al.*, "Curcumin a colorimetric and fluorimetric cyanide probe in aqueous system and living cells," *Anal. Methods*, vol. 11, no. 40, pp. 5169–5176, 2019, doi: 10.1039/c9ay01557d.

[150] R. Siegel, D. Naishadham, and A. Jemal, "Cancer Statistics , 2013," vol. 63, no. 1, pp. 11–30, 2013, doi: 10.3322/caac.21166.

[151] S. H. Hassanpour and M. Dehghani, "Review of cancer from perspective of molecular," *J. Cancer Res. Pract.*, vol. 4, no. 4, pp. 127–129, 2017, doi: 10.1016/j.jcrpr.2017.07.001.

[152] R. L. Siegel, K. D. Miller, and A. Jemal, "Cancer Statistics , 2016," vol. 66, no. 1, pp. 7–30, 2016, doi: 10.3322/caac.21332.

[153] L. A. Torre, F. Bray, R. L. Siegel, and J. Ferlay, "Global Cancer Statistics , 2012," vol. 65, no. 2, pp. 87–108, 2015, doi: 10.3322/caac.21262.

[154] U. Veronesi, P. Boyle, A. Goldhirsch, R. Orecchia, and G. Viale, "Breast cancer," vol. 365, 2005.

[155] Y. Feng *et al.*, "ScienceDirect Breast cancer development and progression : Risk factors , cancer stem cells , signaling pathways , genomics , and molecular pathogenesis," *Genes Dis.*, vol. 5, no. 2, pp. 77–106, 2018, doi: 10.1016/j.gendis.2018.05.001.

[156] A. Tyagi *et al.*, "Nicotine promotes breast cancer metastasis by stimulating N2 neutrophils and generating pre-metastatic niche in lung," *Nat. Commun.*, no. 2021, pp. 1–18, doi: 10.1038/s41467-020-20733-9.

[157] J. E. Shea, "NIH Public Access," vol. 39, no. 4, pp. 425–435, 2011, doi: 10.1097/MPA.0b013e3181c15963.Phenotype.

[158] S. Jones *et al.*, "Core Signaling Pathways in Human Pancreatic Cancers Revealed by Global Genomic Analyses," vol. 321, no. September, pp. 1801–1806, 2008.

[159] D. P. Ryan, T. S. Hong, and N. Bardeesy, "Pancreatic Adenocarcinoma," pp. 1039–1049, 2014, doi: 10.1056/NEJMra1404198.

[160] P. W. Underwood *et al.*, "Nicotine induces IL-8 secretion from pancreatic cancer stroma and worsens cancer-induced cachexia," *Cancers (Basel).*, vol. 12, no. 2, pp. 1–12, 2020, doi: 10.3390/cancers12020329.

[161] M. Xu *et al.*, "HHS Public Access," vol. 47, no. 2, pp. 158–162, 2019, doi: 10.1097/MPA.0000000000000974.Obesity.

[162] W. D. Newhauser, "A Review of Radiotherapy-induced Late effects Research after Advanced Technology Treatments," vol. 6, no. February 2016, pp. 1–11, 2020, doi: 10.3389/fonc.2016.00013.

[163] D. Drotar and E. Kodish, "NIH Public Access," vol. 52, no. 4, pp. 497–502, 2010, doi: 10.1002/pbc.21835.Potential.

[164] J. R. Heath and M. E. Davis, "NIH Public Access," pp. 251–265, 2013, doi: 10.1146/annurev.med.59.061506.185523.Nanotechnology.

[165] Waage et al., "乳鼠心肌提取 HHS Public Access," *Physiol. Behav.*, vol. 176, no. 1, pp. 139–148, 2017, doi: 10.1515/ntrev-2013-0013.Nanotechnology.

[166] Y. Malam, M. Loizidou, and A. M. Seifalian, "Liposomes and nanoparticles :

nanosized vehicles for drug delivery in cancer," 2009, doi: 10.1016/j.tips.2009.08.004.

[167] G. Bozzuto, "Liposomes as nanomedical devices," pp. 975–999, 2015.

[168] M. A. Tomeh, R. Hadianamrei, and X. Zhao, "A Review of Curcumin and Its Derivatives as Anticancer Agents," 2019, doi: 10.3390/ijms20051033.

[169] Z. Jing, "Anti-Tumor Effect of Curcumin on Human Cervical Carcinoma HeLa Cells In Vitro and In Vivo," vol. 19, no. 1, pp. 32–36, 2007.

[170] J. U. N. L. I. Liu, Y. A. N. Y. A. N. Pan, O. U. Chen, Y. U. N. Luan, and X. I. A. Xue, "Curcumin inhibits MCF - 7 cells by modulating the NF - κ B signaling pathway," pp. 5581–5584, 2017, doi: 10.3892/ol.2017.6860.

[171] S. Bimonte *et al.*, "Curcumin AntiCancer Studies in Pancreatic Cancer," pp. 1–12, 2016, doi: 10.3390/nu8070433.

[172] M. Pricci, B. Girardi, F. Giorgio, G. Losurdo, E. Ierardi, and A. Di Leo, "Curcumin and Colorectal Cancer : From Basic to Clinical Evidences," 2020.

[173] W. Liu, Y. Zhai, X. Heng, F. Che, W. Chen, and G. Zhai, "Oral Bioavailability of Curcumin: Problems and Ad- vancements," 2016, doi: 10.3109/1061186X.2016.1157883.

[174] A. Karewicz, D. Bielska, B. Gzyl-malcher, M. Kepczynski, R. Lach, and M. Nowakowska, "Colloids and Surfaces B : Biointerfaces Interaction of curcumin with lipid monolayers and liposomal bilayers," *Colloids Surfaces B Biointerfaces*, vol. 88, no. 1, pp. 231–239, 2011, doi: 10.1016/j.colsurfb.2011.06.037.

[175] R. L. Thangapazham, A. N. U. Puri, S. Tele, R. Blumenthal, and R. K. Maheshwari, "Evaluation of a nanotechnology-based carrier for delivery of curcumin in prostate cancer cells," no. 14, pp. 1119–1123, 2008.

[176] H. Zhang, "Chapter 2 Thin-Film Hydration Followed by Extrusion Method for Liposome Preparation," vol. 1522, pp. 17–22, doi: 10.1007/978-1-4939-6591-5.

[177] E. Commission and M. A. Rahman, "Synthesis and Characterization of Metal Complexes Containing Curcumin (C 21 H 20 O 6) and Study of their Anti-microbial Activities and DNA Binding Properties Synthesis and Characterization of Metal Complexes Containing Curcumin (C 21 H 20 O 6) and Stu," no. January 2014, 2015, doi: 10.3329/jsr.v6i1.15381.

[178] E. El Khoury and D. Patra, "Journal of Photochemistry & Photobiology , B : Biology Length of hydrocarbon chain in fl uences location of curcumin in liposomes : Curcumin as a molecular probe to study ethanol induced interdigitation of liposomes," *JPB*, vol. 158, pp. 49–54, 2016, doi: 10.1016/j.jphotobiol.2016.02.022.

[179] G. K. Athira and A. N. Jyothi, "Innovare Academic Sciences PREPARATION AND CHARACTERIZATION OF CURCUMIN LOADED CASSAVA STARCH NANOPARTICLES WITH IMPROVED CELLULAR ABSORPTION," vol. 6, no. 10, 2014.

[180] A. I. Journal *et al.*, "Application of liposomes in medicine and drug delivery Application of liposomes in medicine and drug delivery," vol. 1401, 2016, doi: 10.3109/21691401.2014.953633.

[181] M. J. Tuorkey, "Curcumin a potent cancer preventive agent : Mechanisms of cancer cell killing," vol. 6, no. 4, pp. 139–146, 2014, doi: 10.1556/IMAS.6.2014.4.1.

[182] N. M. Ali *et al.*, "Synthetic curcumin derivative DK1 possessed G2/M arrest and induced apoptosis through accumulation of intracellular ROS in MCF-7 breast cancer cells," *Cancer Cell Int.*, vol. 17, no. 1, pp. 1–12, 2017, doi: 10.1186/s12935-017-0400-3.

[183] F. Sadat and T. Mirakabad, "A Comparison between the cytotoxic effects of pure curcumin and curcumin-loaded PLGA-PEG nanoparticles on the MCF-7 human breast cancer cell line," no. August, pp. 1–8, 2014, doi: 10.3109/21691401.2014.955108.

[184] D. Sutaria, B. K. Grandhi, A. Thakkar, J. Wang, and S. Prabhu, "Chemoprevention of pancreatic cancer using solid-lipid nanoparticulate delivery of a novel aspirin , curcumin and sulforaphane drug combination regimen," pp. 2260–2268, 2012, doi: 10.3892/ijo.2012.1636.

[185] M. Selim and A. Hendi, "Gold Nanoparticles Induce Apoptosis in MCF-7 Human Breast Cancer Cells," no. March 2014, 2012, doi: 10.7314/APJCP.2012.13.4.1617.

[186] H. B. Ruttala and Y. T. Ko, "Liposomal Co-delivery of Curcumin and Albumin/Paclitaxel Nanoparticle for Enhanced Synergistic Antitumor Efficacy," *Colloids Surfaces B Biointerfaces*, 2015, doi: 10.1016/j.colsurfb.2015.02.040.

[187] D. Press, "Study of the enhanced anticancer efficacy of gambogic acid on Capan-1 pancreatic cancer cells when mediated via magnetic Fe 3 O 4 nanoparticles," pp. 1929–1935, 2011.

[188] A. P. Ranjan, A. Mukerjee, and L. Helson, "Efficacy of Liposomal Curcumin in a Human Pancreatic Tumor Xenograft Model : Inhibition of Tumor Growth and Angiogenesis," vol. 3610, pp. 3603–3609, 2013.

[189] Nsi, "Nanotechnology for Sensors and Sensors for Nanotechnology: Improving and Protecting Health, Safety, and the Environment," *Nanotechnol. Signat. Initiat.*, no. July, pp. 1–11, 2012.

[190] R. D. van Zee and G. S. Pomrenke, "Nanotechnology-Enabled Sensing," *Rep. Natl. Nanotechnol. Initiat. Work.*, 2009, [Online]. Available:

https://www.nano.gov/sites/default/files/NNI-Nanosensors-stdres.pdf.

[191] T. A. Cooper, L. Wan, and G. Dreyfuss, "RNA and Disease," *Hhmi*, vol. 136, no. 4, pp. 777–793, 2009.

[192] B. M. Cullum and T. Vo-dinh, "The development of optical biosensors for Biological Measurement," *Bmj*, vol. 1, no. 4017, pp. 20–21, 1938, doi: 10.1136/bmj.1.4017.20-a.

[193] Y. E. K. Lee, R. Smith, and R. Kopelman, "Nanoparticle PEBBLE sensors in live cells and in vivo," *Annu. Rev. Anal. Chem.*, vol. 2, pp. 57–76, 2009, doi: 10.1146/annurev.anchem.1.031207.112823.

[194] R. Badugu, J. R. Lakowicz, and C. D. Geddes, "A Glucose Sensing Contact Lens: A Non-Invasive Technique for Continuous Physiological Glucose Monitoring," *J. Fluoresc.*, vol. 13, no. 5, pp. 371–374, 2003, doi: 10.1023/A:1026103804104.

[195] D. Patra, R. Aridi, and K. Bouhadir, "Fluorometric sensing of DNA using curcumin encapsulated in nanoparticle-assembled microcapsules prepared from poly(diallylammonium chloride-co-sulfur dioxide)," *Microchim. Acta*, vol. 180, no. 1–2, pp. 59–64, 2013, doi: 10.1007/s00604-012-0903-5.

[196] L. Bechnak, R. El Kurdi, and D. Patra, "Fluorescence Sensing of Nucleic Acid by Curcumin Encapsulated Poly(Ethylene Oxide)-Block-Poly(Propylene Oxide)-Block-Poly(Ethylene Oxide) Based Nanocapsules," *J. Fluoresc.*, vol. 30, no. 3, pp. 547–556, 2020, doi: 10.1007/s10895-020-02528-9.

[197] S. Nafisi, M. Adelzadeh, Z. Norouzi, and M. N. Sarbolouki, "Curcumin binding to DNA and RNA," *DNA Cell Biol.*, vol. 28, no. 4, pp. 201–208, 2009, doi: 10.1089/dna.2008.0840.

[198] E. Sezgin and P. Schwille, "Fluorescence tehniques to study Lipid Dynamics," *Cold Spring Harb. Perspect. Biol.*, vol. 3, pp. 1–32, 2011.

[199] P. Pizzo, C. Scapin, M. Vitadello, C. Florean, and L. Gorza, "Grp94 acts as a mediator of curcumin-induced antioxidant defence in myogenic cells," *J. Cell. Mol. Med.*, vol. 14, no. 4, pp. 970–981, 2010, doi: 10.1111/j.1582-4934.2008.00681.x.

[200] S. Kawakishi, "Involvement of the P-Diketone Moiety in the antioxidative Mechanism of Tetrahydrocurcumin," *Science (80-.).*, vol. 52, no. 4, pp. 519–525, 1996, [Online]. Available: http://www.ncbi.nlm.nih.gov/pubmed/8759023.

[201] S. Shishodia, M. M. Chaturvedi, and B. B. Aggarwal, "Role of Curcumin in Cancer Therapy," *Curr. Probl. Cancer*, vol. 31, no. 4, pp. 243–305, 2007, doi: 10.1016/j.currproblcancer.2007.04.001.

[202] P. Maiti, L. Paladugu, and G. L. Dunbar, "Solid lipid curcumin particles provide greater anti-amyloid, anti-inflammatory and neuroprotective effects than curcumin in

the 5xFAD mouse model of Alzheimer's disease," *BMC Neurosci.*, vol. 19, no. 1, pp. 1–19, 2018, doi: 10.1186/s12868-018-0406-3.

[203] S. S. Ghosh *et al.*, "Curcumin ameliorates renal failure in 5/6 nephrectomized rats: Role of inflammation," *Am. J. Physiol. - Ren. Physiol.*, vol. 296, no. 5, pp. 1146–1157, 2009, doi: 10.1152/ajprenal.90732.2008.

[204] D. Patra, C. Barakat, and R. M. Tafech, "Study on effect of lipophilic curcumin on sub-domain IIA site of human serum albumin during unfolded and refolded states: A synchronous fluorescence spectroscopic study," *Colloids Surfaces B Biointerfaces*, vol. 94, no. 2012, pp. 354–361, 2012, doi: 10.1016/j.colsurfb.2012.02.017.

[205] C. Barakat and D. Patra, "Combining time-resolved fluorescence with synchronous fluorescence spectroscopy to study bovine serum albumin-curcumin complex during unfolding and refolding processes," *Luminescence*, vol. 28, no. 2, pp. 149–155, 2013, doi: 10.1002/bio.2354.

[206] K. Ponnuvel, K. Santhiya, and V. Padmini, "Curcumin based chemosensor for selective detection of fluoride and cyanide anions in aqueous media," *Photochem. Photobiol. Sci.*, vol. 15, no. 12, pp. 1536–1543, 2016, doi: 10.1039/c6pp00254d.

[207] C. Cheng, S. Peng, Z. Li, L. Zou, W. Liu, and C. Liu, "Improved bioavailability of curcumin in liposomes prepared using a pH-driven, organic solvent-free, easily scalable process," *RSC Adv.*, vol. 7, no. 42, pp. 25978–25986, 2017, doi: 10.1039/c7ra02861j.

[208] B. Zheng and D. J. McClements, "Formulation of more efficacious curcumin delivery systems using colloid science: Enhanced solubility, stability, and bioavailability," *Molecules*, vol. 25, no. 12, pp. 1–25, 2020, doi: 10.3390/molecules25122791.

[209] M. Barberi-heyob, E. Arab-tehrany, and M. Linder, "Growth-Inhibitory E ff ect of Chitosan-Coated Cancer Cells," *Mar. Drugs*, vol. 18, 2020.

[210] T. Song, X. Guo, X. Li, and S. Zhang, "Label-free electrochemical detection of RNA based on 'Y' junction structure and restriction endonuclease-aided target recycling strategy," *J. Electroanal. Chem.*, vol. 781, pp. 251–256, 2016, doi: 10.1016/j.jelechem.2016.05.046.

[211] E. El Khoury, M. Abiad, Z. G. Kassaify, and D. Patra, "Green synthesis of curcumin conjugated nanosilver for the applications in nucleic acid sensing and anti-bacterial activity," *Colloids Surfaces B Biointerfaces*, vol. 127, pp. 274–280, 2015, doi: 10.1016/j.colsurfb.2015.01.050.